

HARRISON, HALEY B. Ph.D. Covalent functionalization of BNNTs for low density aerogels. (2021)
Directed by Dr. Jeffrey R. Alston. 132 pp.

Boron nitride nanotubes (BNNTs) and hexagonal boron nitride platelets (h-BNs) have received considerable attention for aerospace insulation applications due to their exceptional chemical and thermal stability. Since synthesis in 1995, there have been many attempts towards developing novel BNNT-based and BNNT-integrated composites, but many advances are limited by the production scale of BNNTs. In this dissertation, recent advances in BNNT synthesis and purification are reviewed and how the increasing availability of gram-scale high purity BNNTs can be investigated for low density composite applications. Such future applications covered in this work include use of h-BNs and BNNTs as nanofillers in polymer aerogels. Polyimide aerogels have great potential for use as flexible, high temperature stable insulation materials. These aerogels can be multifunctional by adding BNNTs into the aerogel structure. As covalent functionalization methods remain limited, we explore methods enabling the addition of unmodified boron nitride nanomaterials including BNNTs into polyimide aerogels as nanofiller, and their limitations due to their strong tendency to aggregate in solution.

COVALENT FUNCTIONALIZATION OF BNNTS FOR LOW DENSITY AEROGELS

by

Haley B. Harrison

A Dissertation

Submitted to

the Faculty of The Graduate School at

The University of North Carolina at Greensboro

in Partial Fulfillment

of the Requirements for the Degree

Doctor of Philosophy

Greensboro

2021

Approved by

Dr. Jeffrey R. Alston
Committee Co-Chair

Dr. Hemali Rathnayake
Committee Co-Chair

DEDICATION

My amazing parents, who taught me perseverance. My beloved sisters; My daughter; and my Grandma who always supported my wildest dreams. To my friends who encourage and support me, and all the people in my life who touch my heart, I dedicate this dissertation.

APPROVAL PAGE

This dissertation written by Haley B. Harrison has been approved by the following committee of the Faculty of The Graduate School at The University of North Carolina at Greensboro.

Committee Co-Chair

Dr. Jeffrey R. Alston

Committee Co-Chair

Dr. Hemali Rathnayake

Committee Members

Dr. Tetyana Ignatova

Dr. Dennis LaJeunesse

Dr. Stephanie L. Vivod,
NASA Glenn Research Center

June 23, 2021

Date of Acceptance by Committee

June 23, 2021

Date of Final Oral Examination

ACKNOWLEDGEMENTS

I would like to acknowledge North Carolina A&T State University, The University of North Carolina at Greensboro, The Joint School of Nanoscience and Nanoengineering, and the North Carolina SPACE Grant for funding that contributed to the completion of this dissertation. I would like to give my warmest thanks to my co-advisors, Dr. Jeffrey Alston, Dr. Hemali Rathnayake, and my committee for lending their time and expertise to support my vision. I acknowledge Dean Sherine Obare for lending her expertise and providing mentorship. Additionally, I would like to acknowledge my external committee member, Dr. Stephanie Vivod for providing her time, lab space, equipment, and expertise as a polymer expert. I would like to acknowledge the BNNT, LLC team, President Dr. Roy Whitney and CEO Tom Henneberg for providing lab space and sharing their knowledge and expertise to enable me to explore new opportunities within the field, and finally, Dr. Lindsey Scammell for providing support, materials, and her expertise during my training.

TABLE OF CONTENTS

LIST OF TABLES	ix
LIST OF FIGURES	x
CHAPTER I: OVERVIEW.....	1
List of Abbreviations	4
CHAPTER II: INVESTIGATING BN NANOPARTICLES AND BNNTS AS NANOFILLER IN POLYIMIDE AEROGELS	6
Introduction.....	6
Synthesis	6
Chemical Vapor Deposition, Induction Heating Boron Oxide Chemical Vapor Deposition .	7
Thermal Chemical Vapor Deposition	8
High Temperature Ball Milling	9
Arc Discharge Method.....	10
Laser Heating/Laser Ablation Methods	11
High Temperature High Pressure Method (HTP).....	12
Solubility, Purification and Dispersion of BNNT.....	12
Solubility.....	13
Individualization of BNNTs using Superacids: Chlorosulfonic acid	14
Wet thermal etching.....	15
Gas-Phase Purification.....	16
Surfactant and Centrifugation Methods	16
Polymer wrapping.....	17
Aerogels	18
Polyimide Synthesis: Towards Polyimide Aerogels.....	19
Polyimide aerogel Synthesis: One-step polymerization	20
Polyimide Synthesis: Two-step polymerization	22
Thermal Imidization of poly(amic acid)	22
Chemical Imidization of poly(amic acid)	23
Crosslinked Polyimide Aerogels.....	24

Altering the Backbone Chemistry.....	25
BN as Porous Aerogels and as Reinforcement	27
Boron Nitride Nanomaterials as Nanofiller into Polyimide Aerogels	28
Polyimide Aerogels.....	29
Preparation of Polyimide Aerogel loaded with h-BN.....	30
Materials	30
BNNT Refinement via Thermal Oxidation.....	31
OW-BNNT Preparation	32
Methods.....	32
Preparation of Polyimide Aerogels, BTC Crosslinks	32
h-BN and BNNT Suspensions	33
Synthesis/Preparation of Crosslinked Monoliths.....	34
Supercritical Fluid Extraction.....	34
General Characterization Methods	36
Density	37
Spectroscopic Analysis: XPS Measurements	37
SEM Measurements	38
FT-IR Spectroscopic Measurements.....	40
Contact Angle Measurements.....	41
Static Thermogravimetric Analysis	43
Conclusions.....	47
CHAPTER III: QUANTIFICATION OF HEXAGONAL BORON NITRIDE IMPURITIES IN BORON NITRIDE NANOTUBES VIA FT-IR SPECTROSCOPY	50
Abstract.....	51
Background.....	51
Removal of Amorphous Impurities	55
BNNT Enrichment	56

Quantification of h-BN Content in BNNTs: X-Ray Diffraction of Boron Nitride.....	57
Quantification of h-BN Content in BNNTs: Fourier Transform Infrared (FT-IR) Spectroscopy of BNNTs and h-BN.....	59
Quantification of h-BN Content in BNNTs: Measuring unknown [h-BN] using FT-IR Absorbance and Internal Standard (Spiking).....	61
Conclusions.....	65
Methods.....	66
Materials	66
Oxidation of as-received Nanomaterials.....	66
High-Temperature Oxidation Discussion	67
Sonication assisted isovolumetric filtration (SAIF).....	68
Surfactant Wrapping	69
Thermal Analysis	69
Powder X-ray Diffraction (XRD).....	69
FT-IR “Spiked” Standard Preparation	70
Determination of Unknown h-BN Concentration.....	71
CHAPTER IV: SONOCHEMICAL FUNCTIONALIZATION OF BORON NITRIDE NANOMATERIALS	75
Abstract.....	75
Background.....	76
Experimental Details.....	77
Materials	77
Ultrasonic Processing.....	78
Discussion.....	81
Conclusions.....	86
Chapter V: INVESTIGATING THE COVALENT FUNCTIONALIZATION OF BORON NITRIDE NANOMATERIALS VIA SONOCHEMICAL ALCOHOLYSIS	88
Abstract.....	88
Introduction.....	89

Enhanced chemical reactivity of BNNTs	91
Sonication assisted alcoholysis	92
On BNNT Functionalization.....	94
Covalent Functionalization of BNNTs	97
Proposed Reaction Scheme.....	98
Methods (BN)	100
Approach: Boron Nitride Purification	100
Filtering Protocol	101
Temperature Control.....	101
Ultrasonication.....	102
Sonotrode Selection	102
Additional Materials	103
Reagents.....	103
Preparation of -CF functionalized h-BN and BNNTs.....	104
Preparation of -NH ₂ Functionalized h-BNs and BNNTs.....	105
On the use of Glycerol: Green Solvent.....	105
h-BN reacted with excess ethanolamine, in glycerol.....	106
BNNT reacted with ethanolamine, in glycerol	107
BNNT reacted with ethanolamine, in n-butylamine	107
Temperature Control.....	108
Characterization	109
X ray Photoelectron Spectroscopy.....	110
Fourier Transform Infrared Spectroscopy (FT-IR).....	111
Dispersity Analysis	113
Amine Functionalized h-BN and BNNTs: UV/Visible Spectrophotometry (in NMP)	114
Discussion and Conclusions	121
BIBLIOGRAPHY.....	122

LIST OF TABLES

Table 1. Polyimide oligomers are synthesized using a combination of, but not limited to, the following monomers. Dianhydrides frequently used as cited in this dissertation include (top to bottom) PMDA, BPDA, and BTDA. Diamines frequently used include (top to bottom) aromatic ODA and DMBZ, and aliphatic DADD. Each of these monomers are selected due to the specific properties they impart on the resulting aerogels.....	26
Table 2. 7 wt. % polyimide aerogel formulation parameters.....	37
Table 3. Contact angle measurements for polyimide aerogels. Addition of BN nanomaterials did not improve hydrophobicity, despite hydrophobic nature of unmodified BNNTs. Due to the low concentration added, the polymer backbone composition has a greater impact on the properties in these studies.	42
Table 4. FT-IR Peak Ratios with Calculated h-BN Weight Percent from Figure 5.	62
Table 5. Sonication energy output calculated in J for each reaction scheme.	105
Table 6. Control sample (Top) was ultrasonication in glycerol, washed and dried. BNNTs were reacted with ethanolamine in glycerol to attach -NH ₂ moieties to the edges and surface of BNNTs. The dried BNNTs were characterized via XPS, and elemental analysis was conducted to determine the composition of the materials. The B/N ratio was also calculated for reference. For a standard as-received BNNT sample, the ratio is 1.08, for NH ₂ -BNNTs, the ratio is 0.86	115
Table 7. Atomic % composition of AR-BNNT (Top) and CF _x -BNNT (Bottom). Confirms attachment of fluoroalkyl groups to BNNT surface.	116

LIST OF FIGURES

Figure 1. Schematic for purification set-up that is used to purify raw BNNTs. Pure oxygen/nitrogen flows into the tube furnace (7), heated in a flask (5) to 90 °C. An alumina crucible containing BNNT sample is placed within the furnace (7). The furnace (7) is plugged with refractory blocks to minimize heat loss, and left at the maximum processing temperature for 24 h.....	15
Figure 2. Dianhydride and diamine monomer polymerize into polyimide oligomer (of n repeating units), releasing water.	20
Figure 3. Example of a linear polyimide.	21
Figure 4. Example of a heterocyclic (aromatic) polyimide. These polyimides are formed by a reaction of aromatic monomers.	21
Figure 5. Semi-aromatic polyimide structure. These polyimides are synthesized with one aliphatic monomer and one aromatic monomer.	21
Figure 6. Polyimide is a polymer of imide monomers.....	21
Figure 7. Chemical imidization at room temperature schematic including crosslinker. This synthesis process is highly customizable, but this follows the general formulation of using PMDA and DMBZ as the monomers, crosslinked with BTC. As viscosity begins to increase, and the polymerization process begins, the solution can be poured into molds for an aging period of 24 h. After aging, the gels go through a series of solvent exchanges to replace the pore fluid (NMP) with acetone.	23

Figure 8. Benzenetricarbonyl trichloride (BTC) was used as a crosslinker to fabricate polyimide aerogels. BTC is a cost-effective alternative crosslinker. Fabricating polyimide aerogels with BTC gel faster (5-20 minutes, compared with an hour or more) than alternatives (TAB or OAPS) and have comparable onset of decomposition. However, increased hydrophilicity remains a challenge that isn't overcome by altering the backbone structure of the oligomers. 25

Figure 9. The figure depicts the temperature vs pressure diagram for carbon dioxide.

Additionally, the supercritical fluid exchange process followed for drying aerogels is depicted using the red arrows. (1) liquid CO₂ is converted to supercritical fluid by increasing the temperature and pressure above the supercritical point, avoiding the phase boundaries, and thereby capillary forces. (2) The supercritical fluid is then converted to gas, and the pressure is reduced to ambient pressures, temperature is reduced and the vessel can be opened, leaving low density, nanoporous aerogels. 36

Figure 10. Polyimide aerogels were sputter coated in a thin ~10 nm layer and adhered to Lacey carbon grids. The resolution of the micrograph is 200 nm showing the unique nanoporous structure of polyimide aerogels. The pore structure can be altered by varying the monomers, their concentration, as well as the crosslinkers. We predict nanoparticles can be trapped in the nanosized pores, and various resulting properties can be characterized..... 38

Figure 11. A representative micrograph of the polyimide aerogel 7 wt % formulation synthesized in this dissertation. 39

Figure 12. FTIR Spectra of polymer aerogels formulated with a 7 w/w polymer concentration, n=60. 41

Figure 13. Contact angle measurements. All samples are slightly hydrophilic..... 42

Figure 14. TGA of polyimide aerogels run in nitrogen, ramp rate 5 °C/minute. This TGA curve shows the char yield, as defined here as the mass remaining at 750 °C to be ~60% for all samples. (Note: sample 1.11% h-BN (blue) was conducted from 0-750°C, so a ~3 C mass loss is accounted for in the graph here.)..... 43

Figure 15. Composite graph of representative TGA curves from the study in an oxidative environment, the onset of thermal decomposition for all samples was calculated between ~515-530 C. The onset of thermal oxidative decomposition is slightly higher for sample. This may be due to the presence of boron nitride nanoparticles..... 44

Figure 16. Onset of decomposition was quantified as the 5% mass loss was calculated for the control sample, 7 wt % DMBZ/PMDA was calculated to be 510 C. 45

Figure 17. Onset of decomposition was quantified as the 5% mass loss was calculated for 0.55% BNNT incorporated polymer aerogel to be 517 C..... 46

Figure 18. High temperature oxidation of commercially produced BNNTs and h-BN. Before: As received BNNTs (AR-BNNTs) After: Oxidized commercial BNNTs (Ox-BNNTs), AR-BNNTs heated in air at 800 °C for 3 h. Bottom: Thermogravimetric analysis of AR-BNNTs (Red) and 98% h-BN (black) heated in air at 10 °C min⁻¹ up to 1000 °C. AR-BNNTs (Blue) heated in air at 10 °C min⁻¹ up to 800 °C then held for 3 h, followed by a thermal cycle down to RT and back to 1000 °C at 10 °C min⁻¹..... 53

Figure 19. XRD spectra of as received commercial hexagonal boron nitride (h-BN) and commercial boron nitride nanotubes (BNNTs) with oxidation and wash products. h-BN peaks near 41°, 43°, 50° and 55° show characteristic 3D ordering.²² Broadening and shifting the (002) peak near 26° is a sign of increasing graphitic plane spacing and curvature.²⁴ B₂O₃ is

the primary product removed from the oxidized commercial BNNTs (Ox-BNNTs) as Wash Recovery. Note* Some cellulose is present due to contamination from sample collection on a cellulose filter membrane. Individual intensity axes are not to scale. 58

Figure 20. FTIR Spectra array of AR-BNNT samples that have been “spiked” with increasing amounts of nanoscale h-BN. Samples are presented from the lowest h-BN concentration (AR-BNNTs) to the highest in the back (pure nanoscale h-BN). The spectra are all normalized to their TO peaks (1350 cm⁻¹) to assist visualization of the increasing out-of-plane versus in-plane transmission (R/TO) peak ratio as the concentration of h-GN in the sample increases. 61

Figure 22. Calibration curve generated from “spiked” standards after determination of [h-BN]_i in AR-BNNTs. Black circles represent calibration standards. Green squares represent enrichment samples and the Calculated Weight Percent from R/TO peak ratios and based on linear best fit (red line) to calibration curve..... 63

Figure 23. Hielscher probe sonicator is used in the stand mounted procedure with titanium and glass probe tip attachments. A chiller loop is hooked up to a jacketed flask, and the reaction vessel is submerged inside to manage temperature. The sonication set up is contained inside a soundproof box. 78

Figure 24. Experimental Parameters of Samples A through F. Output parameter, Fluorine atomic %, measured via X-ray photoelectron spectroscopy (XPS)..... 81

Figure 25. XPS Atomic % analysis of Samples A-F. 82

Figure 26. (Top left) XPS carbon spectra. 1 μm functionalized h-BN platelets (Sample C, red) versus the control, unfunctionalized h-BN material (Sample D, blue). The C-F2 peak is at ~292 eV and the C-F3 peak is at ~294 eV. The carbon peak arising at ~284.1 eV can be

attributed to the presence of adventitious carbon, and C-C bonds contaminating the surface of the material. (Top right) XPS fluorine spectra. 1 μm functionalized h-BN platelets (Sample C, red) versus the control, unfunctionalized h-BN material (Sample D, blue). The binding energy for fluorine is ~ 688 eV. (Bottom left) XPS carbon spectra. <150 nm functionalized h-BN nanopowder (Sample A, blue) versus the control, unfunctionalized h-BN nanopowder (Sample F, red). C1s binding energy in the range of 280-299 eV was evaluated. The functionalized h-BN binding energy corresponding to the C-F2 group was ~ 292 eV. XPS fluorine spectra. <150 nm functionalized h-BN nanopowder (Sample A, red) versus the control, unfunctionalized h-BN nanopowder (Sample F, blue). The binding energy for F1s was ~ 688 eV. 83

Figure 27. (Left) FT-IR spectra of as-received micron size h-BN (Red) versus functionalized h-BN (Blue). (Right) Unfunctionalized spectra subtracted from the functionalized spectra clearly expose -CF2 and -CF3 absorption at $1090\text{-}1290\text{ cm}^{-1}$ 85

Figure 28. h-BN particle dispersion stability is qualitatively assessed by observing stability in fluorinated media (Vertrel-XF pictured). (Left) Sonochemical functionalized sample B, 72 hours after dispersion in Vertrel-XF. (Right) Control (unfunctionalized) sample E, 72 hours after dispersion in Vertrel-XF. 85

Figure 29. Thermolysis induced generation of oxygen or carbon centered radicals in situ for covalent functionalization of BNNTs at boron sites. 93

Figure 30.(a) Schematic depicting two different initiation sites: the "edge" or "surface." 93

Figure 31. Various routes to hydroxylate raw h-BN sheets. 93

Figure 32. h-BN platelets are reacted with perfluorinated bifunctional alcohols in decafluoropentane. 98

Figure 33. BNNTs or h-BN nano-sized platelets (<150 nm) are reacted with a bifunctional alcohol containing amine moieties in unreacted solvents. In these experiments, the solvents primarily used were either glycerol or n-butylamine, yielding amine functionalized h-BN or BNNTs. The non-aqueous solution is sonicated at high power (~70-80 W) and the temperature is controlled, such that a large amount of energy is created within the reaction vessel. This ultrasonication procedure produces short-lived hydroxyl radicals, which reacts with B-N, producing NH₂-BNNTs and NH₂-h-BN nanoparticles..... 99

Figure 34. FT-IR was used to identify the presence of aliphatic C-N groups attached to the BNNT surface. Characteristic peaks are identified at between ~1020-1250 cm⁻¹, which can be attributed to the small molecule attachment. Also shown here are the transverse optical and longitudinal modes (~1350 cm⁻¹) and the out of plane buckling corresponding to the radial mode(~800 cm⁻¹). 111

Figure 35. BNNT has characteristic peaks at 1343 cm⁻¹ and 789 cm⁻¹, corresponding with the radial breathing and transverse optical modes of BNNTs. 112

Figure 36. 150 mg h-BN platelets in solvent. (left) unfunctionalized (right) functionalized. 114

Figure 37. Suspensions of (left) amine-functionalized BNNTs in NMP, (right) unfunctionalized BNNTs after brief sonication..... 115

Figure 38. High resolution C1s spectra of BNNT and NH-BNNT..... 117

Figure 39. N1s high resolution spectra of NH-BNNT compared with BNNT. 118

Figure 40. High resolution spectra valence region BNNT compared with NH-BNNT, highlighting the C2s bonding of surface BNNT(~18.1 eV). 118

Figure 41. O1s high resolution spectra BNNT compared with NH-BNNT 119

CHAPTER I: OVERVIEW

Boron nitride nanotubes (BNNTs) have numerous interesting properties including significant thermal and chemical stability, that make them ideal for use in polymer materials to improve the physical and chemical properties. Due to the exceptional stability of BNNTs, their use as reinforcement has been limited due to the strong intermolecular forces responsible for the agglomeration of BNNTs in solvents and solutions. In this thesis, we explore methods for functionalizing BN nanoparticles and BNNTs and applications enabled by the development of these methods.

First, this dissertation presents a literature review of the synthesis, purification, and functionalization of BNNTs. As proof of concept, the use of h-BN and BNNTs as nanofiller in polyimide aerogels was explored. A 7 wt. % formulation was used to synthesize a series of polyimide aerogels. The aerogels were characterized via Fourier transform infrared spectroscopy (FT-IR), thermal gravimetric analysis (TGA), and Sessile Drop goniometry was used to calculate the contact angle. Methods for dispersing BN nanoparticles in solutions were evaluated. This dissertation also explores methods for quantifying the h-BN content in a sample of as received BNNTs (AR-BNNTs). Controlled covalent attachment across the B-N bond via a sonication initiated alcoholysis approach is presented. A statistical experimental design was employed to optimize factors such as time, temperature, and energy output (Joules) during the procedure, to control heat generated during the sonication process. Alcohols containing one or more additional functional groups were targeted due to the reactivity of short lived -OH radicals. Small molecules including fluoroalkoxy, alkoxy, and amine moieties are explored for their potential to be used as structural reinforcement in polyimide aerogels. In this one-step approach, it has been demonstrated that fluorinated groups can be attached across the B-N bond showing functional

group compatibility in low concentrations. First, we demonstrated h-BN platelets < 150 nm can be covalently functionalized when reacted with fluorinated alcohols to yield -CF₂ and -CF₃ functionalized hexagonal boron nitride nanoparticles (CF₃-h-BN) and (CF₂-h-BN) (in ~1-2% via atomic percentages). Once successful attachment was shown, the technique was reproduced on BNNTs. Attachment of fluoroalkyl groups was confirmed via XPS, Raman and FT-IR. Bifunctional alkanolamines were investigated for attaching aliphatic amine (-NH₂) moieties to across the BN bond. Adequate stability of functionalized h-BN and BNNT nanostructures can be showed in solvents such as NMP, when compared with unfunctionalized BNNTs. This work seeks to improve the compatibility between BN or BNNT nanostructures and composite and polymer matrices such that their properties are improved. This provides a basis for exploring functionalized BNNTs for use as reinforcement in polyimide aerogels. Further summaries of the chapters are expanded below.

In Chapter 1, a literature review on current BNNT synthesis methods, purification, functionalization methods is covered. An overview of polyimide aerogel synthesis and their applications are provided. This review is followed by a demonstration of methods as a proof of concept, which can potentially be used to effectively incorporate h-BN and BNNTs into polyimide aerogels. With this technique, we use a liquid processing approach to incorporate BN nanoparticles and BNNTs into the dilute monomer solution hereby avoiding aggregation that occurs during gelation. This processing route will enable future applications development and expand use of polyimide aerogels for high-temperature environments.

In Chapter 2, we describe methods for quantifying the purity of as received BNNT samples via calculating the concentration of h-BN via an FT-IR spectroscopic technique.

In Chapter 3, we explore sonochemical techniques to develop a one-step route for functionalizing h-BN with fluoroalkoxy groups. We apply DOE methods to optimize on factors such as temperature, time, and energy to reduce potential damage to BNNTs.

In Chapter 4, we demonstrate sonochemical radical initiated fluoroalkoxy covalent functionalization of BNNTs. We characterize the functionalized BNNTs using a variety of spectroscopic and microscopic techniques including XPS, FT-IR, Confocal Raman microscopy and solubility studies. We demonstrate the sonochemical process can be modified, presenting functionalized NH₂-h-BN nanoparticles (f-NH₂-h-BN) and NH₂-BNNTs sonochemical radical initiated amine covalent functionalization of h-BN and BNNTs. We characterize the functionalized BNNTs using spectroscopic and microscopic techniques including XPS, FT-IR. Visual stability is used to evaluate the solubility of BNNTs.

List of Abbreviations

AR-BNNT- as received boron nitride nanotube

ATR -attenuated total reflectance (infrared spectroscopy)

FT-IR -Fourier transform infrared spectroscopy

BNNT -boron nitride nanotube

CNT -carbon nanotube

DMF -N,N-dimethyl formamide

h-BN -hexagonal boron nitride (nanoparticles)

EtOH -ethanol

MeOH -methanol

PFO-ol -perfluoro octanol

PFH-ol -perfluoro hexanol

NMP -n-methyl-2-pyrrolidon

UV-Vis -ultraviolet-visible (spectrophotometry)

TGA -thermal gravimetric analysis

Wt. % -weight percent

XPS -x-ray photoelectron spectroscopy

SEM -scanning electron microscopy

TEM -transmission electron microscopy

SFE -supercritical fluid (extraction)

PMDA -pyromellitic dianhydride

DMBZ -2, 2'-dimethylbenzidine

AA -acetic anhydride

TEA -triethylamine

BTC -1,3,5-benzenetricarbonyl trichloride

Vertrel XF -commercial decafluoropentane

CHAPTER II: INVESTIGATING BN NANOPARTICLES AND BNNTS AS NANOFILLER IN POLYIMIDE AEROGELS

Introduction

Boron nitride nanotubes (BNNTs) are white, optically transparent to visible and IR light, one-dimensional nanostructures that are, in contrast with CNTs, electrically insulating nanostructures regardless of chirality. BNNTs are the structural analogue for CNTs but due to the partial ionic nature of B-N bonds, these h-BN nanoparticles and BNNT materials have numerous distinct properties such as superior mechanical strength, a band gap of ~6 eV, high oxidative resistance, and high thermal conductivity. Additionally, BNNTs have an exceptional capability to be neutron shielding . BNNTs consist of rolled h-BN sheets where the B and N atoms exist in an hexagonal sp^2 hybridized lattice. BNNTs are high aspect ratio materials with a 1-100 nm diameter and can be grown at lengths ranging from 100 nm to several microns. BNNTs are exceptional due to the higher oxidative stability in air, approaching 800 °C, well exceeding the 400 °C oxidation limit of CNTs. This makes BNNTs favorable for a variety of high temperature applications, as BNNTs will not break down in extreme environments where CNTs and other bulk materials fail. Despite their theorized superiority, BNNT advances in applications remain limited as synthesis techniques, purification methods, and covalent functionalization techniques remain difficult to develop due to their (BNNTs) high thermal stability, inert nature, insolubility and hydrophobicity .

Synthesis

Advances in synthesis techniques have allowed for commercial availability of a wide variety BNNTs, but practical use of BNNTs has been limited due to the problems with commercial processing leading to poor quality products with low yield. Since inception, a wide

variety of methods have been developed to grow BNNTs. Many of these methods were inspired by successful techniques developed for CNT synthesis, including arc discharge, chemical vapor deposition (CVD), laser ablation, ball milling, and atom deposition. In 1995, BNNTs were first synthesized via a plasma arc discharge apparatus, producing tubes with a diameter of 1-3 nanometers and lengths up to 200 nm.

Chemical Vapor Deposition, Induction Heating Boron Oxide Chemical Vapor Deposition

Chemical Vapor Deposition (CVD) methods were frequently and successfully used to synthesize CNTs, and many methods exist that have been modified and developed to be applied for the synthesis of BNNTs. These early methods relied on forming carbon based vapors that resulted in carbon contaminated BNNTs. The focus then turned to developing carbon-free catalysts in methods, referred to as boron oxide CVD (BOCVD) methods, including early but limited success using highly toxic borazine as a precursor at 1000 – 1100 °C . In 2002, Tang et al. developed the first successful carbon-free precursor and catalyst, that enabled the group to develop a successful CVD method that could produce bulk amounts of BNNTs. Here, they reacted boron and nitrogen or ammonia in the presence of amorphous NiB/Al₂O₃ catalyst. In another publication, the group reacted a mixture of B₂O₂ and Mg in ammonia to produce BNNTs.

Early development of BOCVD processes yielding BNNTs used an induction heating chamber containing a mixture of carbon free precursors such as B. These precursors are reacted with metal oxides such as MgO and FeO catalysts that produce reactive boron oxide (B_xO_y) vapor, that is then reacted in ammonia (NH₃). After evaporation, small amounts of BNNTs could be collected from the chamber. Lee et al., produced BNNTs at 1200 °C in a conventional resistive tube furnace via a growth vapor trapping method. Here, growth is controlled by using

catalytic nanoparticles coated on Si substrates. This method produces BNNTs in a controlled manner, whereas the traditional CVD methods spontaneously produces BNNTs that are removed from the tube surface. Presently, CVD techniques are favorable when compared with other techniques because they allow for better controllability of growth parameters, precursors, and catalyst type and temperature. BNNT growth by CVD methods consistently produce higher quality and quantity BNNTs. Huang et al., and Li et al., expanded on the preceding work by introducing B and Li₂O as a precursor. The introduction of lithium improved the process, producing pristine, gram-scale quantities of BNNTs .

These advancements allowed for the next phase of CVD methods to develop, where high quality, gram-scale BNNTs could be produced at lower temperatures and at ambient pressures. It can be summarized that, using BOCVD methods, BNNTs can be produced at temperatures from 1100-1500 °C in gram-scale quantities although some impurities, such as B, BN, and metal catalyst are detected. This process was simplified further by using an argon gas atmosphere, developing argon supported thermal chemical vapor deposition (TCVD) methods .

Thermal Chemical Vapor Deposition

CVD methods are highly customizable, and different research groups tend to use a variety of experimental parameters leading to a wide range in the produced BNNT quality and quantity. Additionally, these early methods required a special furnace, high pressures, and high temperatures. In the next phase of development, researchers began using a conventional horizontal tube furnace, in specific ratios of precursors (B, FeO, MgO) to grow BNNTs on silicone/silicone dioxide (Si/SiO₂) substrates at 1100 -1300 °C using a process known as thermal chemical vapor deposition (TCVD) . Lee et al., produced BNNTs using a growth vapor trapping approach (GVT) , where a quartz tube is used to trap growth vapors and form BNNTs. Compared

with BOCVD methods, specific ratios of catalytic nanoparticles (Fe, MgO, Ni) on Si substrates are used to control the growth of BNNTs via an optimized vapor-liquid-solid process (VLS). This work established reproducible methods for producing small quantities of high quality and high purity BNNTs . Wang, X. Z. et al., customized a template-assisted microwave plasma-enhanced CVD approach to synthesize BNNT arrays below 520 °C, under a anodic aluminum oxide template with borane/argon and ammonia/nitrogen precursors. This method is desirable due to the low growth temperature for practical, potentially scalable synthesis enabling commercial applications. However, this method produces highly amorphous BNNTs. The BNNTs produced branched and dendriform BNNTs, which may be of interest for electrical applications .

High Temperature Ball Milling

The formation of BNNTs can be achieved using solid-state processes such as ball milling and annealing, however, the quality of the produced BNNTs is generally low, and the energy and time expended during this process is high. The theory behind the method is that a reaction between boron and nitrogen can be induced through the introduction of defects in the starting powders by adding sufficient mechanical energy (ball milling). To make nanotubes, the treated powders must be annealed at high temperatures (at or above 1200 °C) . This process is appealing because it can produce large quantities of BNNTs, although purity remains questionable. Chen et al., first utilized ball milling as a synthesis method to yield BNNTs by ball milling hexagonal BN (h-BN) powder for many hours (150 h) to generate disordered nanostructures. This was followed by annealing at high temperatures (1300 °C), leading to nucleation and growth of hexagonal shaped BNNTs . The BNNTs produced included different structures, including cylindrical tubes as well as segmented tubular nanostructures, resembling bamboo. These early methods produced

highly contaminated samples; each tube produced during this process was capped with a metal (Fe, Ni, Cr) particle, and contaminated with difficult to remove nanosized h-BN particles. H-BN powders did not grow nanotubes in milled samples that were not heated, showing that the growth of BNNT was due in part to the annealing process. Further research was conducted to improve the ball-milling process to improve the quality and quantity of BNNTs that could be produced . Researchers have attempted using ammonia during the annealing process, but this yielded comparably low quality BNNTs contaminated with large quantities of difficult to remove micro- and nano-structured BN impurities .

To address the high energy concerns arising from the lengthy ball milling and annealing method, a self-propagation high-temperature synthesis (SHS) method was developed using a mixture Magnesium (Mg), Boron Oxide (B_2O_3), and CaB_6 heated in a furnace at $750\text{ }^\circ\text{C}$ to yield a porous precursor. The precursor was heated at $1150\text{ }^\circ\text{C}$ under an ammonia and cooled. The product was extensively washed in harsh acids, yielding BNNTs .

Arc Discharge Method

The first BNNTs experimentally observed were synthesized via plasma arc discharge in 1995 . The arc discharge method is a method requiring expensive, pure cathode and anode materials, offering little control over the synthesis process, and producing small quantities of usable BNNTs (generally, BNNTs were only present in the cathode deposits). Here, a pressed h-BN rod was inserted into a hollow tungsten electrode to form an anode. A pure, rapidly cooled copper electrode was used to form an anode. A constant potential drop of 30 V between the electrode was maintained during discharge in helium gas, maintained at 650 torr. Temperatures inside the chamber exceeded the melting point of tungsten, or 3700 K. N_2 , NH_3 with ZrB_2 or HfB_2 high purity rods have also been used as electrodes, with arcing taking place in a nitrogen

gas environment . Loiseau et al., introduced high purity, hot-pressed 10 mm in diameter hafnium diboride (HfB_2) rods as electrodes. In a nitrogen gas atmosphere, at 700 mbar a stable plasma was established during arcing . Here, a thin layer of electrode deposit was noted, as well as the apparent melting of the anode during synthesis, indicating temperatures inside the vessel reached 3650 K. The BNNT was deposited on the electrode, dispersed in ethanol using ultrasonication and analyzed via TEM. The few layered BNNTs produced via this arc discharge method contained dark, HfB_2 nanocrystals that were encapsulated into the tubes, appearing like cages . From this work, the authors established that energy expended during synthesis had an impact on the tip morphology of the nanotubes, potentially offering an avenue towards control. This behavior contrasts with the random nature seen with carbon nanotubes (CNTs) synthesized via CVD methods . More recently, researchers sought to improve the stability of the arcing process itself, and to increase the quantity of BNNTs that could be produced per batch . Using boron containing trace nickel and cobalt as the electrode and boron or tungsten as the cathode in a nitrogen environment, grey BNNTs were found deposited randomly within the chamber. The BNNTs produced were low in quality, and contaminated with elemental boron, boron oxide, and h-BN.

Laser Heating/Laser Ablation Methods

In the past decades, there has been an increase in attention given towards developing and improving BNNT synthesis techniques. However, even the current state of the art methods that can be used for mass production produce low quality, highly contaminated material while methods that can be used to produce small amounts of high quality, high purity BNNTs remain expensive, requiring lots of time and energy. Additionally, even these methods, requiring high temperatures leave chemically similar h-BN contaminants which are difficult to remove, and

induce defects on the tube surfaces. As these challenges remain despite significant advances in synthesis techniques in the past years, attention has shifted towards improving and developing purification techniques for removing contaminants from as-received BNNTs.

High Temperature High Pressure Method (HTP)

Michael Smith et al., developed a successful high temperature method produces gram-scale quantities of small diameter, few walled, long nanotubes, resembling fibers. Using a pressurized vapor/condenser (PVC) method, condensation of seed particles is forced in a plume of pure boron vapor held at high ambient pressures. This creates a density difference between hot boron vapor (4000 °C) and the surrounding N₂ atmosphere, which is held at room temperature. This difference in temperature produces a buoyancy force and a narrow vertical plume of boron vapor. A cooled metal wire traversing the plume acts as a condenser, leaving boron droplets to form nucleation sites. Seconds later, the sites encounter the N₂ gas leading to the formation of BNNTs . This method has been evolved into a high temperature laser ablation method and remains one of the most highly successful techniques for producing high quality BNNTs.

Solubility, Purification and Dispersion of BNNT

The main impurities of BNNTs are elemental boron (B), boron oxide (B₂O₃), hexagonal boron nitride nanoparticles (h-BNs) and nanofibers. Removing elemental boron and boron oxide can be sufficiently accomplished by thermal oxidation at 800 °C and using more refined syntheses processes, such as the high-temperature-pressure method (HTP). However, removing boron nitride microscale particles, nanoparticles and nanofibers remains a challenge because BN impurities are chemically very similar to BNNTs . Purification approaches include polymer wrapping, non-covalent functionalization, DNA and peptide mediated isolation, and dispersion in aqueous solutions via ionic surfactants. All methods are generally accompanied by some form

of sonication, which temporarily swells and stabilizes nanotube samples, although harsh sonication to increase the solubility generally damages the tubes.

Amin, S. Mahmoud et al., presented a mild high-yield method capable of removing >99% of h-BN impurities without requiring high temperatures or harsh acids, contrasting with most existing methods where damage to the tubes ultimately reduces the yield of purified BNNT produced. In this approach, the authors mixed a mass of BNNT with heptane in a pressure tube which was heated to 90 °C for 5 hours in an oil bath, then cooled. The BNNTs were separated from heptane via decantation and dried under <10 mbar at 250 °C, overnight. The h-BN impurities remained suspended in the supernatant, leaving purified BNNTs with their structural integrity intact.

Improved biological compatibility of BNNTs in aqueous solutions is being explored as the development of biological applications are sought due to the non-toxic nature of BNNTs. One approach by Kode, Venkateswara et al., extensively studied using DNA to purify, wrap, individualize and effectively disperse BNNTs uniformly at concentrations as high as 11.5 wt. %. The purified DNA-BNNTs were isolated via solvent evaporation, leaving aligned BNNT films produced by spontaneous alignment. These films were characterized via SEM. Using DNA harnesses the advantages of stabilizing BNNTs by relying on π - π interactions and can be employed for use in various solvents including alcohols .

Solubility

The solubility of BNNTs and boron nitride containing nanoparticles is an important quantification technique for polymer nanocomposite formulation and development. To determine a set of suitable solvents for BNNTs, Mutz et al., quantified the solubility limit of BNNTs, functionalized BNNTs (FBNNTs) and BN sheets in toluene and THF without the use of

surfactants to aid individualization. The authors presented physical observation, UV-vis and χ values in conjunction with refractometry are reliable techniques for quantifying the solubility behavior of nanoparticle systems. This work presented an early quantifiable picture of the behavior of BN materials in solvent systems. It was concluded functionalization of BNNTs with stearoyl side groups did not improve the dispersion and solubility when compared with unmodified tubes, in contrast with earlier works. It was shown that dimethylformamide (DMF), MeOH and acetone could be used to temporarily stabilize h-BN platelets. Conversely, McWilliams et al., looked at individualizing and dispersing BNNTs with surfactants. It was shown that high molecular weight, nonionic surfactants suspend the highest quantity of BNNTs while ionic surfactants removed h-BN impurities. These suspensions were characterized using a variety of spectroscopic and photoluminescence techniques. These studies have shown great promise for the development of reliable quantification techniques, but for use in polymeric systems, the use of surfactants and difficult to remove solvents such as DMF are avoided.

Individualization of BNNTs using Superacids: Chlorosulfonic acid

Superacids have been used to individualize BNNTs avoids the use of both surfactants and sonication. Moreover, it has been experimentally shown that chlorosulfonic acid acts as a true solvent for BNNTs. 99% pure chlorosulfonic acid (CSA) has been shown to individually disperse BNNTs. It is theorized that CSA protonates nitrogen atoms, causing BNNTs to have a positive net charge. This charge enables a repulsion between tubes. In this process, BNNT is mixed with CSA at a concentration of 100 ppm and stirred for 24-48 h. Cryo-TEM imaging was used to characterize these BNNT/CSA solutions to support these findings. To remove the CSA, the samples are washed with ethyl alcohol and water and vacuum dried at 35 °C for 48 h.

Wet thermal etching

The wet thermal etching approach follows the same approach as simply oxidizing elemental boron and boron oxide and high temperatures. Wet thermal etching is a scalable, selective method that enables large quantities of BNNTs to be purified at one time. Here, as synthesized BNNTs are introduced into a wet oxygen environment at (hot water sourced at 90 °C) to remove elemental boron and hexagonal boron nitride impurities. Pure oxygen or nitrogen flows through a tube furnace set to a temperature between 500 and 715 °C. Compared with other methods, this method is shown to limit the damage to the BNNT surface. This process was shown to be effective at removing contaminants including h-BN nanoparticle impurities at temperature exceeding 700 °C.

Figure 1. Schematic for purification set-up that is used to purify raw BNNTs. Pure oxygen/nitrogen flows into the tube furnace (7), heated in a flask (5) to 90 °C. An alumina crucible containing BNNT sample is placed within the furnace (7). The furnace (7) is plugged with refractory blocks to minimize heat loss, and left at the maximum processing temperature for 24 h.

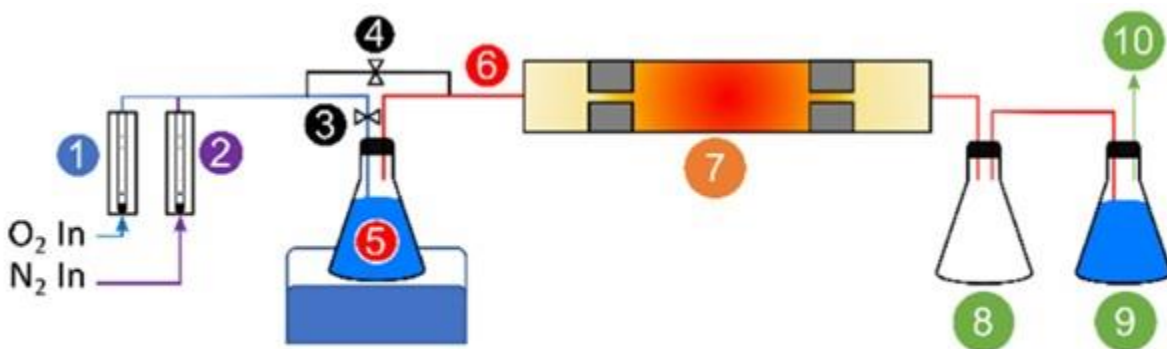


Figure Reprinted (adapted) with permission from (Daniel M. Marincel, Mohammed Adnan, Junchi Ma, E. Amram Bengio, Mitchell A. Trafford, Olga Kleinerman, Dmitry V. Kosynkin, Sang-Hyon Chu, Cheol Park, Samuel J.A. Hocker, Catharine C. Fay, Sivaram Arepalli, Angel A. Martí, Yeshayahu Talmon, and Matteo Pasquali *Chemistry of Materials* **2019** 31 (5), 1520-1527 DOI: 10.1021/acs.chemmater.8b03785). Copyright (2019) American Chemical Society.

Marincel et al., state,

“Pure oxygen and/or nitrogen with a controlled flow rate (using flow meters 1 and 2) flows into the tube furnace (7) via a source of hot water at 90 °C (5) while valve 3 remains open. A bypass valve (4) was used to provide an alternative path for dry oxygen or nitrogen to reach the tube furnace. The stainless-steel tube (6) between the water bubbler and furnace was heated using a heating tape at 90 °C to ensure no loss of steam due to condensation. An alumina crucible containing the sample (h-BN, precipitates, or raw BNNTs) was placed at the center of the tube furnace (7), which was plugged with refractory blocks on both ends to minimize heat loss, for 24 h at the maximum processing temperature. The cooled effluent gas was filtered through water (9) and vented to the atmosphere (10). An empty flask (8) prevented water from (9) from entering the furnace.”

Gas-Phase Purification

Cho et al., took a similar approach developing a simple, scalable one-step process for purifying BNNTs to 85 wt.% using a vertical flow tube operated under pure or diluted chlorine gas flow between 950-1100 °C. This process converts boron and boron nitride platelets into BCl_3 and HCl which can be removed as a gas, leaving pristine BNNTs behind. This process is advantageous over other wet chemical processing techniques as the gas-phase byproducts are entirely soluble in water .

Surfactant and Centrifugation Methods

Ammonium oleate surfactants help improve the stability of BNNTs in solution enabled by non-covalent functionalization on the nanotube surface. Yu et al., synthesized BNNTs via a ball milling and annealing process. 1 mL oleic acid was mixed with 1 mL concentrated ammonia

in 50 mL DI water to prepare the surfactant solution. More recently McWilliams et al., prepared 1 wt.% aqueous surfactant solutions to evaluate the quality and stability of a variety of surfactants for dispersing BNNTs. Surfactants studied include DTAB, CTAC, SDS, Pluronic L81, F87 and 17R4. The samples were bath sonicated and centrifuged. Due to the absorbance region overlapping between surfactants and the BNNTs, the group developed a method using TGA to evaluate the weight corresponding with the surfactant vs the remaining mass of BNNT . Tiano et al., used a co-solvent approach to improve the solubility of BNNTs. For this work, more favorable solvents such as DMAc, DMF and NMP were paired with poor solvents to improve the solubility. BNNTs were suspended in miscible co-solvents were magnetically stirred for up to 96 hours and bath sonicated to exfoliate the bundled nanotubes .

Polymer wrapping

Early research showed solubility of BNNTs could be improved by wrapping with a conjugated polymer, poly(m-phenylenevinylene-co-2,5-dioctoxy-p-phenylenevinylene) (PmPV). This long chain polymer tends to coil into a helical structure, making it easier for the nanotube to wrap the polymer. This enables stronger π - π interactions. These polymer wrapped BNNTs were sonicated in chloroform to break up the tightly bundled BNNTs . Velayudham et al., explored using conjugated polymers poly(p-phenylene ethynylene)s (PPEs) and polythiophene to non-covalently functionalize BNNTs, thereby initiating strong π - π stacking between the polymers and BNNTs.

The authors also used organic solvents such as chloroform, methylene chloride and tetrahydrofuran (THF) to evaluate the stability. Mutz et al., used a similar procedure to non-covalently functionalize BNNTs with stearyl chloride. In these cases, heating the sample to 700 °C removes the polymer, as evidenced by a change in color from yellow to white, coinciding

with complete oxidation (removal) of the polymer and/or solvent. Sang-Woo et al., used copolymers with hydrophilic groups Pluronic P85 and F127 were used to wrap BNNTs and improve the quality of dispersions of BNNTs in aqueous solutions. Triblock copolymer wrapped BNNTs were sonicated for 30 minutes to 1 hour and centrifuged before analysis. Despite the promising evidence of dispersion in aqueous solution, the BNNTs were shortened due to the ultrasonication.

Aerogels

Aerogels are a class of low density solid materials characterized by their large internal surface area, high thermal stability, and small pore sizes. Presently, aerogels can be synthesized from a wide variety of materials using sol-gel techniques, followed by delicate removal of pore fluid via supercritical CO₂ extraction. The supercritical CO₂ extraction process an important development for aerogel development, as it enables liquid to be removed from the pores of the gel, replaced with gas in such a way that the particle network does not collapse due to capillary forces. The most popular aerogels are silica aerogels, with interest in polymer and polymer/clay composites, as well as carbon-based aerogels increasing in recent years. The low density silica aerogels we recognize today were realized by S. S. Kistler in 1931, as he tested the hypothesis that the pore fluid could be removed from the delicate pore structure of the silica jelly using a closed autoclave system to harness a supercritical fluid exchange. It was shown that alcohol replaced with supercritical ether could be used for inorganic aerogels and propane was used to make organic aerogels. It was shown that if the vapor pressure could be exceeded and the temperature remained above critical temperature of the liquid, as the supercritical point is passed, the liquid converts directly into a gas, preserving the delicate silica gel's porous structure, which would not contract due to capillary forces.

The sol-gel process is a widely used method for synthesizing silica aerogels. The process more broadly refers to a process in which a solution “sol” undergoes a sol-gel transition, wherein the solution transitions to a gel, and solvent is removed, leaving a rigid porous mass. It is noted that in a gel, the liquid within the porous network does not flow out. A one phase solution of a precursor, such as silane or metal alkoxides or ceramic oxides in an alcohol and water, in the presence of a catalyst, undergoes a sol-gel transition to rigid two phase system consisting of a solid (silica) with solvent-filled pores. Further, this process is highly customizable and has been used in a variety of ways for aerogel formulation.

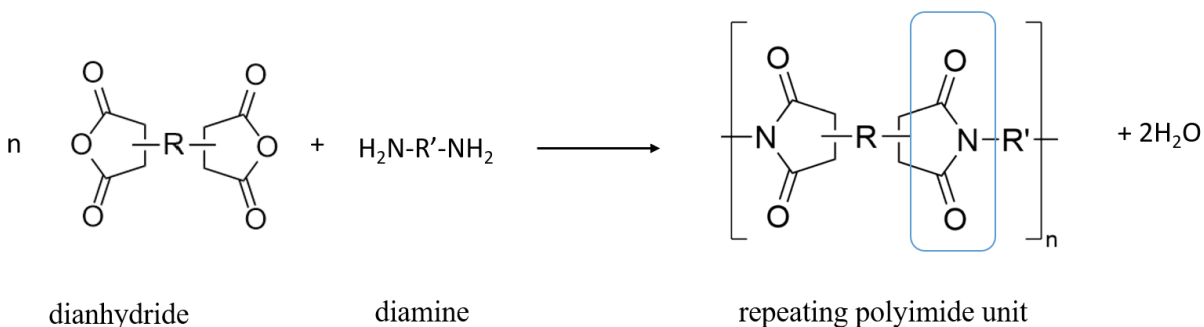
Aerogels can also be made using a variety of organic, cellulose and inorganic polymer systems, if polymerization can occur in highly diluted solutions. Organic aerogels have attracted significant attention, but due to their lower thermal stability at high temperatures. Conversely, inorganic polymer aerogels are high performing polymers with a higher thermal stability and high glass transition temperature, making them favorably suited for aerospace insulation applications.

Polyimide Synthesis: Towards Polyimide Aerogels

Polyimides are prepared from dianhydride and diamine monomers, resulting in a repeating imide structural backbone. Polyimides are characterized by their thermal and oxidative stability thermally due to the stiff aromatic backbones. The benefit of studying polyimide aerogels lies in the fact that the chemistry is well known, with a variety of affordable, widely available monomers available for synthesis. Polyimides are often used in aeronautic and aerospace applications due to their high thermal and mechanical stability, making them optimal for use in harsh environmental conditions. Polyimides are formed via step-growth polymerization via condensation reactions or through addition polymerization.. Polyimide

aerogel chemistry is unique as the monomers used can be tailored towards enhancing certain properties leading to better moisture resistance, flexibility and strength.

Figure 2. Dianhydride and diamine monomer polymerize into polyimide oligomer (of n repeating units), releasing water.



Polyimide aerogel Synthesis: One-step polymerization

First synthesized in 1908, aromatic polyimide aerogels were synthesized by equimolar mixtures of tetracarboxylic acid dianhydride and diamine in the presence of high boiling point dipolar aprotic amide solvents to produce completely cyclized polyimides. This synthesis route did not take off at first, because of limited processing methods, and insolubility due to the backbone rigidity. Due to these complications, a solvent-based route was necessary to process polyimides and that was discovered and popularized by DuPont™ in the 1950's. DuPont commercially produced a polyimide film, known as Kapton based on PMDA and 4,4' diaminodiphenyl ether via two-step polymerization.

Polyimides are characterized by the composition of their main chain, and the interactions between the monomers. They can be made through the reaction of aliphatic monomers, yielding aliphatic (linear) polyimides, through the reaction of aromatic monomers, yielding aromatic

heterocyclic polyimides, or through a combination of aromatic and aliphatic monomers, yielding semi-aromatic polyimides.

Figure 3. Example of a linear polyimide.

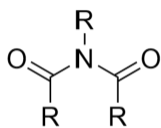


Figure 4. Example of a heterocyclic (aromatic) polyimide. These polyimides are formed by a reaction of aromatic monomers.

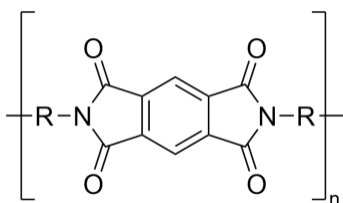


Figure 5. Semi-aromatic polyimide structure. These polyimides are synthesized with one aliphatic monomer and one aromatic monomer.

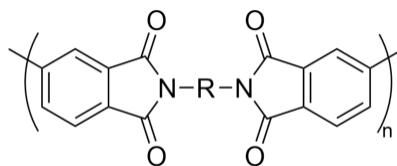
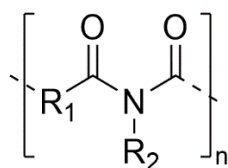


Figure 6. Polyimide is a polymer of imide monomers.



Polyimide Synthesis: Two-step polymerization

The two-step polymerization popularized the use of polyimides, owing to the ability to overcome processing and solubility issues formerly seen with the one-step process. Here, a dianhydride is reacted with a diamine in ambient conditions, in a suitable dipolar aprotic solvent to yield poly(amic acid). The most popular solvent for polyimide aerogel synthesis is n-methyl 2-pyrrolidinone (NMP) but other Lewis-base solvents can be used, including N, N-dimethylformamide (DMF), N, N-dimethylacetamide (DMAc), and tetramethyl urea (TMU). Poly(amic) acid is cyclized, to yield a desired polyimide. This method is highly customizable, but it has been shown that the structure of the diamine and solvent choice impact the reaction rate more significantly than the dianhydride structure, and much research has been conducted to study these structure-property relationships. An example of the two-step process, a pyromellitic dianhydride (PMDA) monomer is reacted with a p-phenylenediamine dianhydride, forming a poly (amic acid). This is followed by the second step where poly (amic acid) is dehydrated under vacuum via chemical vapor deposition, forming a polyimide.

Thermal Imidization of poly(amic acid)

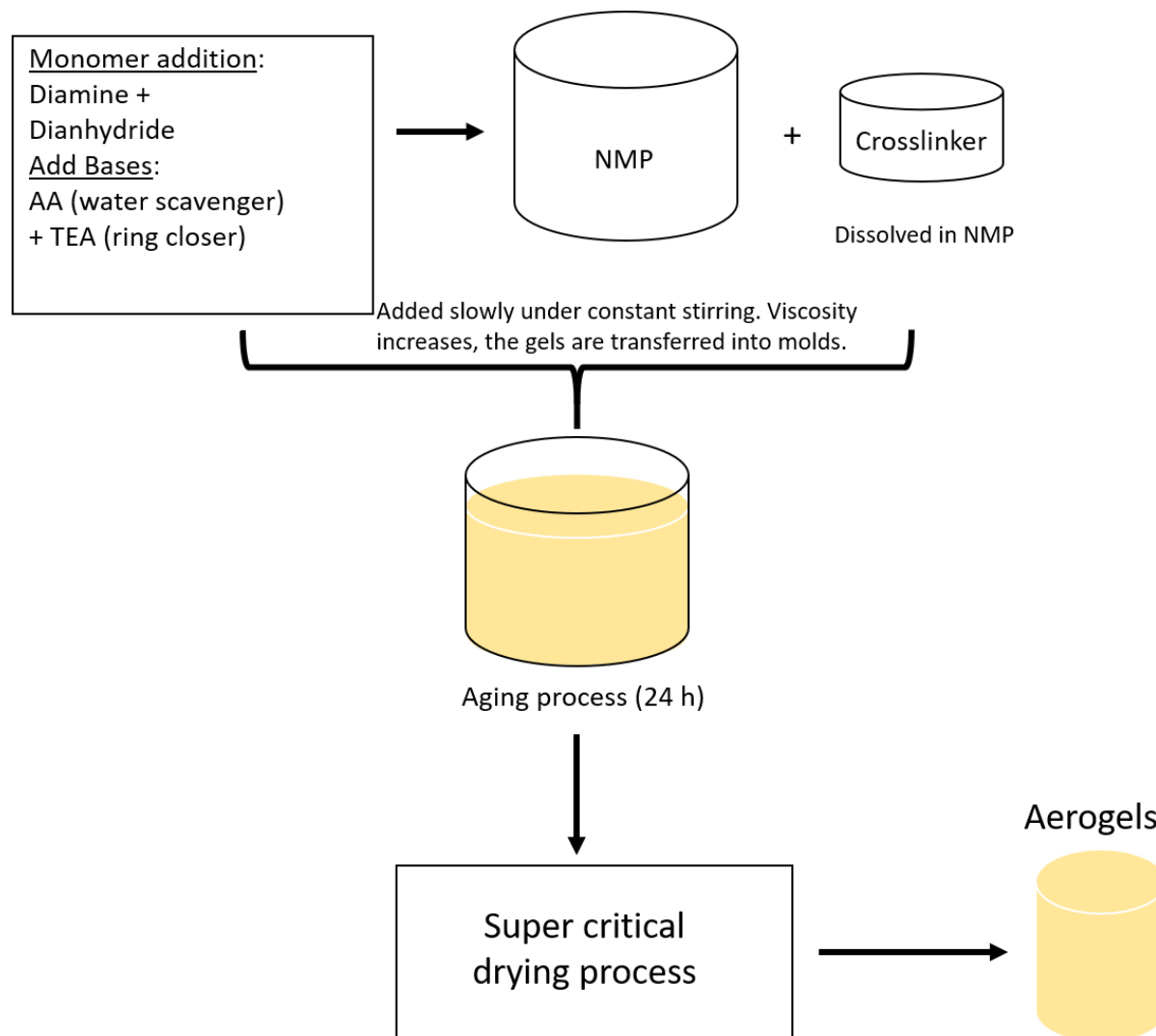
Thermal imidization is the conversion of the poly(amic acid) to a complete polyimide by incremental heating. This route is used for making films or coating forms of polyimides. Poly (amic acid) is cast, and heated between 100-350 °C. The heating cycle selection can be altered to impact the imidization. The completeness and consistency of this process has been debated. This method requires a very concentrated, highly viscous high molecular weight poly (amic acid) solution.

Chemical Imidization of poly(amic acid)

Conversely, low energy chemical imidization methods, occurring at room temperature to yield polyimides and polyimide aerogels have been extensively explored. This method provides a low-energy, time saving route to yield completely imidized polyimide polymers. Endrey et al., employed dehydrating agents acetic anhydride and a basic catalyst pyridine. The procedure is explained as follows: poly(amic) acid film was immersed at room temperature in a benzene solution containing the acetic anhydride pyridine mixture. A time later, the polyimide film is removed and dried. Endrey explored the use of other conversion catalysts including propionic anhydride, n-butyric anhydride and acetic benzoic anhydride. In chemical imidization, the reagents treat poly (amic acid) with aliphatic carboxylic acid dianhydrides and a tertiary amine at ambient temperatures in a process that can be optimized. The tertiary amine reacts with an anhydride, due to its susceptibility to nucleophilic attack. The final polyimide formed is insoluble and precipitates out. If imidization is incomplete, polyimide can precipitate out before all amic groups have cyclized into an imide. Thermal treatments can be used to complete the process. Mary Meador et al., and Haiquan Guo et al., showed complete imidization could be achieved in solution at polymer concentrations as low as 7 wt. % using a combination of diamines and dianhydrides with n repeating units in NMP. Chemical imidization was achieved completely at room temperature using acetic anhydride as a water scavenger, catalyzed by pyridine.

Figure 7. Chemical imidization at room temperature schematic including crosslinker. This synthesis process is highly customizable, but this follows the general formulation of using PMDA and DMBZ as the monomers, crosslinked with BTC. As viscosity begins to increase, and the polymerization process begins, the solution can be poured into molds for an aging

period of 24 h. After aging, the gels go through a series of solvent exchanges to replace the pore fluid (NMP) with acetone.

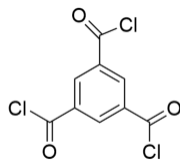


Crosslinked Polyimide Aerogels

Polyimide aerogels are highly customizable as the backbone oligomers can be selected depending on the properties desired. Like altering the monomers, adding crosslinkers can further improve the modulus and flexibility of the otherwise rigid polyimide structure. Finding a chemically suitable and affordable crosslinker has been challenging, as most of the early crosslinkers successfully incorporated for increasing the properties of polymer aerogels were

expensive and not commercially available. Here, 1,3,5-benzene tricarbonyl trichloride (BTC) Polyimide aerogel work includes using crosslinkers such as 1,3,5-triaminophenoxybenzene (TAB), 2,4,6-tris(4-aminophenyl) pyridine (TAPP), 1,3,5-tris-(aminophenyl)benzene (TAPB), or octa(aminophenoxy) silsesquioxane (OAPS). Unfortunately, these crosslinkers are not commercially available or expensive so other alternatives must be established. Mary Meador et al., utilized an amine capped oligomer crosslinked with 1,3,5-benzenetricarbonyl trichloride (BTC) to synthesize a mechanically strong polymer aerogel. This approach combines various properties including low thermal conductivity with excellent mechanical properties as compared with silica and polymer-silica aerogels. Although this aerogel proves to be a cost-effective alternative, its use is limited due to the hydrophilicity that arises in the fabricated polyimide aerogel, due to the hydrophilicity of the carbonyl groups when a BTC crosslinker is added.

Figure 8. Benzenetricarbonyl trichloride (BTC) was used as a crosslinker to fabricate polyimide aerogels. BTC is a cost-effective alternative crosslinker. Fabricating polyimide aerogels with BTC gel faster (5-20 minutes, compared with an hour or more) than alternatives (TAB or OAPS) and have comparable onset of decomposition. However, increased hydrophilicity remains a challenge that isn't overcome by altering the backbone structure of the oligomers.

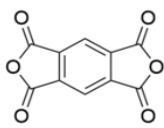
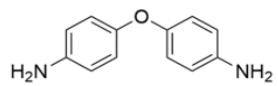
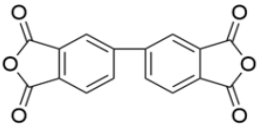
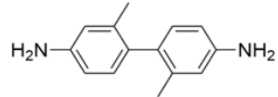
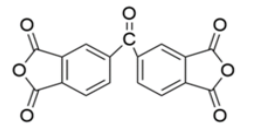
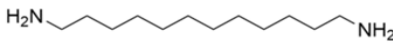


Altering the Backbone Chemistry

It has been shown that the backbone chemistry has a more significant structure-property relationship than the crosslinker, so significant work has been done to develop polyimide

aerogels with improved properties based on the backbone chemistry. Haiquan Guo et al., recently explored altering the oligomer to reduce shrinkage and moisture uptake by incorporating 1,12-docyl diamine (DADD) with DMBZ into the diamine and 3,3',4,4'-biphenyltetracarboxylic dianhydride crosslinked with 1,3,5-triaminophenoxybenzene (TAB). Here it was shown that improvements could be made to the flexibility and moisture resistance at the expense of the transparency.

Table 1. Polyimide oligomers are synthesized using a combination of, but not limited to, the following monomers. Dianhydrides frequently used as cited in this dissertation include (top to bottom) PMDA, BPDA, and BTDA. Diamines frequently used include (top to bottom) aromatic ODA and DMBZ, and aliphatic DADD. Each of these monomers are selected due to the specific properties they impart on the resulting aerogels.

Dianhydride	Diamine
	
	
	

Polyimide aerogels are generally yellow to brown and hazy. Stephanie Vivod et al., explored making polyimide aerogels more transparent and less yellow by combining dianhydrides pyromellitic dianhydride (PMDA) with 4,4'-hexafluoroisopropylidene di(phthalic

anhydride) (6FDA) and DMBZ as the diamine crosslinked with BTC. The authors predicted adding fluorine atoms or $-CF_3$ groups, weak electron donating groups would suppress the charge transfer interactions would thereby reduce the yellowing and improve the transparency of the synthesized aerogels. In this study, eighteen batches of polyimide aerogels were selected, the polymer concentration varied from 7-10 wt. % altering the concentration of 6FDA in place of PMDA. It was found that the formulation containing 25 mol % 6FDA has the highest optical transparency, which was attributed to the smaller, more uniform pore distribution. The formulation containing 50 mol % 6FDA had a lower optical transparency and a broad pore size distribution. The formulation containing 0 mol % 6FDA was intermediate between the two. The authors concluded the pore size distribution and surface area may have a bigger impact on the optical transparency. Additional work is ongoing to reduce the yellow color of the polyimide aerogel.

BN as Porous Aerogels and as Reinforcement

It is known that reinforcement such as crosslinking within a polymer network enhances structural properties. By reducing the motion of polymer chains, beneficial structural properties are enhanced, increasing tensile strength and flexural modulus, and temperature stability. Commercially available silica and polyimide aerogels are high surface area and low density, with tailorable properties. Aerogel reinforcement has been studied extensively for carbon nanotubes (CNTs), but applications are limited due to the resulting materials being opaque and black. BN has been studied as a reinforcement material, and Porous BN aerogels material can be synthesized via reacting complexes of boron oxide and amines with nitrogen containing gases, or by carbothermic conversion of graphene aerogels via vapor phase reaction. Song, Yangxi et al., synthesized BN aerogels using a carbon aerogel template via a template assisted, catalyst-free

method ultimately synthesizing an aerogel with a mass density lighter than air (1.225 kg/m^3). This template assisted method, using a borazine precursor, allows BN aerogels to copy the carbon structure and grow on the carbon substrates via template assisted chemical vapor deposition (CVD). The resulting BN aerogels are hydrophobic and oleophilic and have a continuous 3D network with the desired high specific surface area and low density. These properties were shown to be controllable across a large system. Due to their inherent chemical and thermal stability, aerogels with a three-dimensional, highly crystalline sp^2 -bonded B-N have also been synthesized via a carbothermic reduction process. A freeze casting process was utilized to fabricate non-covalent functionalized boron nitride nanosheets (BNNS) and polymer aerogels. Despite these successes, the resulting BN based aerogels remain brittle and rigid, and are currently limited to few applications.

Boron Nitride Nanomaterials as Nanofiller into Polyimide Aerogels

Polyimide aerogels are a unique group of lightweight, low density solids classified by their unique nanoporous structure. The chemical structure, backbone and crosslinker of polyimide aerogels can be modified extensively to yield a variety of properties. Polyimides are formed by a two-stage, step-growth condensation polymerization of diamines and dianhydrides. This forms intermediate poly (amic acid) which is then chemically or thermally imidized. In this chapter, a chemical imidization process is used and the entire process is carried out at ambient temperatures. Once the gels have aged, the fluid is extracted via a supercritical fluid extraction process to produce low density, nanoporous aerogels. Here, unfunctionalized boron nitride nanostructures ($1\mu\text{m}$ or $<150 \text{ nm}$ in diameter h-BN platelets, Sigma Aldrich) and BNNTs (BNNT LLC, Newport News, VA) were used as fillers for reinforcement in the synthesis of polyimide aerogels. The objective of this research was to study the feasibility of using favorable

solvent systems such as NMP, to stabilize the BN materials using liquid processing techniques. In this work, we looked for obvious signs of incompatibility such as h-BN/BNNT settling and/or incomplete gelation.

Boron nitride nanomaterials are insoluble in all solvent systems, and like many other unfunctionalized nanomaterials, do not remain in suspension for long periods of time. BNNTs specifically do not individualize without chemical modification. Instead, due to their strong Van der Waals forces, they form large clumps resistant to ultrasonication in non-polar solvents, and swell in alcohols. Despite their low solubility, some research has been done to show BNNTs can be slightly disaggregated and suspended for short periods of time in polar aprotic solvents such as N,N-dimethyl formamide (DMF), N-methyl pyrrolidinone(NMP), and N,N-dimethyl acetamide (DMAc). To avoid these challenges, we used ultrasonication to disaggregate h-BN/BNNTs in NMP before performing polyimide synthesis. We explored direct addition of unfunctionalized h-BN and BNNTs, relying on the higher viscosity of the gelation solution to “trap” particles in suspension. h-BN/BNNTs were suspended in NMP in desirable concentrations to create a stock solution (5 or 10 mgmL⁻¹). This solution is sonicated briefly at low power, (20 W for 10 minutes, pulsed), and set aside before polyimide aerogels were fabricated.

Polyimide Aerogels

This work established that h-BN could be suspended in NMP to yield quasi stable colloidal solutions that can be used for created BN incorporated polyimide aerogels. This background provides a potential route for future applications wherein functionalized BNNTs can be uniformly dispersed at varying concentrations into the polyimide pore structure and backbone to improve modulus, increase onset of degradation, and improve thermal properties.

Polyimide aerogels were synthesized via chemical imidization in diluted systems to yield low density structurally robust materials. The synthesis procedures were performed at ambient temperatures in a ventilated hood; using methods previously reported via Vivod, 2019. These methods were modified as necessary and reproduced as follows:

Mass was measured using an XSE 104 analytical balance from Ohaus Scientific, Inc., and volumetric measurements were taken using an adjustable volume pipettor with a volumetric range of 0.5-5.0 mL with an accuracy of 0.5 to 2.0 %. Reactions were performed in glass jars using magnetic stir bars until desired viscosity occurred. The viscous fluids were then poured into various molds and covered with parafilm, reducing atmospheric exposure to water vapor during gelation. Each batch of viscous gels were poured into molds selected for the type of analysis being performed. 20 mL syringes were used to create cylindrical samples for chemical analysis, 9 mm by 9 mm square molds were used for optical and thermal testing.

Preparation of Polyimide Aerogel loaded with h-BN

For polyimide aerogel synthesis, a 10 mL volumetric pipette was used with plastic pipette tips supplied by Fisher Scientific. Polyimide aerogel synthesis was conducted in 100 and 200 mL glass jars. Large hexagonal stirbars were used to stir the viscous solutions until gelation commenced. Gels were poured into silicone molds and left to age. Upon completion of the full aging process, the gels were removed from the silicone molds and submerged in solvent, in Tupperware vessels large enough to contain 4x the volume of pore solvent. The vessels are covered with matching Tupperware lids to keep the solutions air-tight.

Materials

Monomers 2,2-dimethylbenzidine (DMBZ), pyromellitic dianhydride (PMDA) and crosslinkers 1,3,5- benzene tricarboxyl trichloride (BTC) were purchased from Sigma-Aldrich.

Bases Acetic anhydride (AA) and triethylamine (TEA) were purchased from Sigma-Aldrich. Hexagonal boron nitride nanoparticles, (h-BN) <150 nm were purchased from Sigma-Aldrich. After being exposed to the atmosphere, dianhydrides required vacuum drying at 120 °C for 24 h. All other materials listed above were used as received. Unrefined BNNTs were supplied by BNNT Materials, LLC (Newport News, VA).

BNNT Refinement via Thermal Oxidation

Unfunctionalized boron nitride polymorphs, including oxidized and washed BNNTS (OW-BNNTs), as-received purified BNNTS (AR-BNNTs), and h-BN nanoparticles (<150 nm) were suspended in NMP via probe sonication. A desired mass of BN nanoparticles were weighed and added to a stock solution of NMP. The reaction vessel (~50 mL glass jar) was submerged into an ice bath to control temperature for the duration of the sonication. The nanoparticle/NMP solution was probe sonicated at 20 W power for 10 minutes, pulsed for 10 seconds on and 5 seconds off. These nanoparticle/NMP solutions were made to evaluate (1) the changes in gelation behavior by adding nanomaterials (2) the aggregation behavior in solution, if obvious to the eye. The suspended solution was further diluted to be used as a cosolvent during the synthesis of polyimide aerogels. Initially, two nanoparticle/NMP stock solutions were prepared. The first solution concentration contained 10 mg/mL h-BN/NMP, and the second stock concentration was 10 mg/mL OW-BNNT/NMP. The stock solutions were used to make further dilutions at 5 mg/mL for each stock solution. These stock solutions were further diluted into a total volume of ~90 mL NMP during the fabrication of polyimide aerogels, to yield polyimide aerogels. In this batch of aerogels, 5 formulations were prepared containing 0% BN nanoparticles as the control, 0.55 wt. % h-BN nanoparticles, 1.11% h-BN nanoparticles, 0.55wt. % OW-BNNTs, and 1.11 wt. % OW-BNNTs in the total polymer.

OW-BNNT Preparation

~100 mg of unrefined BNNT fluff was placed in a ceramic crucible and heated in a Thermo Scientific Thermolyne benchtop muffle furnace at 800 °C for 1 h to oxidize contaminants, removing unreacted B and boron oxide (B_2O_3). This leaves a bright white bundle of BNNTs. After 1 hour, the oxidized BNNTs are left to cool until the unit reaches ambient temperature (25 °C). The oxidized BNNT fluff is then placed into a large glass beaker (500 mL) with >400 mL of warm water. A stirbar is placed in the solution which is subsequently covered with parafilm and stirred vigorously for 48 h to break up large clumps. The water is replaced with >200 mL of EtOH and stirred for an additional 24 h. The oxidized BNNTs are filtered using a Buchner set up and rinsed three to five times in DI H_2O , and oven dried at 100 °C for 1-2 h to remove remaining solvent before use, yielding OW-BNNTs.

Methods

Preparation of Polyimide Aerogels, BTC Crosslinks

A 1,3,5-benzenetricarbonyl trichloride (BTC) crosslinker formulation was used to form mechanically strong polyimide aerogels. BTC was selected due to its commercial availability, and well established backbone chemistry. We also selected this formulation due to its reliability and fast gelation rate as we anticipated solely studying the impact of boron nitride nanomaterials on the structure. Here, 2,2'-dimethylbenzidine (DMBZ) was used as the diamine and pyromellitic dianhydride (PMDA) was used as the dianhydride to synthesize the polyimide oligomers. The oligomers ($n=60$) were then crosslinked with BTC to form gels. The concentration of the total polymer in the gelation solution was held constant at 7 wt. %. Repeating units within the oligomer unit was held constant at 60. This formulation was utilized

to establish control parameters, with special attention towards chemical and mechanical properties.

While working to evaluate low concentrations of BN nanoparticles in solution to evaluate particle stability in solution and optimize on gelation time, polyimide aerogel formulation was held constant, and the type of boron nitride nanomaterial and concentration added to the gelation solution were altered. H-BN (<150 nm) platelets and oxidized and washed BNNTs (OW-BNNTs) were. Further qualitative work was done to study particle stability in NMP solutions only.

h-BN and BNNT Suspensions

To prepare control polyimide aerogels, 7 wt. % polyimide aerogel formulations were prepared in varying molds without the addition of BN nanoparticles. To prepare polyimide aerogels with h-BN nanofiller, a 5 mg/mL suspension of h-BN in NMP was prepared. To prepare a 5 mg/mL suspension of h-BN in NMP, 100 mg of h-BN nanoparticles (<150 nm) were weighed and added to 20 mL of NMP. The solution was ultrasonicated at 20 W in a probe tip sonicator for 10 minutes (Pulse 10 seconds on / 5 seconds off). The temperature was controlled by submerging the reaction vessel in an ice bath. Likewise, a 10 mg/mL suspension of h-BN nanoparticles (<150 nm) was prepared, adding 200 mg of h-BN nanoparticles to 20 mL of NMP. This solution was likewise ultrasonicated at 20 W using a probe tip sonicator for 10 minutes. (Pulse 10 seconds on / 5 seconds off). A 10 mg/mL BNNT suspension was prepared following the same manner as above, and further diluted to yield a 5 mg/mL suspension. The h-BN/NMP or BNNT/NMP solutions were diluted with a volume of NMP under constant stirring before the addition of DMBZ, preceding the polymerization and subsequent gelation procedure.

Synthesis/Preparation of Crosslinked Monoliths

Polyimide aerogels were prepared based on a formation of 100 mol % PMDA, $n = 60$ and a polymer concentration at 7%. DMBZ was used as the diamine and BTC was used as the crosslinking monomer. The formation was produced as follows. 3.76 g (17.7 mmol) DMBZ was dissolved in 80 mL NMP under constant stirring. Once fully dissolved, 3.84 g (17.6 mmol) PMDA was added under constant stirring, until fully dissolved. 13.32 mL Acetic anhydride (AA) followed by triethylamine (TEA) (2.45 mL) was added and stirred until homogenously mixed. The solution is left to mix for 15 minutes. Under constant stirring, a solution containing 0.0512 g (0.19 mmol) BTC dissolved in 5 mL NMP was added. Immediately after mixing, the solution is poured into molds. Within one hour, the solution will begin to crosslink and form gels. The gels are covered and left to age for 24 h before extraction. After the gels are aged, they are extracted into 75% acetone in NMP and soaked for 24 hours. This is followed by three 24 h solvent exchanges in 100% acetone. The pore fluid is then removed from the gels via supercritical solvent extraction. This process includes multiple cycles of soaking and rinsing the gels in subcritical and supercritical CO₂. This process is extensively documented by Meador et al.

Supercritical Fluid Extraction

Supercritical Fluid Extraction is the process by which fluid-filled gels are converted to aerogels. This involves multiple cycles of subcritical and supercritical CO₂ soaking and rinsing. The gels were submerged in acetone in a sealed chamber at 78 bar and 25 °C. The chamber was then set to soak for 30 min followed by a subcritical liquid CO₂ flush equal to the volume of the chamber and repeated four times. Then the temperature in the chamber was ramped to 35 °C to reach a supercritical state of CO₂ and held for 30 min followed by slow venting (10 g/min) for

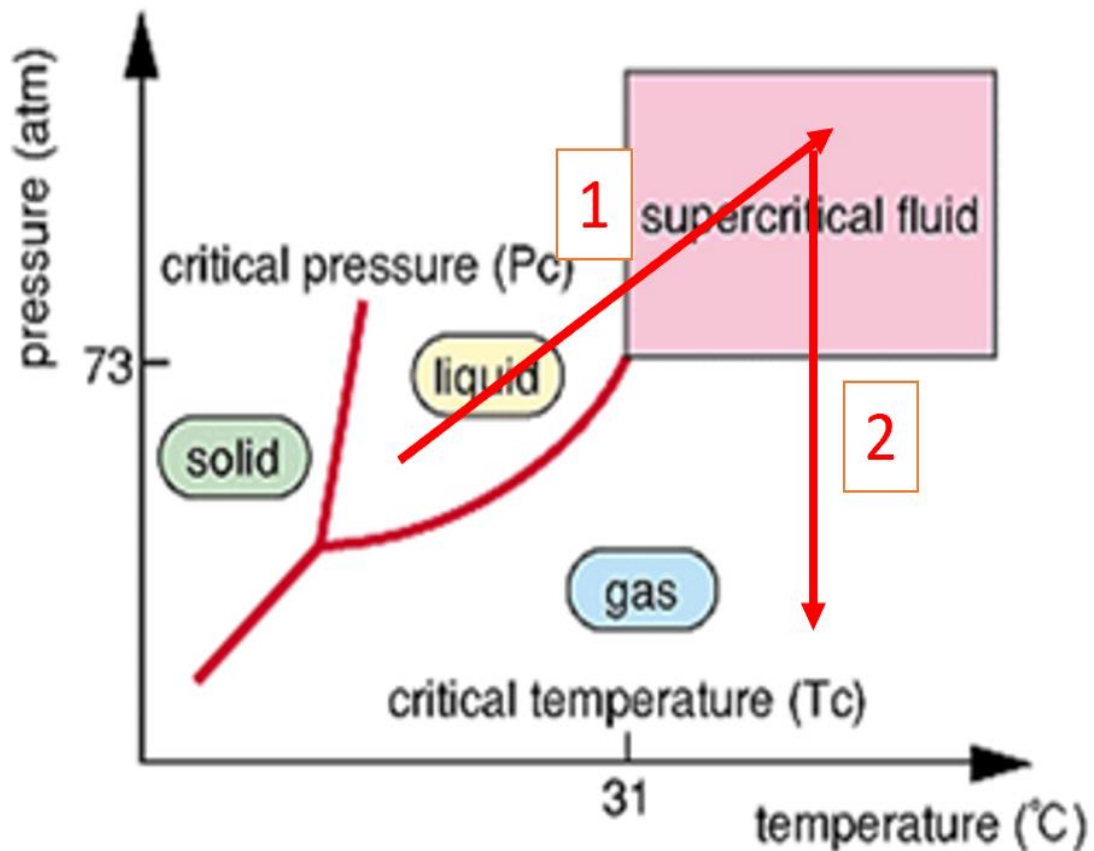
approximately 2 h. This is followed by vacuum drying overnight at 75 °C to remove any residual acetone. The Supercritical Fluid Extraction process can be explained as follows.

Liquid CO₂ supercritical fluid extraction (SFE) is performed via a fully automated process, using Wonderware software in a multi-chamber high pressure system (Accudyne Industries, LLC). All aerogels fabricated and referenced within this dissertation were prepared at NASA Glenn Research Center (Cleveland, Ohio). After aerogels are fully exchanged into acetone, they are exchanged one more time into fresh acetone, and submerged into a stainless steel vessel. The steel vessel is rated for 300 psi/100 °C. During the first phase of the supercritical fluid exchange process, the vessel pressure is increased to 78 bar at ambient temperature (~25 °C) and the acetone is exchanged with liquid CO₂, replacing the pore fluid. The sealed vessel remains at this temperature and pressure for 30 minutes and drained at a controlled rate of 9 g/minute, strictly controlled by the automated software, based upon a specific weight corresponding with the full weight required to replace contaminated CO₂ with clean CO₂. This process is cycled four times, to ensure all acetone is removed from the pores of the gel and replaced with liquid CO₂. The temperature is then increased to 35 °C and pressure is increased to 90 bar, above the supercritical point of CO₂ (above 73 bar and 32°C to convert the liquid CO₂ directly to supercritical CO₂ without crossing phase boundaries. The reason for going through this extensive process is to avoid building interfacial pressures inside the system that lead to pore collapse due to surface tension and capillary forces. When gels are dried at ambient pressures and temperatures, the pores collapse within an aerogel, the gel densifies and becomes brittle and weak. These densified materials are often characterized as xerogels. Once the supercritical phase is reached, while the temperature is maintained the pressure is slowly decreased. The CO₂ within the vessel and the pores of the aerogel is transitioned to the gas phase. When the process is over,

the vessel is opened and the gaseous CO₂ within the pores can be exchanged with air, yielding aerogels. The nanoporous aerogels are dried in a vacuum oven at 65 °C to remove any solvent.

Figure 9. The figure depicts the temperature vs pressure diagram for carbon dioxide.

Additionally, the supercritical fluid exchange process followed for drying aerogels is depicted using the red arrows. (1) liquid CO₂ is converted to supercritical fluid by increasing the temperature and pressure above the supercritical point, avoiding the phase boundaries, and thereby capillary forces. (2) The supercritical fluid is then converted to gas, and the pressure is reduced to ambient pressures, temperature is reduced and the vessel can be opened, leaving low density, nanoporous aerogels.



General Characterization Methods

Skeletal density of the specimens was measured using 1340 helium pycnometer. Scanning Electron Microscopy (SEM) was performed on a Zeiss Auriga field emission microscope after sputter coating samples. Fourier Transform Infrared Spectroscopy (FT-IR) was conducted using an Agilent FT-IR with a single point ATR detector. Small area X-Ray Photoelectron Spectroscopy (XPS) was conducted using the Thermo Scientific Escalab Xi+ with an Al $K\alpha$ source (200 μm).

Table 2. 7 wt. % polyimide aerogel formulation parameters.

Stock h-BN in NMP ($\text{mg}\cdot\text{mL}^{-1}$)	stock BNNT in NMP ($\text{mg}\cdot\text{mL}^{-1}$)	Vol BN solute (mL)	Concentration hBN/NMP gelation solution ($\text{mg}\cdot\text{mL}^{-1}$)	Average Density (g/cm^3)
0	0	0.00	0.00	0.1070
5	0	10	0.56	0.0890
10	0	10	1.11	0.0910
0	10	10	1.11	0.1280
0	5	10	0.56	0.0750

Density

Aerogel density was measured manually in triplicate using calipers, and an average was taken over several monoliths made with the same formulation/ loading of nanoparticle. All aerogels had an average density ranging from ~ 0.07 ~ 0.10 g/cm^3 .

Spectroscopic Analysis: XPS Measurements

X-ray photoelectron spectroscopic spectra were collected via an Thermo Scientific Escalab Xi+ Microprobe. Survey scans and high resolution surface elemental analysis was conducted using a monochromatic Al $K\alpha$ monochromator with a spot size ranging from 200-500 μm . Due to the insulating nature of all samples (Polyimide aerogel monoliths and BN powder samples) a low-energy electron flood gun was used to compensate for charging at the surface.

All samples (polyimide and silica aerogel monoliths and BN nanopowder samples) were adhered to carbon tape or double sided copper tape, which was then adhered to the sample holder before analysis.

SEM Measurements

Scanning electron microscopy (SEM) was conducted on a Zeiss Auriga FIBSEM to obtain micrographs of the pore structure of polyimide aerogel samples. The samples were sputter coated with a conductive material (gold) in a thin ~10 nm layer and adhered to Lacey carbon grids.

Figure 10. Polyimide aerogels were sputter coated in a thin ~10 nm layer and adhered to Lacey carbon grids. The resolution of the micrograph is 200 nm showing the unique nanoporous structure of polyimide aerogels. The pore structure can be altered by varying the monomers, their concentration, as well as the crosslinkers. We predict nanoparticles can be trapped in the nanosized pores, and various resulting properties can be characterized.

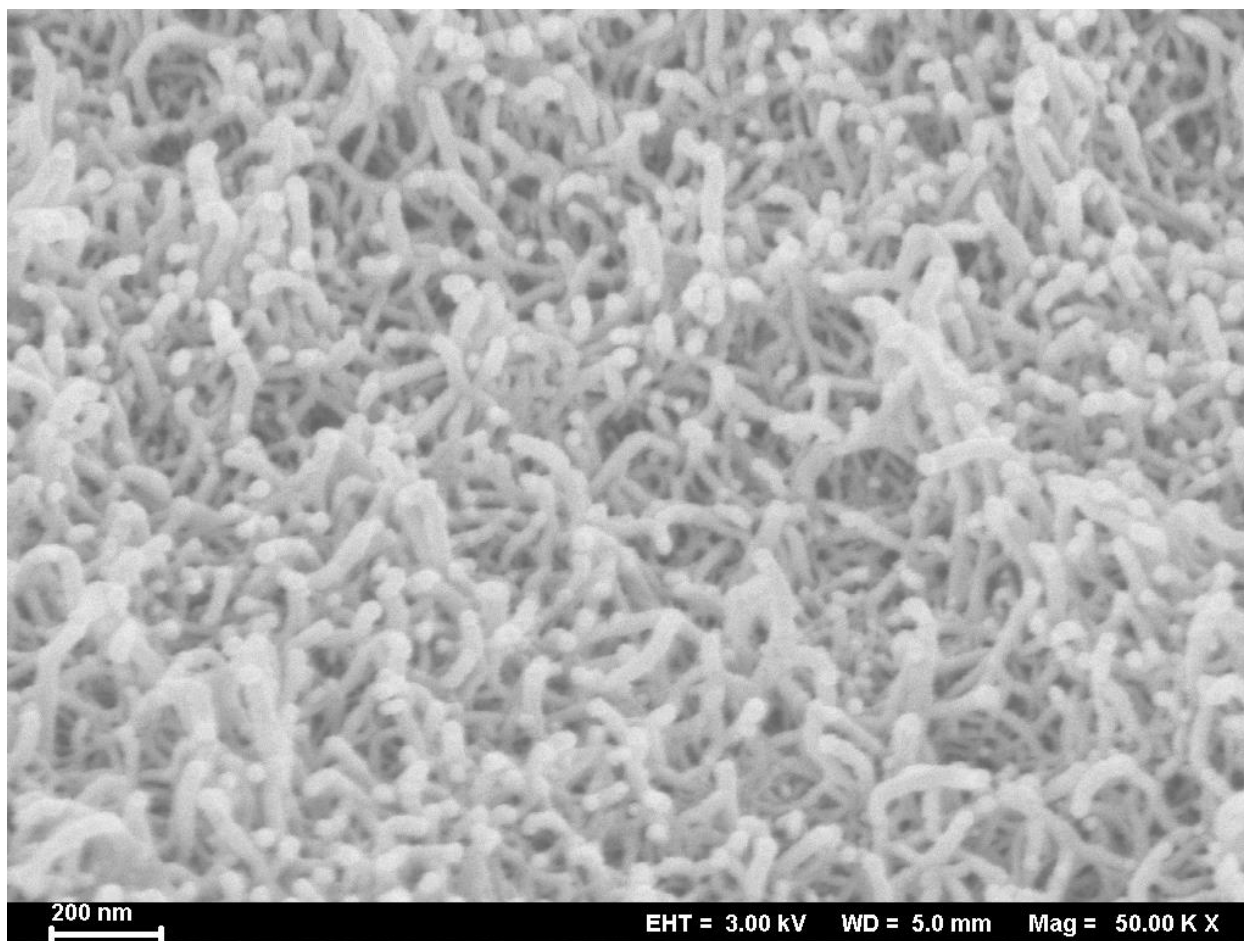
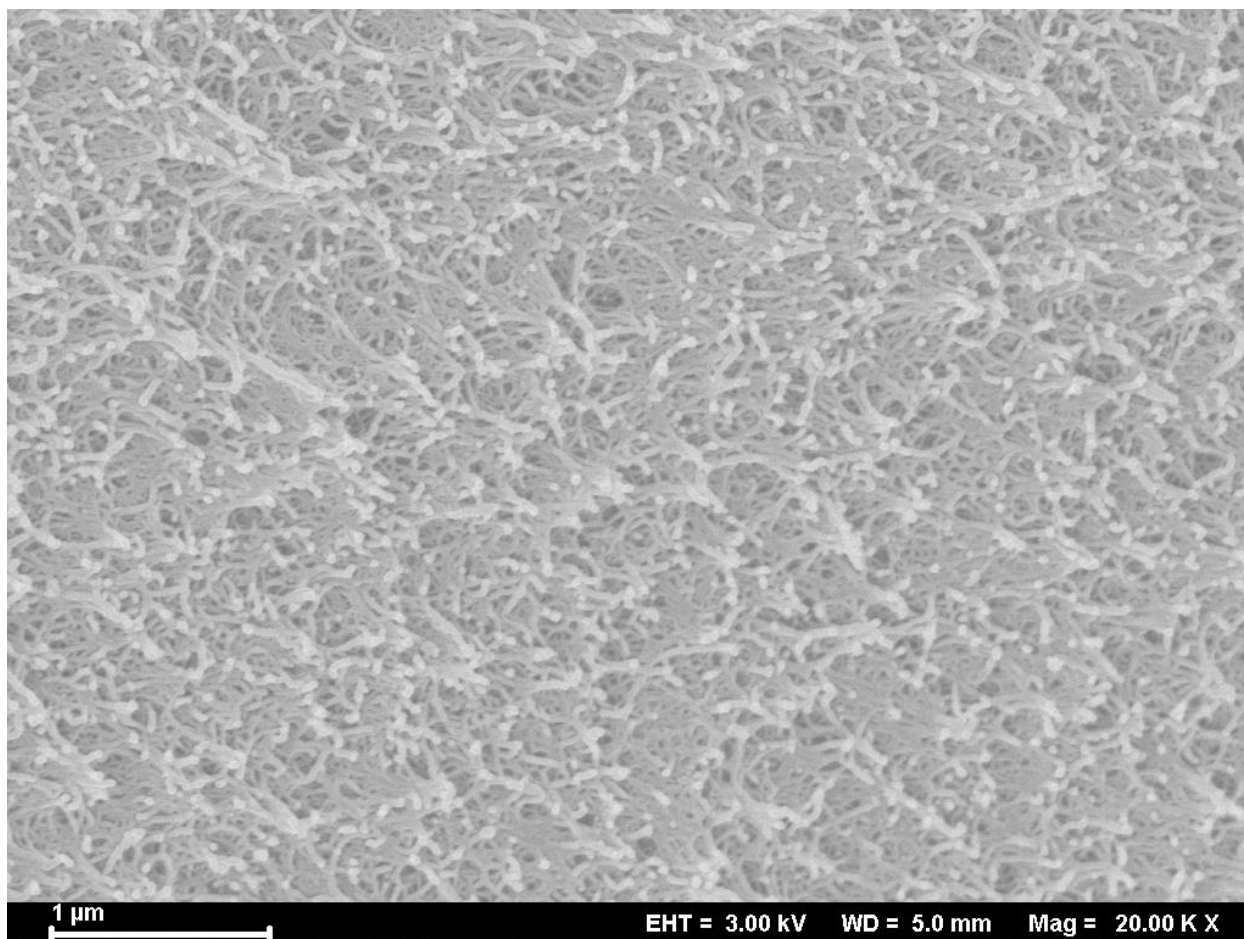


Figure 11. A representative micrograph of the polyimide aerogel 7 wt % formulation synthesized in this dissertation.



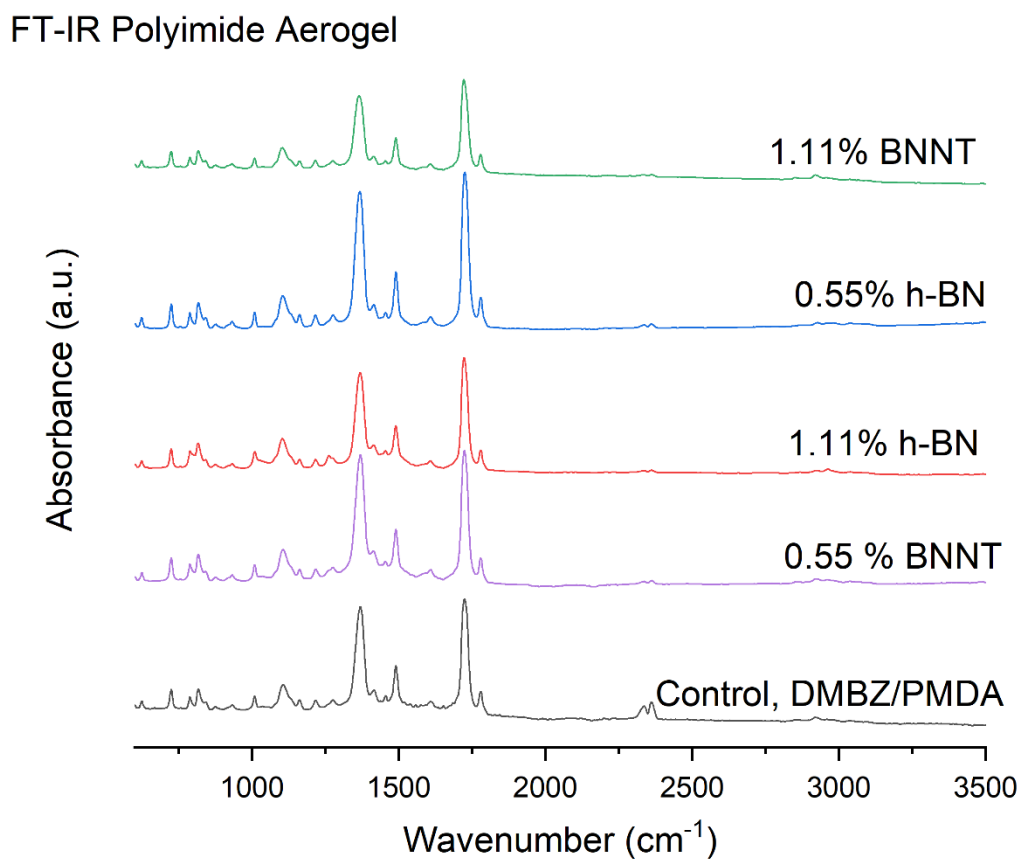
FT-IR Spectroscopic Measurements

Fourier Transform Infrared Spectroscopy was used as surface characterization technique for boron nitride polymorph samples as well as polyimide aerogels. Measurements were conducted on an Agilent Nicolet FT-IR with a single point detector. Powdered samples were pressed directly between the crystal and a flat tip for chemical identification of functional groups, and characterization of the vibrational and rotational energy modes of the BNNT structure. Spectra were collected for all samples from 400-4000 cm^{-1} . Either 20 or 100 scans were collected at 1 sensitivity.

The spectra contain characteristic bands correlated with polyimides. This includes peaks at 1367 cm^{-1} (ν C-N, imide), 1719 cm^{-1} (symmetric ν imide, C=O), 1774 cm^{-1} (asymmetric ν

imide, C=O), and aliphatic C-H stretching vibration correlate with peaks at 2925 and 2854 cm^{-1} . The peak in the control sample, DMBZ/PMDA at $\sim 2300 \text{ cm}^{-1}$ can be assigned to C-C stretching.

Figure 12. FTIR Spectra of polymer aerogels formulated with a 7 w/w polymer concentration, n=60.



Contact Angle Measurements

Static contact angle measurements were taken using the Sessile drop goniometry technique, with water as the probe liquid. The hydrophobic nature of BN nanomaterials was expected to increase the contact angle, but due to the low concentration of nanofiller within the

pore structure(0.55-1.11 wt %), the hydrophilic nature of the polyimide, (crosslinked with hydrophilic BTC,) dominated the hydrophilicity.

Figure 13. Contact angle measurements. All samples are slightly hydrophilic.

Static Contact Angle (water)

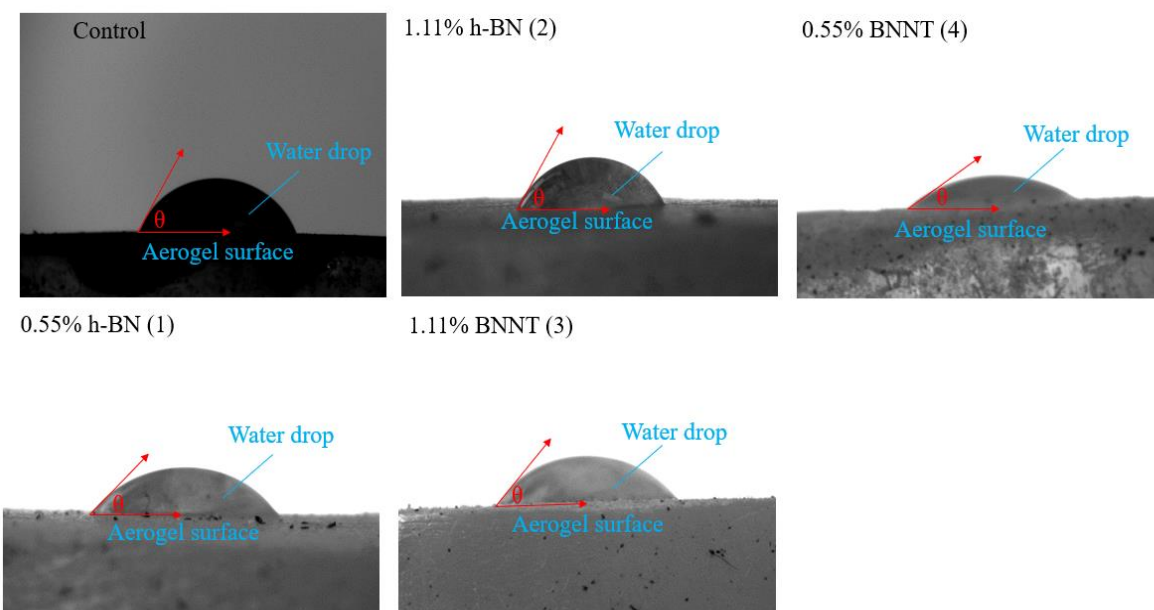


Table 3. Contact angle measurements for polyimide aerogels. Addition of BN nanomaterials did not improve hydrophobicity, despite hydrophobic nature of unmodified BNNTs. Due to the low concentration added, the polymer backbone composition has a greater impact on the properties in these studies.

Sample	Angle ($\theta^\circ \pm 3^\circ$)
Control	70
0.55% h-BN	70
1.11 % h-BN	55
1.11 % BNNT	56
0.55% BNNT	44

Static Thermogravimetric Analysis

Static thermogravimetric Analysis (TGA) was investigated in an inert atmosphere using a Mettler Toledo TGA. Analysis was conducted on a Q500 TA instrument using 5-100 mg of solid under both air and N₂, at a controlled heating rate of 5 °C/min. Thermal analysis was measured to determine thermal decomposition via weight change of material at increasing temperatures from ambient to ~730 °C (Figure 14). The onset of thermal oxidative decomposition for each sample was between ~510 -517 °C, as decomposition was primarily dominated by the polyimide chemistry. Likewise, all samples were analyzed in an inert N₂ atmosphere, showing weight loss of 40% for all samples. Char yield (residual weight, including carbon) is determined as 60% under nitrogen at 735 °C.

Figure 14. TGA of polyimide aerogels run in nitrogen, ramp rate 5 °C/minute. This TGA curve shows the char yield, as defined here as the mass remaining at 750 °C to be ~60% for all samples. (Note: sample 1.11% h-BN (blue) was conducted from 0-750°C, so a ~3 C mass loss is accounted for in the graph here.)

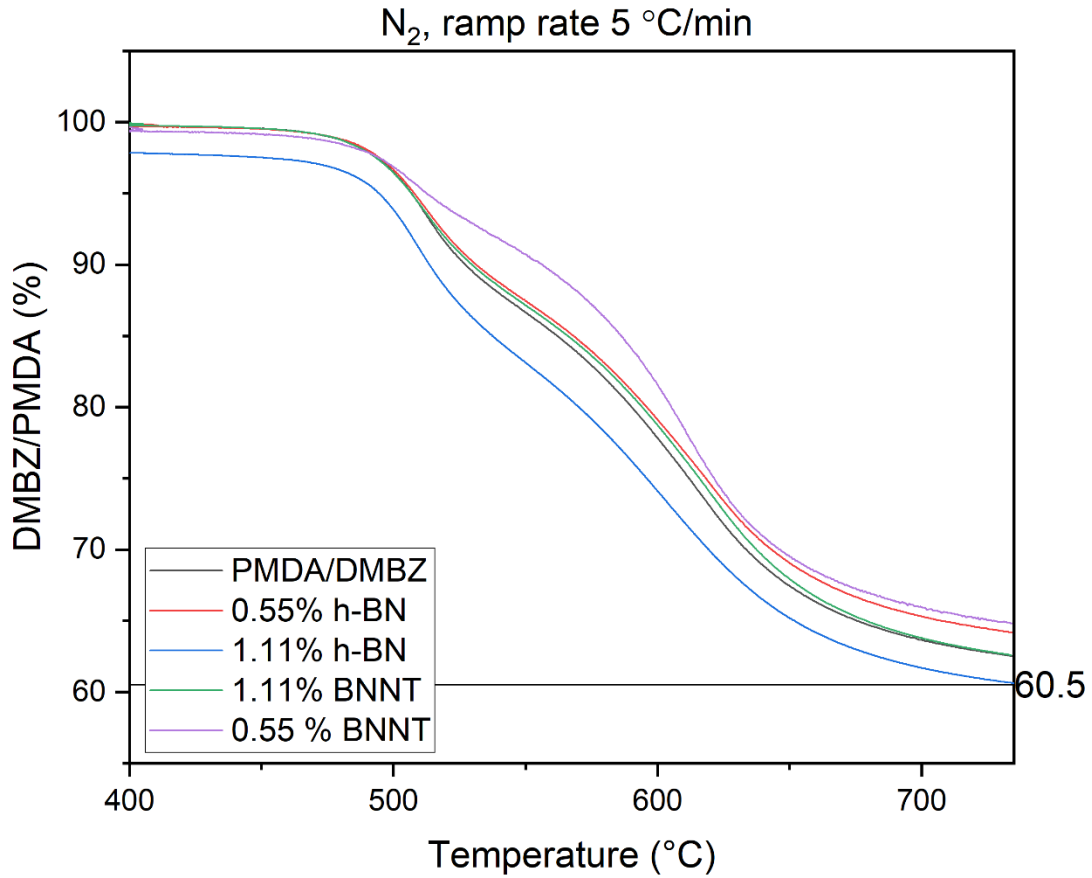


Figure 15. Composite graph of representative TGA curves from the study in an oxidative environment, the onset of thermal decomposition for all samples was calculated between ~515-530 C. The onset of thermal oxidative decomposition is slightly higher for sample. This may be due to the presence of boron nitride nanoparticles.

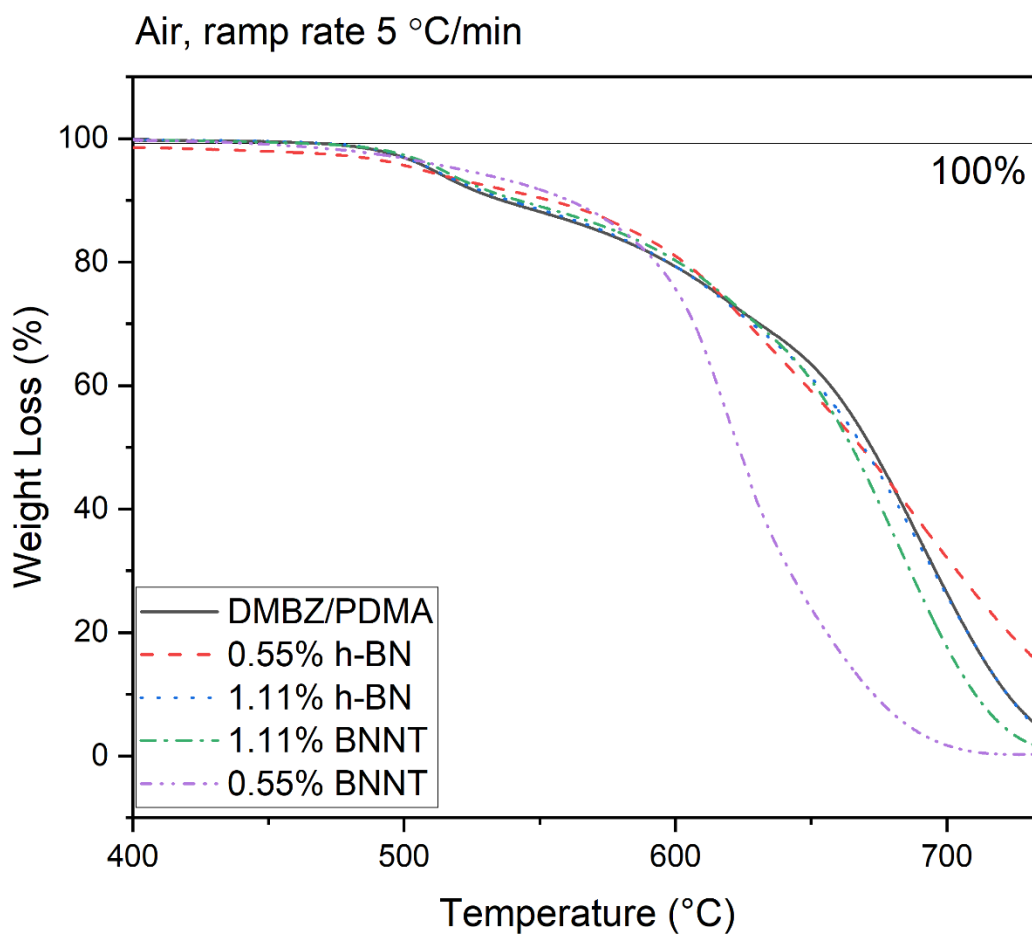


Figure 16. Onset of decomposition was quantified as the 5% mass loss was calculated for the control sample, 7 wt % DMBZ/PMDA was calculated to be 510 C.

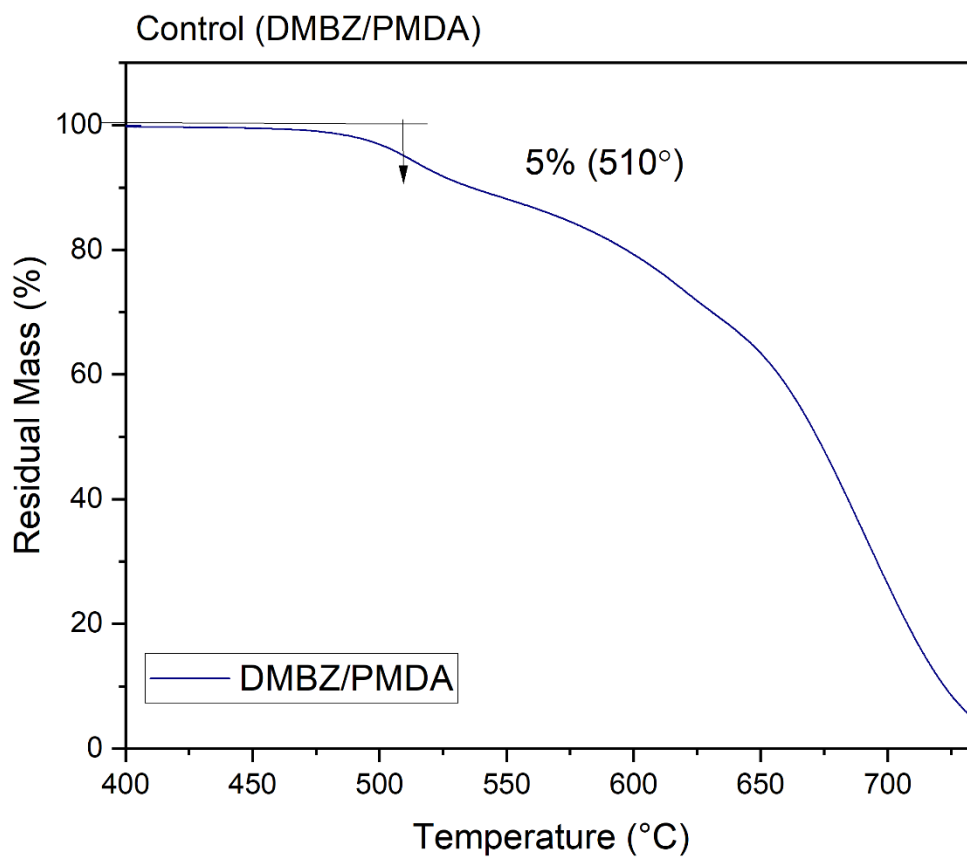
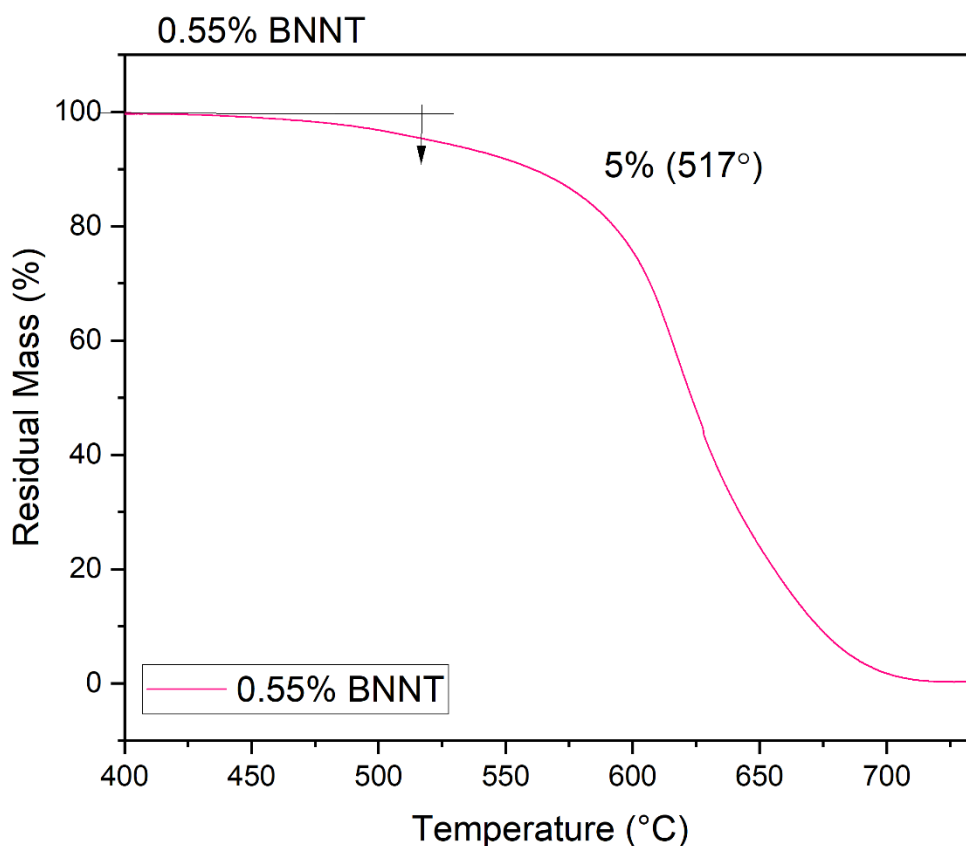


Figure 17. Onset of decomposition was quantified as the 5% mass loss was calculated for 0.55% BNNT incorporated polymer aerogel to be 517 C.



Conclusions

The development of techniques that can be used to incorporate boron nitride nanoparticles and nanotubes into polyimide aerogels was presented. H-BN nanoparticles (<150 nm) and OW-BNNTs were dispersed in NMP via ultrasonication preceding the gelation of polyimide aerogels, under constant stirring. The presence of BNNT and h-BN in polyimide aerogel's pore structure was presented, and the resulting polyimide aerogels were characterized extensively to understand their properties. Spectroscopic properties of the synthesized aerogels were characterized via FT-IR, SEM, and XPS techniques. The contact angle was calculated and evaluated via static Sessile drop goniometry to evaluate wettability. This work lays the

foundation for future incorporation of BN nanoparticles and BNNTs, where individualization of BNNTs via functionalization can be explored, leading to increasing the concentration of BN in polyimide aerogels without increasing the mass to improve properties such as heat transfer. These methods serve as contributions to the field of integrated low density polymers with a fundamental understanding of how to fabricate and characterize BN nanoparticle incorporated polyimide aerogels.

Chapter III Quantification of Hexagonal Boron Nitride Impurities in Boron Nitride Nanotubes
via FT-IR Spectroscopy

Reproduced from Ref. with permission from the Royal Society of Chemistry. Haley Harrison, Jason T. Lamb, Kyle S. Nowlin, Andrew J. Guenther, and Ajit D. Kelkar and Jeffrey R. Alston Kamran B. Ghiassi. "Quantification of Hexagonal Boron Nitride Impurities in Boron Nitride Nanotubes Via FT-IR Spectroscopy." *Nanoscale Advances* (2019). Print.

CHAPTER III: QUANTIFICATION OF HEXAGONAL BORON NITRIDE IMPURITIES IN BORON NITRIDE NANOTUBES VIA FT-IR SPECTROSCOPY

Haley Harrison,^a Jason T. Lamb,^b Kyle S. Nowlin,^d Andrew J. Guenther,^c Kamran B. Ghiassi,^c

Ajit D. Kelkar,^d Jeffrey R. Alston^d

^a*Joint School of Nanoscience and Nanoengineering, University of North Carolina at Greensboro, Greensboro, NC 27401, USA.*

^b*ERC, Incorporated, Edwards AFB, CA 93524, USA.*

^c*Air Force Research Laboratory, Aerospace Systems Directorate, Edwards AFB, CA 93524, USA.*

^d*Joint School of Nanoscience and Nanoengineering, North Carolina A&T State University, Greensboro, NC 27401, USA.*

**Email: jralston1@ncat.edu*

Electronic Supplementary Information (ESI) available: [details of any supplementary information available should be included here]. See DOI: 10.1039/c8na00251g

Abstract

Preparation of high-quality boron nitride nanotubes (BNNTs) from commercially available stock is critical for the comprehensive experimental study of BNNTs and eventual industry adoption. Separation of h-BN and BNNTs is a significant challenge, and equally so, quantification of relative h-BN content in mixed samples is a major challenge due to their nearly identical properties. This work introduces a simple method of quantifying h-BN content in BNNTs based on FT-IR analysis. Quantification of relative h-BN content is demonstrated following two effective BNNT enrichment methods, surfactant wrapping and centrifugation, and a novel sonication-assisted isovolumetric filtration. Powder XRD analysis and FT-IR spectra of enriched samples show clear trends throughout the processes. The relative intensity of the FT-IR buckling mode (800 cm^{-1}) in h-BN/BNNT samples appears to be linearly proportional to the total h-BN content. We propose and demonstrate that FT-IR peak ratios of the Transverse and Buckling modes of h-BN/BNNT samples can be used to calibrate and quantify h-BN content in BNNT samples. Using this method, as-received BNNTs can be quantifiably enriched from low purity commercial feedstocks, enabling future development and study of BNNTs.

Background

Typical composition of commercially available BNNTs is ~ 50 wt. % BNNTs, ≥ 20 wt. % graphite-like hexagonal boron nitride (h-BN) and amorphous boron and BNH derivatives. High-temperature oxidation followed by water washing have been demonstrated as a suitable method to effectively eliminate amorphous impurities. However, quantifying and separating h-BN from BNNTs remains a significant challenge. Quantification of relative h-BN content in mixed h-BN/BNNT samples is a major challenge due to the nearly identical properties of h-BN and BNNTs and often involves laborious use on electron microscopy to assess the sample

constitution. In this work, we demonstrate, for the first time, a readily available and practical method of quantifying h-BN sheet content in BNNT samples. The technique, based on FT-IR analysis, is demonstrated after utilizing two different BNNT enrichment methods, surfactant wrapping and centrifugation, and sonication-assisted isovolumetric filtration. Powder XRD analysis, electron microscopy and FT-IR spectra of enriched samples show clear h-BN reduction trends throughout the processes. Our FT-IR quantification technique combined with any enrichment process will enable the use of lower cost, easily accessible commercial BNNT sources; which can now be quantifiably enriched for more in-depth study of BNNTs and more rapid development of BNNT based technologies.

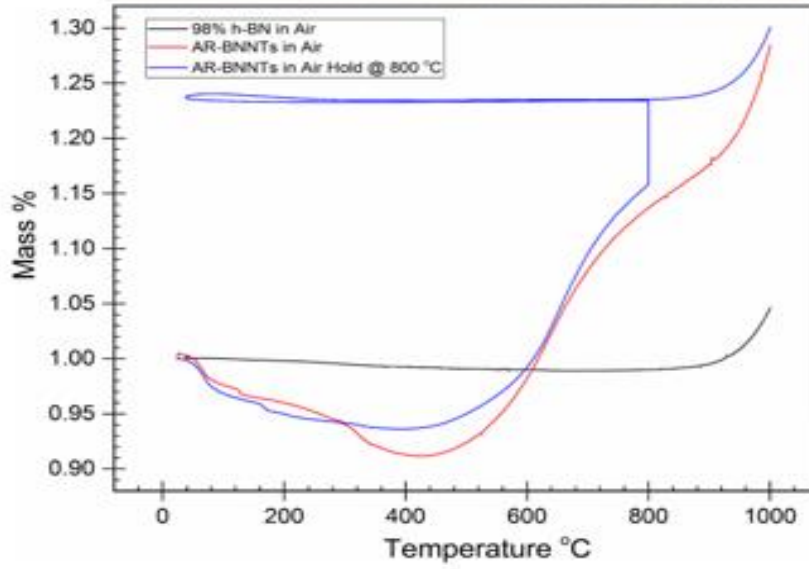
Boron nitride nanotubes (BNNTs) exhibit similar properties to carbon nanotubes (CNTs), but possess much higher chemical and thermal stability, positioning them as important new nanomaterials for future applications in high-temperature composites and components in for use in harsh environments. Integrating BNNTs into composite systems designed to withstand challenging environments requires that we study nanotube properties, and ultimately their surface chemistry; so that BNNTs can be made compatible with those composite matrices. To accomplish these studies researchers will need gram-scale quantities of BNNTs of relatively high purity. Much like CNTs, BNNTs can be synthesized as a high purity product, but current synthesis technology is limited to producing a few milligrams of high purity product per batch. The immediate challenge BNNT research faces is the acquisition of sufficient quantities of pure material.

Laboratory-scale synthesis with relatively high BNNT purity is often metal catalyzed, and purification involving acid is needed to remove metal impurities. Removal of amorphous impurities is commonly achieved by oxidation of the sample at elevated temperatures in H₂O or

O₂ containing atmosphere, which is then removed via solvent wash to dissolve B₂O₃. This procedure is effective for laboratory-scale synthesis methods, which produce relatively pure BNNTs where the primary impurities include a low wt. % of metal catalyst and small amounts of amorphous BN with a few imperfect BNNTs and h-BN. To produce gram-scale quantities of material, commercial producers are using variations of high temperature and high-pressure vapor synthesis methods with laser or plasma assistance. While high quantity production is possible, these processes are not optimized to the extent of producing highly pure material. The most readily available sources, Tekna and BNNT, Llc. offer BNNT feedstock that is less than 50 wt. % BNNTs with the remaining composition consisting of hexagonal boron nitride (h-BN) and amorphous BNH derivatives. (Figure 18)-Before is a representative image of as-received commercial grade BNNTs, highlighting the need for further purification. Because metal catalyst is not used to produce these samples, these feedstocks do not require the acid-wash-removal of metal catalyst, however a natural byproduct of this BNNT production processes includes large amounts of h-BN, which have nearly identical chemical and thermal properties to BNNTs. Amorphous and hexagonal BN is the primary contaminant of commercially produced BNNTs and due to the chemical composition and property similarities to BNNTs, removal h-BN is a major challenge.

Figure 18. High temperature oxidation of commercially produced BNNTs and h-BN.

Before: As received BNNTs (AR-BNNTs) After: Oxidized commercial BNNTs (Ox-BNNTs), AR-BNNTs heated in air at 800 °C for 3 h. Bottom: Thermogravimetric analysis of AR-BNNTs (Red) and 98% h-BN (black) heated in air at 10 °C min⁻¹ up to 1000 °C. AR-BNNTs (Blue) heated in air at 10 °C min⁻¹ up to 800 °C then held for 3 h, followed by a thermal cycle down to RT and back to 1000 °C at 10 °C min⁻¹.



Removal of Amorphous Impurities

Large-scale commercial batches of BNNTs can appear grey to light brown in color due to the presence of boron and amorphous h-BN material (Figure 18-Before). To identify an appropriate oxidation temperature, thermogravimetric analysis (TGA) can be used to observe the mass response of the raw material as it is heated in air (Figure 18-Bottom). During heating to 400 °C, the raw material can lose as much as 10 wt. % volatile mass. With further heating in the presence of oxygen amorphous boron oxidizes to B_2O_3 , and if moisture is present B_2O_3 can convert to boric acid. Either process leads to conversion of amorphous material and mass gains approaching 130 wt. % of the starting sample. As mass gain plateaus, the amorphous material is becoming fully oxidized, until the temperature climbs towards 800 °C, at which point h-BN and BNNTs begin to oxidize. A sample in which amorphous material is fully oxidized displays a characteristic TGA curve analogous to high purity (98%) h-BN (Figure 18-Bottom). A pure or fully oxidized sample shows a characteristic steady mass up to the onset of h-BN and BNNT oxidation. Based on TGA analysis, a tube furnace set at 800 °C was used to oxidize large quantities of as-received BNNTs (AR-BNNTs). A striking visual transformation occurs (Figure 18-After) during the oxidation process, changing the AR-BNNTs from grey to a bright white material primarily containing oxidized boron species, h-BN and BNNTs (Ox-BNNTs). At the start of the oxidation process, the sample is plunged directly into the center of the 800 °C tube furnace with an air atmosphere. Rapid oxidation produces the characteristic, however short-lived, flash of boron green flame upon insertion indicating the presence of elemental boron. After oxidation, the bulk material can be washed with warm water or alcohol using gentle bath sonication followed by filtration to effectively dissolve and remove the oxidized material which leaves a sample containing h-BN and BNNTs (OW-BNNTs, where OW is oxidized-washed). SI

Figure 1 presents full FT-IR spectra (4000 cm^{-1} to 500 cm^{-1}) of BNNTs at different stages of the oxidation process, highlighting the appearance and removal of oxide in the samples.

(Figure 18)

BNNT Enrichment

This study describes two methods for the removal of h-BN for the enrichment of OW-BNNT samples: sonication-assisted isovolumetric filtration (SAIF), and surfactant wrapping and centrifugation followed by high-temperature oxidation. SAIF involves the dispersion of OW-BNNTs in a mixture of dimethylformamide (DMF) and acetone. DMF-Acetone mixtures have been previously demonstrated as having favorable solvent parameters to promote BNNT disaggregation and dispersion. A tip-probe ultrasonicator is used to form the initial dispersion which is then transferred to the funnel of a vacuum filtration apparatus. Signal from dynamic light scattering (DLS) of dispersion filtrate through various pore size membranes was used to select a nanopore membrane that selectively passed particles and particle agglomerates with an intensity size distribution near 100 nm. For SAIF to be effective, sonic energy is constantly supplied to the OW-BNNT dispersion while the permeate passes through the membrane.

During sonication, the dispersion volume is simultaneously replenished with neat solvent from an addition funnel above the filtration apparatus. A detailed diagram of the SAIF apparatus is provided in SI Figure 2. Shear forces help prevent BNNT and h-BN agglomeration and reaggregation, while the agitation and intense convection produced by the sonication prevents caking on the filter membrane. The small pore size of the membrane ($\sim 200\text{ nm}$) in concert with the aforementioned dispersion factors creates an environment in which the smaller and lower aspect ratio h-BN particles diffuse through the membrane at a high rate while the high aspect ratio BNNTs impinge on the membrane and redisperse. Removal of h-BN in this way produces a

BNNT rich sample (SAIF-BNNTs) that can be collected directly on the membrane. SAIF decreases relative h-BN content as a function of time as smaller particles, h-BN and chopped BNNTs, diffuse through the membrane. However, the risk of damaging BNNTs also increases with time and is exacerbated in the presence of alcohols and water.

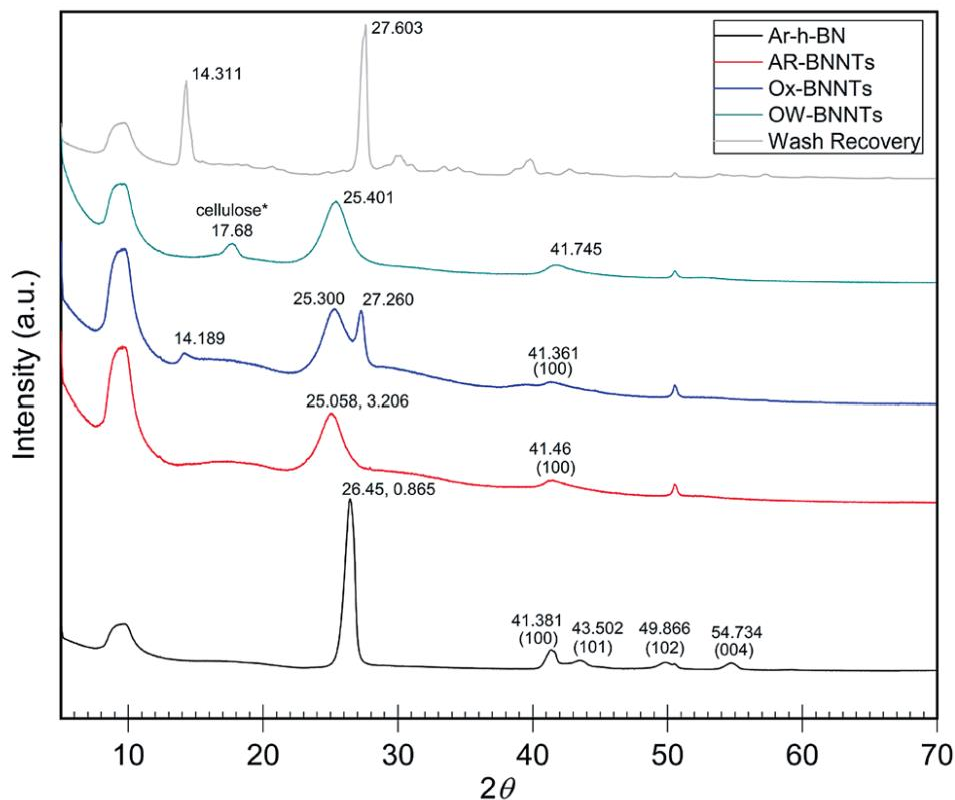
Surfactant wrapping and centrifugation, or “density gradient separation”, is a more gentle and effective purification technique previously demonstrated on carbon nanotubes (CNTs). However, for CNTs, the usefulness of the recovered product can be limited due to the difficulty of completely removing surfactant from the nanotubes. High thermo-oxidative stability offers BNNTs a unique advantage over CNTs for this method and an easy solution to the surfactant removal problem. If metal free surfactants are selected, after centrifugation and sample collection, one can simply heat (400 - 600 °C) the surfactant-wrapped BNNTs in air to oxidize and volatilize the organic material without damaging the BNNTs. During separation, when centrifugal force is applied to the OW-BNNT dispersion, differences in surfactant interaction and coverage cause differences in buoyancy and will cause BNNTs and h-BN to precipitate from dispersion at different rates. Supernatant fractions can then be collected and heated to remove the surfactant. Triton X-100 (TX-BNNTs) proved to be the most effective surfactant in this study, producing slightly higher BNNT enrichment than dispersions made with Span 20 and Tween 20.

Quantification of h-BN Content in BNNTs: X-Ray Diffraction of Boron Nitride

When analyzing BN nanomaterials, distinguishing between BNNTs and h-BN sheets is a major challenge. Analogous studies with graphene and CNTs, carbon analogs of h-BN and BNNTs, respectively, have been conducted exploring this albeit simpler challenge for carbon nanomaterials. Studies employing X-ray diffraction (XRD) show that increased curvature of the graphitic plane (graphene → CNT) leads to decreases in the (002) Bragg plane intensity and

results in broadening of the full width at half maximum (FWHM) of the peak. This trend is attributed to the graphitic plane interlayer spacing and manifests similarly in BN analogs. Figure 19 shows XRD spectra of high purity (> 98 wt. %) h-BN, AR-BNNTs, Ox-BNNTs, and OW-BNNTs. The h-BN diffractogram shows the characteristic set of higher angle peaks due to the three-dimensional order h-BN. AR-BNNTs show the expected broadening for the (002) reflection, indicating a much higher BNNT content (graphitic plane curvature) in the AR- BNNT versus h-BN samples. The (002) 2θ for h-BN is 26.45° , compared to 25.06° for as-received BNNTs; and the FWHM is 0.865° and 3.206° , respectively. XRD diffractograms obtained for TX-BNNTs and SAIF-BNNTs are included in SI Figure 4. All show increasing down-shift of the (002) plane and increased broadening, while the Ox-BNNT spectra clearly show the presences of B_2O_3 . Crystallization of molten α - B_2O_3 at ambient pressure is strongly kinetically unfavored which will limit the amount of diffraction seen in XRD, however, characteristic peaks are seen at 14° and 27° . Narrow, higher angle (002) peaks suggest higher content of h-BN, broader and lower angle (002) peaks would suggest increased curvature and increasing three-dimensional disorder from higher content BNNTs.

Figure 19. XRD spectra of as received commercial hexagonal boron nitride (h-BN) and commercial boron nitride nanotubes (BNNTs) with oxidation and wash products. h-BN peaks near 41° , 43° , 50° and 55° show characteristic 3D ordering.²² Broadening and shifting the (002) peak near 26° is a sign of increasing graphitic plane spacing and curvature.²⁴ B_2O_3 is the primary product removed from the oxidized commercial BNNTs (Ox-BNNTs) as Wash Recovery. Note* Some cellulose is present due to contamination from sample collection on a cellulose filter membrane. Individual intensity axes are not to scale.



Quantification of h-BN Content in BNNTs: Fourier Transform Infrared (FT-IR)

Spectroscopy of BNNTs and h-BN

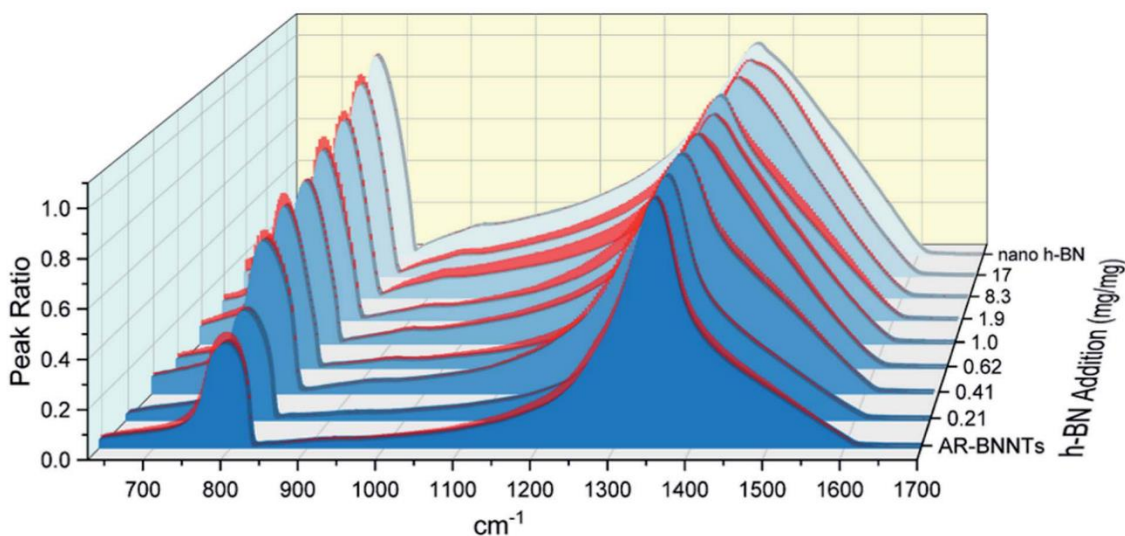
FT-IR spectroscopy of boron nitride provides us with the crucial insight into the morphology differences of the h-BN and BNNT allotropes, needed to properly quantify h-BN content in BNNT samples. Graphene-like BN nanomaterials, with a hexagonal BN network, present characteristic structural vibrations in the low-frequency region of an FT-IR spectra. For stacked sheets of h-BN, two in-plane optical phonon modes, transverse optical (TO) and longitudinal (LO) modes, resonate near 1350 cm^{-1} , and are equal in both the x- and y- axes. Buckling of the hexagonal plane also occurs, and these out-of-plane buckling, (R) modes, resonate near 800 cm^{-1} . To the best of our knowledge, Chee Huei et al. was first to demonstrate experimentally that when highly pure, monodisperse BNNTs are analyzed, the discrete TO and

LO in-plane frequencies can emerge. The LO longitudinal vibrations along the axis resonate sharply at 1369 cm^{-1} , and a second signal (1545 cm^{-1}) appears for tangential (T) circumferential in-plane modes. These T modes should be diameter (curvature) dependent but seem to only be visible for highly pure, crystalline BNNTs. More often, for mixed BNNT samples and those with higher h-BN content, T and LO peaks broaden and overlap. For simplicity, we refer to the broadened, combined peak as TO for this study.

An early computational study by Wirtz et al. offers a detailed explanation of the Raman and IR active modes of h-BN sheets and BNNTs. Ab initio calculations from their work predict a diameter dependence of three distinct BNNT radial buckling modes that converge to become the h-BN out-of-plane buckling mode at approximately 818 cm^{-1} as BN tubes becomes more like h-BN sheets, or more simply, the nanotube diameter approaches infinity ($D \rightarrow \infty$).

These combined computational evidence of Wirtz and FT-IR spectra from pure BNNT synthesis examples inspired us to look more closely at a previously unnoticed spectral feature. It appears that the relative intensity of the out-of-plane versus in-plane transmission (R/TO) for pure BNNTs is approximately 95% lower than the equivalent transmissions in pure h-BN. We suspect this is due to the strain induced in the BN bonds as the bending radius of the BN plane increases from h-BN (planar) to smaller and tubes. Straining the bonds of the h-BN sheet would stiffen the out-of-plane buckling modes and reduce translational freedom in the z-axis. Translational restriction in the z-axis would drastically limit the change in dipole moment that occurs during the buckling stretch, explaining the much lower activity of the absorption and the large difference in R/TO ratio observed for pure BNNTs.

Figure 20. FTIR Spectra array of AR-BNNT samples that have been “spiked” with increasing amounts of nanoscale h-BN. Samples are presented from the lowest h-BN concentration (AR-BNNTs) to the highest in the back (pure nanoscale h-BN). The spectra are all normalized to their TO peaks (1350 cm⁻¹) to assist visualization of the increasing out-of-plane versus in-plane transmission (R/TO) peak ratio as the concentration of h-GN in the sample increases.



Quantification of h-BN Content in BNNTs: Measuring unknown [h-BN] using FT-IR Absorbance and Internal Standard (Spiking)

The dramatic difference in low-frequency absorption of pure h-BN versus pure BNNTs provides a convenient indicator to be used as a marker for quantifying h-BN content in mixed h-BN/BNNT samples. The linear relationship of the out-of-plane (R) mode versus [h-BN] is demonstrated by “spiking” AR-BNNTs with known amounts of pure nanoscale h-BN platelets. By normalizing the FT-IR absorbance to the TO peak the effect of increasing h-BN content in BNNT samples can easily be observed. Figure 20 is a 3-dimensional array of FT-IR spectra ranging from unspiked AR- BNNTS to pure h-BN, illustrating the relationship of R/TO peak

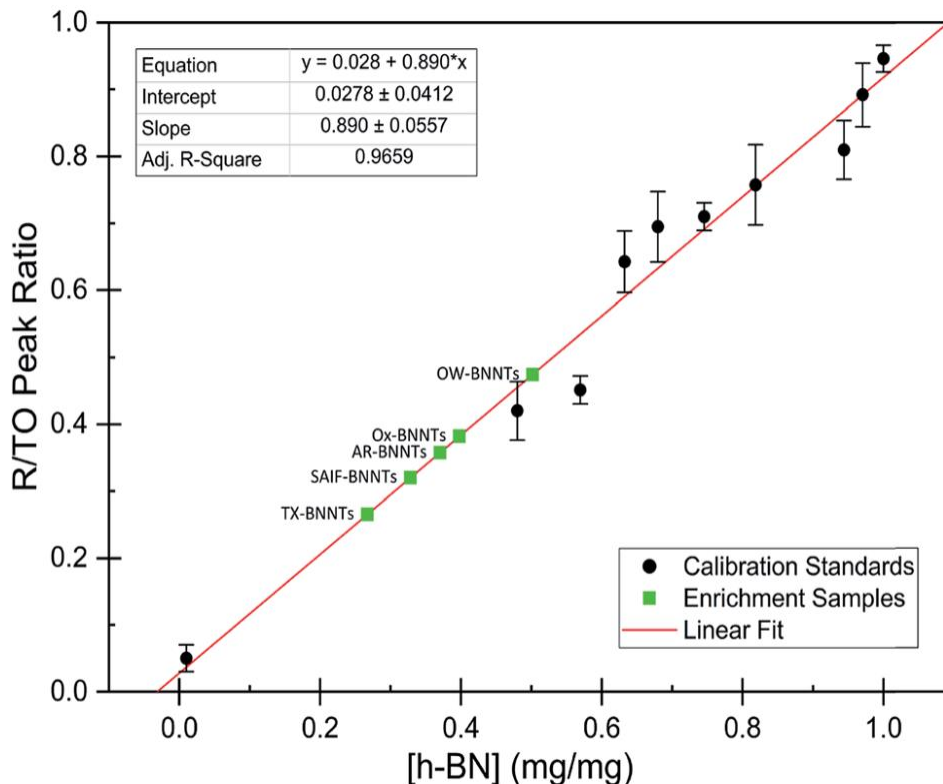
ratio and h-BN. From the “spiking” technique we also gain the ability to calculate the unknown true concentration of h-BN in a BNNT sample. From the concentration/peak ratio relationship detailed below in Equations 1 – 6, we can use readily available nanoscale h-BN as an internal standard to quantify the amount of h-BN in as-produced BNNTs. Using Equation 5, plotting $(R_{f+s})(m_T/m_0)$ versus (m_S/m_0) , the peak ratio versus standard addition is compared showing the linear relationship of peak ratio to h-BN content in BNNT samples. From Equation 5 and Equation 6 we determined the concentration of h-BN in our as-received material was 0.31 ± 0.02 mg h-BN per mg AR-BNNTs. The calculated value of h-BN concentration can then be used to form a calibration curve that can be used to calculate the h-BN concentration of any BNNT sample. Figure 5 and Table 4 show the calibration curve generated from the “spiked” standards after the initial h-BN concentration was calculated. From the calibration curve it is clear that FT-IR R/TO peak ratios can be an effective and straight forward method of quantifying the h-BN content of processed samples.

Table 4. FT-IR Peak Ratios with Calculated h-BN Weight Percent from Figure 5.

Sample	R/TO ratio	h-BN wt%	$\sigma \pm\%$
AR-BNNTs	0.357	0.37	0.0248
Chee <i>et al.</i>	0.0507	0.0257	0.00351
h-BN	0.98	1	—
Ox-BNNTs	0.382	0.398	0.0265
OW-BNNTs	0.475	0.502	0.0329
SAIF-BNNTs	0.32	0.328	0.0222
TX-BNNTs	0.266	0.267	0.0184
SP20-BNNTs	0.395	0.413	0.0274
TW20-BNNTs	0.52	0.553	0.036

From Figure 21, we see that as the BNNT samples are enriched from the as-received state (AR-BNNTs) towards BNNT samples with less h-BN content (SAIF-BNNTs and TX-BNNTs), the R/TO ratio decreases towards the spectra of pristine BNNTs, with [h-BN] of 0.33 and 0.27 mg h-BN per mg of enriched BNNT sample, respectively.

Figure 21. Calibration curve generated from “spiked” standards after determination of [h-BN]i in AR-BNNTs. Black circles represent calibration standards. Green squares represent enrichment samples and the Calculated Weight Percent from R/TO peak ratios and based on linear best fit (red line) to calibration curve.



Of further note, is the observation that the frequency of the out-of-plane mode increases (760 cm^{-1} to 814 cm^{-1}) as h-BN content is reduced (Figure 3). The FT-IR observations presented herein are in agreement with BN nanotube lattice dynamics calculations where the low-

frequency absorption of the spectrum is due to in-plane and out-of-plane modal coupling, and as the sheet rolls into a tube and this characteristic behavior leads to stiffening in the low-frequency tube mode and reduction of the change in dipole moment during stretching. Our results and observations support the assumption that rolling the h-BN plain into BNNTs stiffens the R mode frequency and can explain the reduced intensity of the low frequency absorption of BNNTs versus that of h-BN sheets.

As expected, the measured R/TO ratios are proportional to h-BN weight percent of the measured samples. Figure 21 displays the measured R/TO ratios for all the enrichment samples from this study and includes the calculated h-BN weight percent. Figure 21 is a plot of the enriched samples overlaid on the [h-BN] calibration curve with a slope of 0.890 and intercept of 0.028. According to the manufacturer specification, AR-BNNTs are approximately 50 wt. % BNNTs and 30 wt. % h-BN, with other amorphous material composing the remaining mass. The measured R/TO ratio for AR-BNNTs is 0.36, which by the equation of the calibration curve is 37 wt. % h-BN content. A slightly higher weight percent (50 wt. % h-BN) for OW-BNNTs is calculated which is expected and correlates with the removal of amorphous boron during the high-temperature oxidation and washing step. The R/TO ratio and calculation is provided for the Ox-BNNT sample; however, it should be noted that the oxide content of the sample produces FT-IR absorptions that overlap with the R and TO peaks, making this method unusable for h-BN wt. % calculations for samples with high oxide content. The SAIF process and density gradient separation appears to have been effective at removing a small quantity of h-BN producing enriched BNNT samples of 33 wt. % and 27 wt. % h-BN, respectively.

Conclusions

BNNTs are relatively new nanomaterials with high thermo-oxidative and chemical stability, piezoelectric properties, and have a high radiation absorption cross-section. These properties, along with near-mechanical equivalence to carbon nanotubes positions BNNTs as an important component in advance nanocomposites. However, high purity BNNTs have not yet been produced at commercially significant quantities. Until such a time, new techniques to prepare and refine lower quality commercially available stock into high-quality BNNTs will be critical for the future development of BNNT technologies and for our ability to conduct comprehensive experimental studies. While ongoing advances continue to develop and improve the synthesis of BNNTs, enrichment methods will continue to be used, and until now a simple and reliable method to quantify enrichment has been lacking.

This work demonstrates a simple method based on “spiking” any unknown BNNT sample with standard of high purity h-BN which is inexpensive and readily available. FT-IR is a versatile measure technique with a variety of probe and instrument arrangements which could possibly allow this measurement technique to be used in situ during synthesis to optimize process on the fly. We have shown that via FT-IR absorbance spectroscopy and the measurement of R/TO peak ratios can be a simple method to quantify the weight % of h-BN in mixed samples. While XRD can also be utilized as a complementary analysis to help distinguish between samples with varying degrees of impurities. In the interest of demonstrating the quantification several crude BNNT enrichments have been shown. From these results we see that surfactant wrapping with centrifugation and sonication assisted isovolumetric filtration are potentially useful methods to enrich low quality commercial BNNT feedstocks. The enrichment methods demonstrated herein have not been optimized in any way.

Boron nitride nanotubes are a newly available commercially produced nanomaterial that offers some exciting qualities and properties that will enable major advancements in composite technology. However, commercial production is a nascent synthesis technology, which has not yet simultaneously produced both large quantities and high purity BNNTs. At the time of publication, several companies have begun offering higher purity BNNTs, enriched through proprietary processes before shipment. However even in these cases quantification of h-BN is subjective and is accomplished via tedious combinations of TGA, SEM and TEM analysis. It is our hope with the reporting of this simple FT-IR based quantification technique we will enable both commercial and small research labs to be able to optimize their synthesis and enrichment methods, to enable more in-depth studies of BNNTs and more rapid development of BNNT based technologies.

Methods

Materials

All materials were purchased and used without further purification. Methanol (99%) and dimethyl formamide (DMF) was purchased from Fisher Scientific. AR-BNNTs were supplied by BNNT, Llc and BNNano. Boron nitride nano platelets (h-BN, 99%) < 150 nm particle size was purchased from Sigma Aldrich.

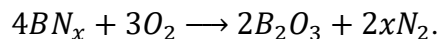
Oxidation of as-received Nanomaterials

88 mg of as-received boron nitride nanotubes (AR-BNNTs) were thermally treated at 800 °C in a Lindeberg Blue M tube furnace for 3 hours in air atmosphere. AR-BNNTs are initially gray in color, and after thermal treatment, the fully-oxidized material (Ox-BNNTs) are bright white (Figure 18), gaining 29 mg in mass. The Ox-BNNTs are dispersed in 100 mL of MilliQ 18.2 MΩ deionized water (DI-H₂O) and shaken vigorously by hand to further break up the

bundles. The mixture is stirred vigorously overnight to fully dissolve B_2O_3 , followed by vacuum filtration through a 0.8 μm pore-size cellulose membrane to separate the remaining BNNTs and residual h-BN impurities (OW-BNNTs) from the boron oxide solution. The solids are washed on the filter 3 times with 100 mL aliquots of DI- H_2O , then collected and dried under vacuum at 100 $^{\circ}\text{C}$ for 24 h.

High-Temperature Oxidation Discussion

The first step toward purification and enrichment of commercially produced BNNTs is a high-temperature oxidation and removal of amorphous material. Oxidation of amorphous boron at room temperature is a kinetically hindered process, but at sufficiently high temperatures ($> 600\text{ }^{\circ}\text{C}$) in oxygen-containing atmosphere, amorphous B_xN_y will rapidly react with $O_{2(g)}$ to form $B_2O_{3(s)}$ and release $N_{2(g)}$, depending on the B_xN_y species. Of particular note, the oxidation temperatures used for this study (750 -800 $^{\circ}\text{C}$) were sufficiently high to ignite the boron within the BNNT mass creating a corona of the characteristic green flame emission spectra of elemental boron. Boron oxide softens at 325 $^{\circ}\text{C}$ and melts near 450 $^{\circ}\text{C}$. It has been noted that sample weight gain during high-temperature oxidation of boron materials is often significantly lower than expected from the reaction



$B_2O_{3(s)}$ is slowly removed from the oxidized material by slow evaporation of $B_2O_{3(l)}$ during the oxidation process. This is likely due to a significant vapor pressure of $B_2O_{3(l)}$ at temperatures approaching 800 $^{\circ}\text{C}$. After high-temperature oxidation removal is achieved via hot water washing, which solubilizes $B_2O_{3(s)}$, as seen in the recovery products of the hot water wash.

B₂O₃ is clearly visible in the FT-IR spectra of unwashed oxidized BNNT material and can be recovered from the wash water (XRD -Figure 19, FT-IR – Figure S11).

Sonication assisted isovolumetric filtration (SAIF)

OW-BNNTs are added to 50:50 vol% DMF: Acetone (~0.25 mg/mL) and ultrasonicated with a ¼” tapered tip probe at 30% amplitude for 10 minutes to disperse the BNNTs. Membrane porosity was selected by analysis of dynamic light scattering (DLS) data, comparing intensity size distribution of the BNNT dispersion before and after filtration through membranes of decreasing pore sizes. PTFE membrane filters with porosity below 0.45 µm produce significantly lower intensity size distribution, so membranes with pore sizes below 450 nm are suitable for retaining BNNTs. The probe tip is positioned in the dispersion above the filter membrane to minimize damage to the membrane during sonication. The dispersion was continuously sonicated during filtration in a pulsing sequence, alternating ON for 10 seconds, OFF for 15 seconds. Sonication simultaneously maintains BNNT/h-BN disaggregation and provides a forced convection current within the funnel body to keep the long aspect ratio BNNTs from caking on the membrane surface during filtration. As the dispersion was sonicated on the filter membrane a small pressure differential was produced ($\Delta P \sim 100$ mPa) using a vacuum pump to slowly pull filtrate through the membrane at a controlled flow rate. A neat mixture of 1:1 DMF-Acetone was simultaneously added to the supernatant to maintain dispersion volume in the filter funnel. During this process, both BNNTs and the remaining h-BN contaminants are well dispersed in the solvent mixture and continuously recirculate throughout the funnel body due to the convection currents produced by sonication. Mass flow through the membrane is driven by the small pressure differential while h-BN selectivity through the filter membrane is based on the

combination of pore size selectivity and the large diffusion coefficient difference between high aspect ratio BNNTs and the relatively small h-BN particles.

Surfactant Wrapping

1 wt. % solutions of the surfactants (Span 20®, Tween 20®, and Triton X100®) in deionized water DI-H₂O were added to ~100 mg of the oxidized and washed BNNTs (OW-BNNTs) in a 100 ml: 50 mg solution to OW-BNNTs ratio. They were stirred vigorously overnight. The following day, the dispersion was centrifuged at 10 G for 10 minutes. The supernatant and solids were collected separately and then dried in a 105 °C oven under nitrogen overnight. The resultant viscous liquid supernatant and powdered solids were further heat treated in a 400 °C tube furnace under a 20 ml/min air flow to oxidize and volatilize the surfactant and leave behind BNNTs.

Thermal Analysis

Thermogravimetric analysis (TGA) experiments were carried out on a TA Instruments Q5000 TGA under a 20 mL/min flow of air using high temperature rated platinum sample pans. Heating rates were at 10 °C/min unless otherwise noted.

Powder X-ray Diffraction (XRD)

XRD experiments were performed at room temperature using a Bruker D2 PHASER equipped with a Cu-K_α ($\lambda = 1.5418 \text{ \AA}$) and a LYNXEYE compound silicon strip detector. Samples were prepared by grinding the material into a fine powder form and placed on a poly (methyl methacrylate) (PMMA) sample holder. Data acquisition was conducted while rotating the sample at 60 rpm, and the pattern was acquired from 5-70° 2 θ at 2.0° 2 θ per min, with an integration step size of 0.02° 2 θ .

FT-IR “Spiked” Standard Preparation

Fourier Transform infrared (FT-IR) spectroscopy analysis was performed on a Thermo Scientific Nicolet iS50 FT-IR equipped with a MIRacle Diamond stage and a diamond crystal window attenuated total reflectance (ATR) accessory. The experiments were performed with 32 scans at a resolution of 4 cm^{-1} ranging from $4,000\text{--}525\text{ cm}^{-1}$. An ambient background scan was taken before each sample acquisition.

To determine the unknown concentration of h-BN in as-received BNNTs, standard samples were prepared. 125 mg h-BN was dispersed in 50 ml MeOH solution followed by pulsed sonication for 20 minutes at 30 W output power from a probe-tip sonicator to disperse the material homogeneously and form a stock nano h-BN solution (2.5 mg/ml). 100 mg AR-BNNTs were dispersed in 20 ml MeOH solution followed by pulse sonication for 20 minutes at 30 W output power to disperse the stock AR-BNNT solution. 10 mL aliquots of the stock AR-BNNT solution were distributed into separate vials. Aliquots of increasing volume of the h-BN stock dispersion were then added to the AR-BNNT sample vials. The mixed dispersions were tip-probe sonicated again for 20 minutes at 30 W output power to homogenize the dispersions. Afterwards, the samples were capped loosely and left in a warm oven ($\sim 50\text{ }^{\circ}\text{C}$) to evaporate the methanol and leave behind a dry solid AR-BNNT sample “spiked” with a specific amount pure nanoscale h-BN. FT-IR spectra of the dry samples is then collected (Figure 21).

Determination of Unknown h-BN Concentration

To calculate the unknown concentration of h-BN in the original AR-BNNT sample we use the following relationships,

$$[hBN]_f = [hBN]_i \times \frac{m_0}{m_T} \quad (1)$$

$$[hBN]_S = 1_{mg/mg} \times \frac{m_S}{m_T} \quad (2)$$

where m_0 , m_S , and m_T , are the mass of the AR-BNNTs, mass of “spiked” h-BN, and total mass of the sample in the vial, respectively. $[h-BN]_i$ is the initial unknown concentration of h-BN in the AR-BNNTs, $[h-BN]_f$ in the unknown concentration of all h-BN in a “spiked” sample vial after standard addition, and $[h-BN]_S$ is the known concentration of standard in the “spiked” sample. The initial h-BN concentration $[h-BN]_i$ in the AR-BNNTs can then be determine by the equivalent ratios;

$$\frac{[hBN]_i}{[hBN]_f + [hBN]_S} = \frac{R_i}{R_{f+S}} \quad (3)$$

R_i and R_{f+S} are the initial AR-BNNT R/TO peak ratio and “spiked” ratio, respectively.

Substituting equations 1 and 2 into equation 3 gives,

$$\frac{[hBN]_i}{[hBN]_i \left(\frac{m_0}{m_T} \right) + 1_{mg/mg} \left(\frac{m_S}{m_T} \right)} = \frac{R_i}{R_{f+S}} \quad (4a)$$

which can be rearranged to

$$R_{f+S}[hBN]_i = R_i \left[[hBN]_i \left(\frac{m_0}{m_T} \right) + 1_{mg/mg} \left(\frac{m_S}{m_T} \right) \right] \quad (4b)$$

Multiplying both sides by, $\frac{m_T}{m_0[hBN]_i}$ creates the linear form

$$R_{f+S} \left(\frac{m_T}{m_0} \right) = R_i + \frac{R_i}{[hBN]_i} \left(\frac{m_S}{m_0} \right) \quad (5)$$

So, by plotting $R_{f+S} \left(\frac{m_T}{m_0} \right)$ versus $\left(\frac{m_S}{m_0} \right)$, solving for $[h-BN]_i$ is found when $y = 0$ by;

$$0 = R_i + \frac{R_i}{[hBN]_i} (x) \quad (6a)$$

$$\text{so, } [hBN]_i = -(x) \quad (6b)$$

where x is the x-intercept of linear regression fit of the plotted data. Once $[h-BN]_i$ is obtained, $[h-BN]_f$ can be calculated for the “spiked” samples. The “spiked” samples, along with data points for pure h-BN and the FT-IR data from Chee Huei et al. interpreted as “99% pure BNNTs”, can be used to establish a calibration curve of R/TO ratio versus $[h-BN]$. In this way, $[h-BN]_i$ of any sample can be calculated from a calibration curve.

Conflicts of interest

There are no conflicts to declare.

Acknowledgments

Research funded in part by AFRL Education Partnership Agreement (16-EPA-RQ-12) DOD DAF Air Force Research Laboratory (AFRL). Summer support was provided by the Draelos Science Scholars program. Work performed in part at the Joint School of Nanoscience and Nanoengineering, a member of the Southeastern Nanotechnology Infrastructure Corridor (SENIC) and National Nanotechnology Coordinated Infrastructure (NNCI), which is supported by the National Science Foundation (Grant ECCS-1542174).

Correspondence and Requests for materials should be addressed to: E-mail: jralston1@ncat.edu,
Telephone: (336) 285-2861

Notes

See supplemental information.

Chapter IV MRS Advances: Sonochemical Functionalization of Boron Nitride Nanomaterials.

Reprinted by permission from Springer Nature Customer Service Centre GmbH [the Licensor]: [Springer Nature [MRS Advances] Harrison, Haley B., and Jeffrey R. Alston. "Sonochemical Functionalization of Boron Nitride Nanomaterials." *MRS Advances* 5.14-15 (2020): 709-16. Print. [COPYRIGHT] (2020)

CHAPTER IV: SONOCHEMICAL FUNCTIONALIZATION OF BORON NITRIDE NANOMATERIALS

Haley B. Harrison, Jeffrey R. Alston

Abstract

Boron nitride nanotubes (BNNTs) and hexagonal boron nitride platelets (h-BNs) have received considerable attention for aerospace insulation applications due to their exceptional chemical and thermal stability. Presently, making BN nanomaterials compatible with polymer and composite matrices is challenging. Due to their inert and highly stable structure, h-BN and BNNTs are difficult to covalently functionalize. In this work, we present a novel sonochemical technique that enables covalent attachment of fluoroalkoxy substituents to the surface of BN nanomaterials in a controlled and metered process. Covalent functionalization is confirmed via colloidal stability analysis, FT-IR, and x-ray photoelectron spectroscopy (XPS).

Background

BNNTs and h-BN are white, large bandgap (5.5-5.8 eV) semiconducting materials, with numerous exciting properties such as superior mechanical strength, high oxidation resistance, high thermal conductivity, and neutron shielding capabilities. Improving poor dispersion and interfacial quality of nanomaterials are critical to enhancing the functionality of polymer composites. Unfortunately, due to the unique structure, and chemical and thermal stability of h-BN and BNNTs, standard functionalization methods are either insufficient, or too aggressive, causing damage to particle structure and properties. New controllable functionalization techniques must be explored to advance covalent BNNT surface modification.

Development of effective covalent and non-covalent surface modification methods have proven more challenging compared with graphitic materials due to the strength and stability of the B-N covalent bond, and resistance to oxidative treatments. The current hypothesis in the field is that controlled functionalization of boron nitride nanomaterials is unachievable due to the significant chemical and thermal stability of the B-N bonds. Most functionalization methods presented are uncontrolled, require harsh solvents and conditions, and ultimately destroy the nanostructure of the materials, eliminating the “nano-derived” benefits. Various approaches have been taken to develop functionalized BN nanomaterials with the overall goal being increased solubility and improved interfacial qualities between the BN material and composite matrices. Both covalent and non-covalent liquid-phase surface modification methods of nanomaterials have been developed, but these methods require large amounts of toxic, corrosive, or volatile solvents. Less popular, solid-phase methods have been developed to reduce or eliminate the need for harsh solvents. Unfortunately, these methods require costly large scale production involving thermal treatment, with high-energy radiation or strong mechanical forces.

Liquid-phase surface modification methods involving heating, sonication, mechanical stirring and separation techniques have been theorized and employed, but controllability and customization remain elusive. Radical mediated and reactive oxygen methods have been reported for covalent chemical surface functionalization of h-BN. When BNNTs are treated by sonication in solutions of aqueous ammonia they sharpen, shorten and unzip producing nanoribbon structures. However it has been demonstrated that alcohol can coordinate with a BN bond, and once activated, can cleave the BN bond, releasing ammonia. Altering the surface chemistry of BN nanoparticles is still in the early research stages and controlling the process to any degree has proven to be a challenging task.

Experimental Details

Materials

Perfluorohexane (99%, MW 338.04 g/mol), 2H, 3H-perfluoropentane, (Vertrel XF, 100%, MW 252.05 g/mol), 1H, 1H, 2H, 2H- Perfluoro-1-octanol (97%, MW 364.1 g/mol) were purchased from Sigma Aldrich and used as received. Hexagonal BN (MW 24.82 g/mol) in the form of boron nitride nanopowder (99%, <150 nm per manufacturer), and microscale platelets (98%, ~1 μm per manufacturer) was also supplied from Sigma Aldrich. Probe sonication was conducted at 26 kHz, with a 200 W Hielschler UP200St ultrasonic homogenizer fitted with a 7 mm titanium sonotrode. A Thermo Scientific ESCALAB Xi was used for photoelectron spectroscopy. An Agilent diamond ATR FT-IR was used for ATR FT-IR spectroscopy.

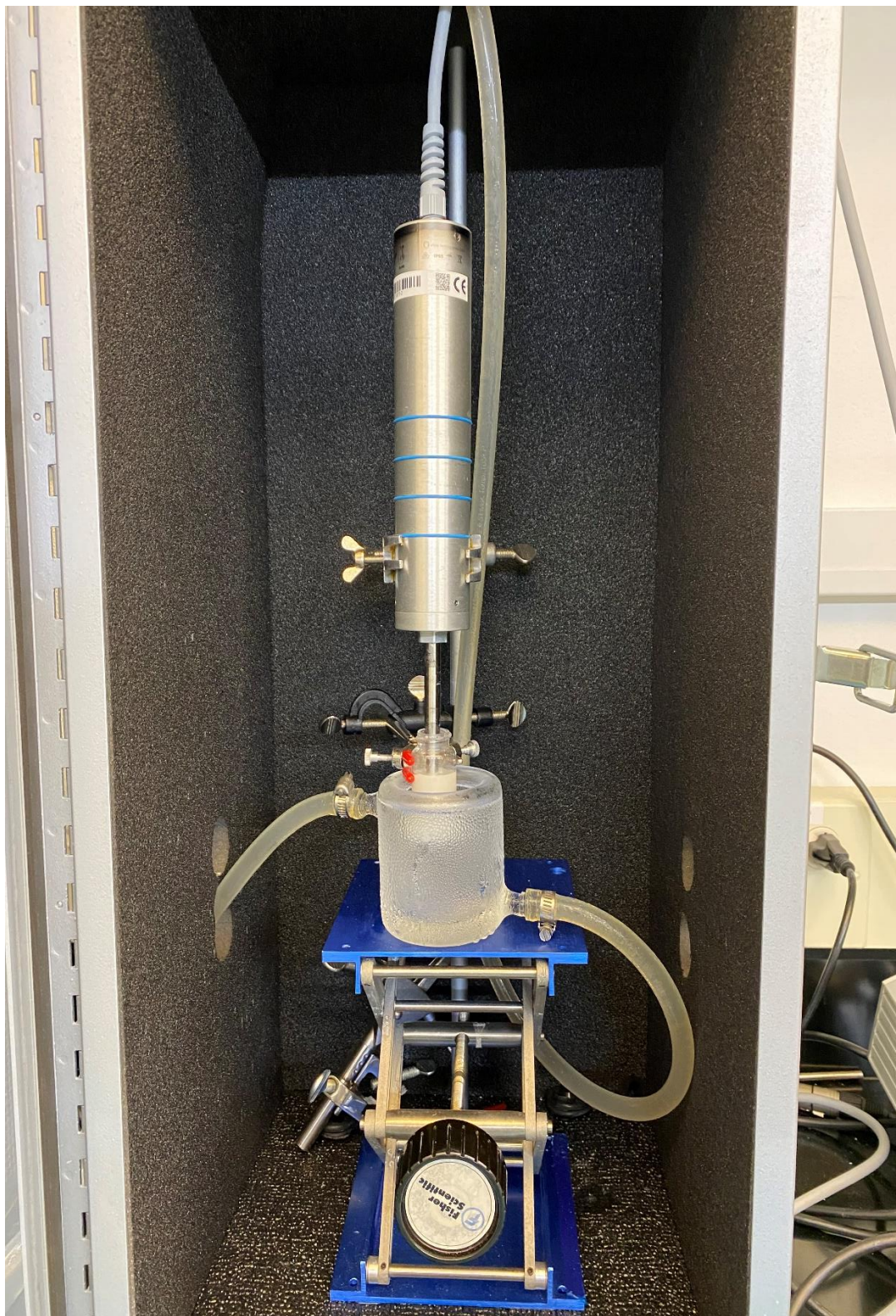
XPS spectra were collected using a twin crystal monochromatic Al K α source (500 μm), and a pass energy of 20.0 eV, with a spot size of 200 μm . XPS measurements were conducted on dry powdered samples. To prevent charging at the surface, all sample surfaces were probed in the presence of a low energy electron flood gun. Thermo Scientific Avantage Data System

software was used for the acquisition and processing of the data. Using a smart background, atomic percentages were calculated from the absolute peak intensity signal of each element detected in the survey spectra of each sample. Elements detected in the survey spectra were studied at characteristic binding energies (BE) to assess the intensity (count/second) of each signal. Characteristic binding energies were compared with data from the XPS Knowledge Database. The fluorine spectra were collected by targeting a binding energy of 688 eV. The carbon spectra were collected by targeting a binding energy range of 284-294 eV. ATR FT-IR spectra were collected in the wavenumber range of 400-4000 cm^{-1} using a diamond ATR crystal and the spectra are compiled from the average of 20 scans per sample. FT-IR measurements of as-received materials were conducted on dry powdered samples at room temperature with no further preparation. FT-IR spectra of functionalized samples were collected of dry powder samples after being washed and dried, as described in the following section.

Ultrasonic Processing

A stand mounted probe ultrasonicator UP200St (26 kHz) from Hielscher Ultrasound Technology was used for all experiments. The instrument has the capacity to reach 200 W output, but for many of the experiments within the thesis, the optimal energy output was 80 W. The ultrasonicator probe tip was changed depending upon the area of the reaction vessel and volume of liquid being homogenized. (Figure 22)

Figure 22. Hielscher probe sonicator is used in the stand mounted procedure with titanium and glass probe tip attachments. A chiller loop is hooked up to a jacketed flask, and the reaction vessel is submerged inside to manage temperature. The sonication set up is contained inside a soundproof box.



A series of sonotrodes were evaluated for the completion of this work. Titanium sonotrodes of different sizes were used depending upon the task at hand, volume and viscosity of liquid being sonicated. For homogenization only, for volumes of 2 mL up to 50 mL, a tapered 3 mm², 120 mm length probe tip was used. For homogenizing small volumes of liquids in microcentrifuge tubes, a titanium vial tweeter was employed to avoid splashing and loss of material. The vial tweeter was partially submerged into a deep (~25 cm depth) sheet of crushed ice to control temperature. For sonochemical reactions, either a 39 mm² or an 154 mm² titanium, bell shaped probe tips were used with for volumes up to 100 mL. For homogenization in viscous solvents or strong bases, a glass and titanium 530 mm², 200 mm long probe tip was employed for volumes up to 100 mL. Ultrasonication was conducted within a soundproof box.

For experiments requiring low energy sonication, a Branson UltrasonicsTM bath sonicator was used. The bath was degassed for 5 minutes before use. Mass was measured using a Mettler Toledo digital precision analytical balance as necessary. For solid nanopowders, wax weigh paper was used, and the balance was tared before and after each measurement was taken. Scoopulas and spatulas were cleaned with ethanol and wiped with a Kimwipe before and after each use. Volumetric measurements were taken using 100 uL, 200 uL and 1000 uL pipettes and plastic pipette tips, supplied by Fisher Scientific.

h-BN dispersions in 20 mL scintillation vials were held in a jacketed flask during sonication to control the temperature within the reaction vial. A thermocouple in the flask constantly monitored the temperature during the reaction, which was maintained at $-17\text{ }^{\circ}\text{C} \pm 3\text{ }^{\circ}\text{C}$. The temperature inside the vial was periodically measured. The cold jacketed flask enabled relative control of the temperature within the reaction vessel, which remained approximately 15 °C for the duration of each reaction. The reflected power of the probe sonicator was controlled

between 33 and 85 W. Application of sonic energy was pulsed to control the buildup of waste heat with a pulse sequence of 10 seconds on / 30 seconds off. Due to differences in reflected power between samples, the energy received by each sample was limited by the total energy input into during sonication. (Figure 23) shows the average reflected power for each sample, and the difference in total energy received by the different samples, 33000 to 384000 J. After sonication, functionalized h-BN was collected via vacuum filtration. The h-BN was washed on the filter four times with 40 mL aliquots of Vertrel XF to remove unreacted perfluoroalkyl species, followed by excessive washing with MeOH to remove the Vertrel XF. Any residual wash solvents were then removed by drying samples in an oven at 100 °C for over 24 hours.

Figure 23. Experimental Parameters of Samples A through F. Output parameter, Fluorine atomic %, measured via X-ray photoelectron spectroscopy (XPS).

Sample	h-BN mass (g)	Reactant (PFO) (g)	Average Reflected Power (W)	Total Energy (J)	Fluorine (Atomic %)
A	0.15	0.0016	85	384000	5.22
B	0.15	0.0016	80	96000	2.56
C	0.15	0.0079	33	33000	1.75
D	0.15	0.0000	0	0	0.00
E	0.15	0.0000	85	96000	0.00
F	0.15	0.0016	0	0	0.00

Discussion

In this study, we compare the level of fluoroalkoxy functionalization of sonochemically treated h-BN samples. The experimental parameters for each experiment, sample (A-F), are outlined in Figure 1. (Figure 24) presents the resulting elemental composition, as determined by XPS analysis, of each sample after the received treatment outlined in Figure 1. Sample A was

irradiated with a total energy of 384000 J in the presence of PFO (1.6 mg). Samples D and F received no sonic energy and were shaken by hand for approximately 2 min. Sample C was sonicated at lower power and lower output energy only receiving a total of 33000 J. The purpose of increasing the reactant concentration while decreasing total energy received was to assess the relative impact of the experimental factors, PFO concentration, and energy input. (Figure 1).

Figure 24. XPS Atomic % analysis of Samples A-F.

Element	Sample A Atomic %	Sample B Atomic %	Sample C Atomic %	Sample D Atomic %	Sample E Atomic %	Sample F Atomic %
B 1s	47.38	50.51	50.83	21.12	35.93	45.08
C 1s	3.98	3.00	3.63	14.44	28.08	16.13
N 1s	39.42	39.89	40.22	56.05	28.48	33.22
O 1s	3.77	3.79	3.58	8.4	7.51	4.38
F 1s	5.22	2.56	1.75	0	0	0

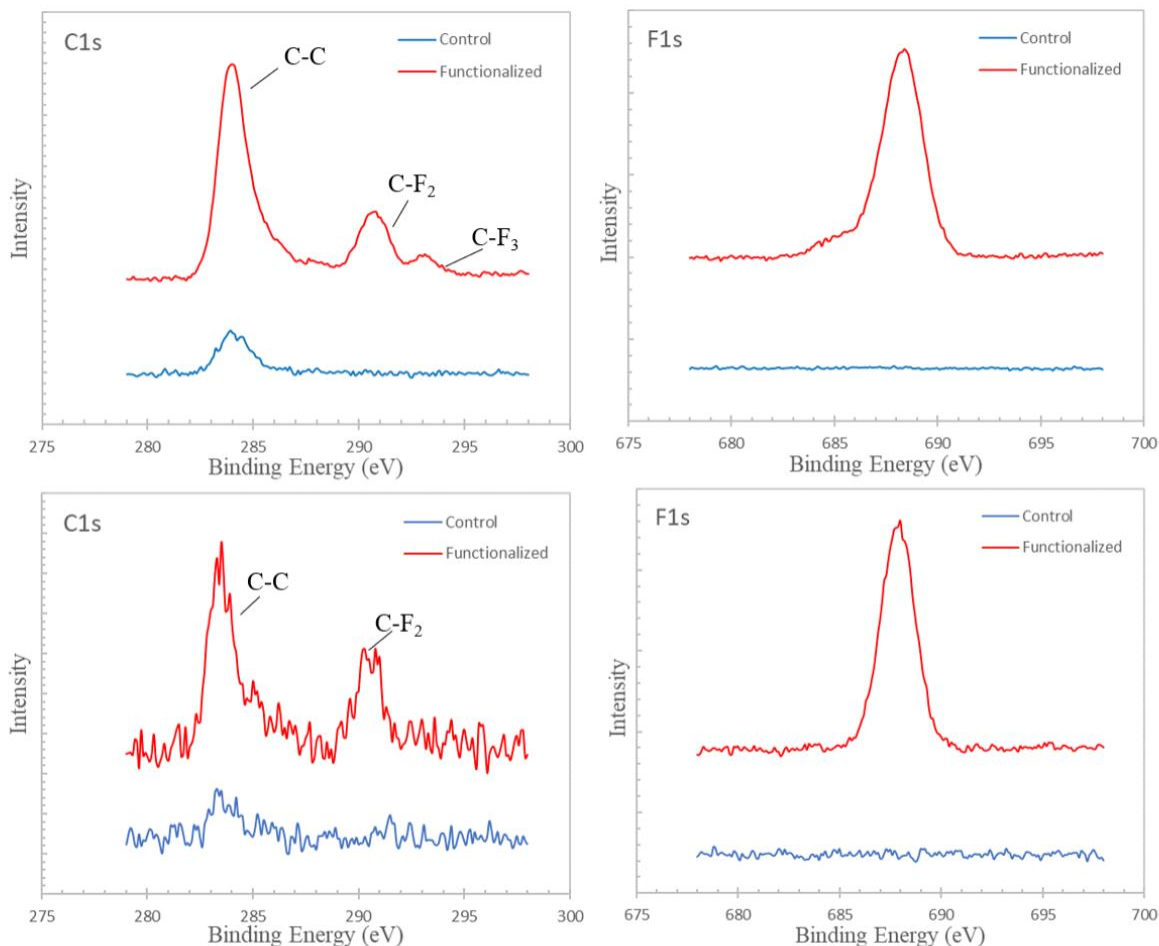
To study the elemental composition of the functionalized samples, x-ray photoelectron spectroscopy (XPS) was employed to probe the surface of the powdered samples. Boron nitride materials are electrically insulating, which can lead to shifting and distortion of the XPS spectra, so a low energy electron flood gun was used to limit charging. Conveniently, BN materials should not contain carbon signal in XPS. Some background carbon is always observed due to surface contamination (~285 eV). However, this is clearly discernable from carbon C1s signal related to the attachment of fluoroalkoxy groups (Figure 3). For sample A-C, after the sonochemical functionalization, corresponding characteristic peaks associated with C-F2 (~292 eV) and C-F3 (~294 eV) binding energies were observed. These peaks are not visible in sample D which was not in the presence of PFO and did not receive sonic irradiation. Similarly, there is also no evidence of C-F bond addition for sample F, which was shaken in the presence of PFO

without ultrasonic irradiation. Fluoroalkoxy addition is also supported by the presence of a fluorine F1s peaks for irradiated samples in the presence of PFO and zero signal for the controls. Figure 3 shows the XPS spectra of samples A, C, D, F, which are representative of all the samples. Similar results are observed for all sonochemically functionalized h-BN samples.

The XPS atomic percentages were recorded for all samples (Figure 4). The fluorine signal as a confirmation of functionalization is ideal because fluorine is not a natural contaminant of h-BN, in the same way the carbon signal could be. Here, the atomic % of fluorine clearly increases proportionally with the additional ultrasonic irradiation but does not appear after simply combining h-BN and PFO in solution. Fluorine signal is also not present for Sample D indicating fluorine does not adhere as a residue from the unreacted alcohol or fluorinated solvent. In this way, the F atomic % can be used as an indicator of fluoroalkoxy attachment to the h-BN.

Figure 25. (Top left) XPS carbon spectra. 1 μm functionalized h-BN platelets (Sample C, red) versus the control, unfunctionalized h-BN material (Sample D, blue). The C-F2 peak is at ~ 292 eV and the C-F3 peak is at ~ 294 eV. The carbon peak arising at ~ 284.1 eV can be attributed to the presence of adventitious carbon, and C-C bonds contaminating the surface of the material. (Top right) XPS fluorine spectra. 1 μm functionalized h-BN platelets (Sample C, red) versus the control, unfunctionalized h-BN material (Sample D, blue). The binding energy for fluorine is ~ 688 eV. (Bottom left) XPS carbon spectra. <150 nm functionalized h-BN nanopowder (Sample A, blue) versus the control, unfunctionalized h-BN nanopowder (Sample F, red). C1s binding energy in the range of 280-299 eV was evaluated. The functionalized h-BN binding energy corresponding to the C-F2 group was ~ 292 eV. XPS fluorine spectra. <150 nm functionalized h-BN nanopowder (Sample A, red)

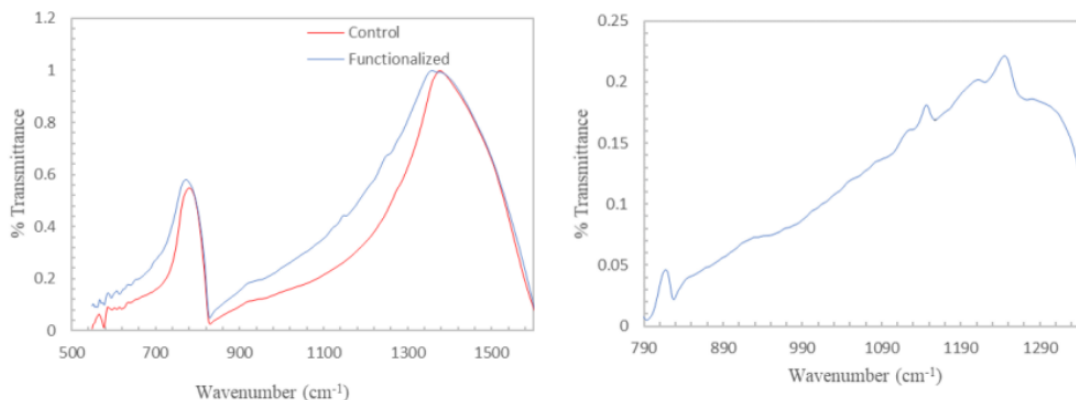
versus the control, unfunctionalized h-BN nanopowder (Sample F, blue). The binding energy for F1s was ~688 eV.



FT-IR analysis, while not as conclusive as XPS, also suggests that C-F bond containing moieties were added to the h-BN samples. h-BN materials, both BN sheets and nanotubes, have two strong FT-IR signals. h-BN has active FT-IR absorptions for in-plane stretching (1350 cm^{-1}) and out of plane bending (800 cm^{-1}). Unfortunately, these strong h-BN absorptions overlap with many FT-IR C-F signals and we are controlling functionalization to a low stoichiometric level, however by subtracting the spectra of unfunctionalized h-BN from fluoroalkoxy functionalized h-BN material we can confirm presence of fluoroalkoxy functional groups. (Figure 26) shows the

ATR FT-IR subtracted spectra of unfunctionalized and functionalized h-BN. After subtraction, peaks corresponding to C-F, C-F₂, C-F₃ stretching and bending modes (~1145, ~1190, ~1250 cm⁻¹) begin to appear.

Figure 26. (Left) FT-IR spectra of as-received micron size h-BN (Red) versus functionalized h-BN (Blue). (Right) Unfunctionalized spectra subtracted from the functionalized spectra clearly expose -CF₂ and -CF₃ absorption at 1090-1290 cm⁻¹.



Sonochemical functionalization of h-BN fluoroalkyl moieties qualitatively shows enhanced particle stability when compared with unfunctionalized particles in fluorinated media (Vertrel XF) after ultrasonication. The samples were dispersed using gentle sonication, left undisturbed for 72 hours, and photographed.

Figure 27. h-BN particle dispersion stability is qualitatively assessed by observing stability in fluorinated media (Vertrel-XF pictured). (Left) Sonochemical functionalized sample B, 72 hours after dispersion in Vertrel-XF. (Right) Control (unfunctionalized) sample E, 72 hours after dispersion in Vertrel-XF.



Conclusions

This work demonstrates that controlled covalent functionalization of h-BN can be achieved using ultrasonication. Herein, we use non-aqueous liquid-phase solutions with low quantities of fluorinated alcohol as a reactant with h-BN. In this reaction, we believe ultrasonic cavitation induces the production of short-lived fluoroalkoxy and hydroxyl radicals. At the same time, the cavitation microbubbles created in the solution collapse, which generates enough energy to destabilize the B-N bond. This is supported by our results which show increased colloidal stabilization of functionalized particles, as well as indicative FT-IR, and elemental analysis of fluoroalkyl groups covalently attached at the surface and edges of the h-BN materials.

We offer a simple alternative to uncontrolled or harsh chemical functionalization of hexagonal BN particles. B-N bonds can be destabilized using ultrasonic energy as a result of acoustic cavitation., in conjunction with the generation of free radicals. This high powered ultrasonication allows the controlled addition of small quantities of reactant for covalent attachment of fluoroalkyl groups h-BN nanomaterials. With this method, it will be possible to covalently functionalized h-BN and BNNTs in a controllable manner that retains the structure and more importantly the properties of the nanoscale boron nitride allotropes. By controlling

functionalization to low stoichiometric amounts without damaging structure and properties, the demonstrated technique will allow nanoparticle compatibilization in a variety of matrices and provide a better chance to improve dispersion and stabilization without damaging the structure.

Future work will seek to further elucidate the reaction mechanism, apply this ultrasonication procedure to purified commercial BNNTs, and expand the range of reactant systems to more widely used, less volatile non-aqueous solvent systems for generation of free radicals for polymer compatibilization.

CHAPTER V: INVESTIGATING THE COVALENT FUNCTIONALIZATION OF BORON NITRIDE NANOMATERIALS VIA SONOCHEMICAL ALCOHOLYSIS

Abstract

Boron nitride nanotubes (BNNTs) are one-dimensional nanostructures with a wide bandgap of ~6.0 eV. BNNTs have excellent mechanical, thermal and electronic properties, making them uniquely suited for use as structural reinforcement in composites, or for use in a variety of electrically insulating materials. Despite their unique properties, successful BNNT incorporation into composites and low density polymer materials has been limited due to their strong van der Waals intermolecular forces, leading to agglomeration in solution. Furthermore, BNNTs high thermo-oxidative stability (exceeding 800 °C) make covalent functionalization methods relying on oxidation to activate reactive sites on BNNTs surfaces and edges, coupled with the stability of the B-N bond. For BNNTs to be used more widely in advanced composite applications, more work needs to be done to improve the compatibility of BNNTs with various liquid media through covalent functionalization. Here, we present fluoroalkyl-functionalized BNNTs and provide evidence of NH₂-functionalized BNNTs using a one-step non-aqueous sonochemical approach. Several bifunctional alcohols were investigated that produce short-lived ·OH radicals in solution, enabling controlled attachment of small fluoroalkyl molecules containing -CF₃ and -CF₂ groups. Likewise, small aliphatic bifunctional alcohols containing -CH and -NH₂ moieties were investigated to add -NH₂ groups across the B-N bond in small concentrations. This approach presents the chemical reactivity of B-N and BNNTs can both be made reactive via sonication assisted alcoholysis. This work presents a highly customizable

approach for future functionalization, via attachment of larger aliphatic molecules, and potentially even molecules containing aromatic functional groups.

Introduction

Boron nitride nanotubes (BNNTs) are a unique one dimensional nanostructured material analogous to the carbon nanotube (CNT), with a hexagonal B-N network. BNNTs continue to receive interest in the scientific community due to the potential for their use in aerospace and aeronautical structural applications. Recent advances in synthesis techniques have improved access to BNNTs for improving purification and dispersion methods and encouraged the development of a variety of BNNT composites. BNNTs are white, optically transparent in the visible region, radiation shielding and electrically insulating with a wide band gap approaching 6 eV. Additionally, BNNTs have exceptional mechanical strength and toughness, with a thermo-oxidative stable exceeding 800 °C in air. Despite these amazing properties and improvements in BNNT availability, development of effectively BNNT incorporated composites and polymers has been limited due to the lack of adequate controllable and non-destructive covalent functionalization methods and techniques. The thermo-oxidative strength of the B-N covalent bond makes many methods successfully applied for covalent functionalization of CNTs ineffective. Existing methods rely on employing harsh acids to cleave the B-N bond, which is uncontrollable, and leads to significant damage to the BNNT structure, thereby limiting the properties. Additionally, BNNTs are insoluble in many solvents relevant for low density polymer applications, limiting effective incorporation into polymeric systems where adequate and stable dispersion of the nanostructures is required.

Despite significant progress in developing non-covalent functionalization methods and recent progress in showing the effectiveness of superacids for solubilizing BNNTs, development

of more controlled, customizable surface functionalization techniques are desired. Developing efficient functionalization techniques can improve the stability of BN and BNNT nanomaterials in solution and improve the shelf life of stable solutions for use in commercial applications. This will enable successful incorporation of BN and BNNT nanostructures into low density polymer composites. Enhanced stability in solution and solubility of BNNTs is essential for improving the properties of h-BN and BNNT incorporated polymer aerogels, where the high viscosity of the polymer solution and long gelation and aging processes lead to aggregation in solution. Further, showing successful covalent functionalization has further implications leading to improved compatibility between BNNTs and polymer matrices.

Development of effective covalent and non-covalent surface modification methods have proven more challenging compared with graphitic materials due to the strength and stability of the B-N covalent bond, and resistance to oxidative treatments. BNNTs are nonreactive due to the lack of covalent chemistry available to the empty orbital on the B sites within the tube. Early work showed promising results on h-BN materials, by generating oxygen and nitrene free radical species via thermolysis, but these methods have not been translated successfully to BNNTs due to the destructive nature harsh acids have on the tubes. Although the impressive properties of BN nanomaterials are well known, practical composite applications are limited due to high surface energy, and the strong tendency to aggregate. It is well known that the poor dispersion and interfacial quality of nanomaterials must be improved, it is critical to enhancing the functionality of polymer composites.

Various approaches have been taken to develop functionalized BN nanomaterials with the overall goal being increase in solubility and improved interfacial qualities between the BN material and composite matrices. The covalent and non-covalent surface modification methods

of nanomaterials can be developed in the liquid phase, requiring large amounts of toxic, corrosive and volatile solvents. Less popular solid phase methods have been developed to reduce or eliminate the need for harsh solvents. Unfortunately, these methods effectuate their own set of challenges and limitations: requiring costly large scale production involving thermal treatment, and high-energy radiation or strong mechanical forces.

Enhanced chemical reactivity of BNNTs

BNNTs have unique chemical properties due to the higher electronegativity of nitrogen (3.04) compared with boron (2.04). This leads to asymmetric charge distribution, where the valence charges are localized to the N atom. This leads to a weaker delocalization of pi electrons in BNNTs, when compared with CNTs which have fully delocalized electron clouds. It has been postulated that this weaker delocalization can enhance the reactivity of BNNTs, enabling routes towards radical activity that can be used for developing functionalization methods.

Covalent liquid phase surface modification consists of two steps, oxidation of h-BN, and introduction of hydroxyl groups onto the surface. For BNNTs, in this process, BNNTs are dispersed in harsh acidic solutions, and sonicated for long periods of time, yielding oxidized BNNTs. Liquid phase surface modification methods involving heating, sonication, mechanical stirring and separation techniques have been theorized and employed, but controllability and customization remain elusive. A simple method for producing chemically functionalized BNNTs via strong oxidation and silanization through 3-aminopropyl-triethoxysilane (APTES) has been successfully shown to add amino groups onto the surface. Although successful, reliance on highly oxidative acids is not desirable and has not been successful for h-BN materials. Reactive oxygen and nitrogen and nitrene radical species have been reported for covalent chemical surface functionalization of h-BNs. Covalent radical initiated functionalization approaches of boron

nitride nanosheets (BNNS) via thermolysis and subsequent hydrolysis using strong reactive agents, high temperatures and pressures were used to generate the oxygen radicals. Huang et al used an autoclave treatment of BNNTs in water-dimethyl sulfoxide to activate BN bonds through coordination for hydrolysis. Previous success with multiwalled carbon nanotubes functionalized with APTES led to improved compatibility with polymers in nanotube-based polymer matrix composites. In these cases, very little control over functionalization is offered and results are not replicated when applied to BNNTs.

Sonication assisted alcoholysis

Sonication has been shown to destabilize the B-N bond, attaching hydroxyl groups on the edge and surface of h-BN and BNNTs (Figures 24, 25). Sonication assisted exfoliation of h-BN has been used to obtain HO-BNNS by directly sonicating bulk h-BN in water without the use of additional surfactants. HO-BNNS are partially oxidized in the hydrolysis process, leading to the attachment of OH groups in small quantities. BNNTs sharpen, shorten and unzip producing BNNRs when BNNTs are treated by sonication in solutions of aqueous ammonia. More recently, Sang Woo et al., showed polymer wrapped BNNTs were shortened after probe-tip ultrasonication in ethanol and H₂O. In this reaction, ammonia coordinated to the B atom as a Lewis base, followed by hydrolysis of the BN bond. Sonication of multiwalled BNNTs induces alcoholysis, leading to sidewall peeling, producing boron nitride nanoribbons (BNNRs). In these cases, low energy bath sonication was employed, for long durations of time (2-50 h). It has been presented that alcohols coordinate to a BN bond, are activated, (Figure 28) and another alcohol cleaves the BN bond through sonication assisted alcoholysis, releasing ammonia. Another method that has been used to exfoliate h-BNs to produce OH-BNNS is ball milling in the presence of chemical agents such as NaOH, KOH and urea (Figure 27). Here, shear-force

exfoliation is coupled with chemical functionalization to produce -OH radicals. While this process is useful for h-BNs, due to the damaging nature of this method it has not translated to use for BNNTs.

Figure 28. Thermolysis induced generation of oxygen or carbon centered radicals in situ for covalent functionalization of BNNTs at boron sites.



Figure 29.(a) Schematic depicting two different initiation sites: the "edge" or "surface."

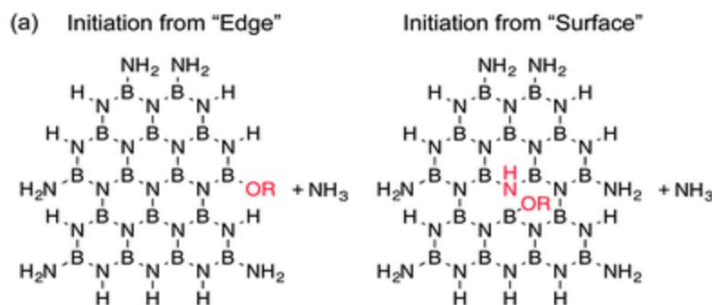
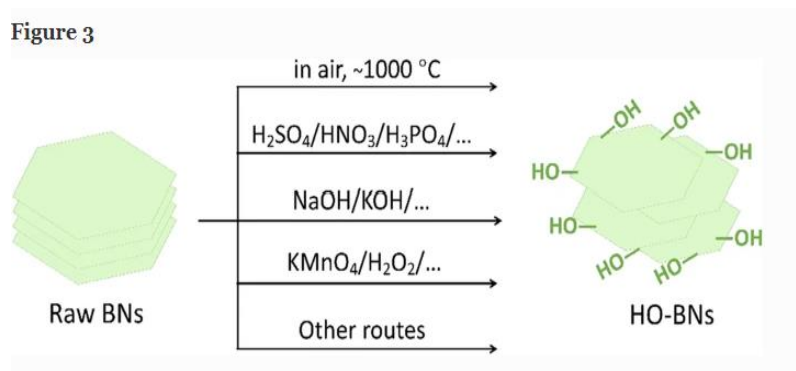


Figure 30. Various routes to hydroxylate raw h-BN sheets.



Reprinted with permission from Ren, J., Stagi, L. & Innocenzi, P. Hydroxylated boron nitride materials: from structures to functional applications. *J Mater Sci* **56**, 4053–4079 (2021).

<https://doi.org/10.1007/s10853-020-05513-6> CC BY license.

On BNNT Functionalization

Boron nitride nanomaterials with a hexagonal lattice structure analogous to that of graphene and carbon nanotubes are relative newcomers in the high performance nanomaterials family, having been predicted and synthesized in the mid-1990's. The bright white hexagonal boron nitride allotropes are wide bandgap (~6 eV) insulators and due to their graphite-like structure hexagonal boron nitride (h-BN) and boron nitride nanotubes (BNNTs) exhibit similar Young's modulus and shear modulus, 1.8 TPa and 7 GPa, respectively. They also have excellent thermal conductivity, which is among the highest of insulating and semiconducting materials, recently measured at 751 W/mK for a pristine monolayer at room temperature. Understandably, BNNTs and h-BN are receiving significant attention as high performing fillers and reinforcement for use in nanocomposites to improve composite properties. However, It is well known that poor dispersion quality and high interfacial energy between nanomaterials and a composite matrix must be improved to gain the full benefit and functionality of nanoparticle-polymer composites. The bonds of h-BNs and BNNTs are quite stable making them relatively chemically inert and also thermally stable in air around 800 °C . Due to the strength and stability of the B-N covalent bond, and resistance to oxidative treatments, this has led to challenges in the development of effective covalent surface modification methods, which have proven more challenging compared to non-covalent methods and chemical examples with graphitic materials like graphene and carbon nanotubes. Although the impressive properties of BN nanomaterials are well known,

practical composite applications are limited due to high surface energy and the strong tendency to aggregate.

Various approaches have been taken to develop functionalized BN nanomaterials with the overall goal being increase in solubility and improved interfacial qualities between the BN material and composite matrices. Covalent and non-covalent surface modification methods of nanomaterials have been developed in the liquid phase, requiring large amounts of toxic, corrosive and volatile solvents. Less popular solid phase methods have been developed to reduce or eliminate the need for harsh solvents. Unfortunately, these methods effectuate their own set of challenges and limitations: requiring costly large scale production involving thermal treatment, and high-energy radiation or strong mechanical forces.

Covalent liquid phase surface modification consists of two steps, oxidation of h-BN, and introduction of hydroxyl groups onto the surface. In this process, BNNTs are dispersed in harsh acidic solutions, and sonicated for long periods of time, yielding oxidized BNNTs. Liquid phase surface modification methods involving heating, sonication, mechanical stirring and separation techniques have been theorized and employed, but controllability and customization remain elusive. A simple method for producing chemically functionalized BNNTs via strong oxidation and silanization through 3-aminopropyl-triethoxysilane (APTES) has been successfully shown to add amino groups onto the surface. Although successful, reliance on highly oxidative acids is not desirable and has not been successful for h-BN materials. Reactive oxygen, nitrogen and nitrene radical species have been reported for covalent chemical surface functionalization of h-BNs. Covalent radical initiated functionalization approaches of boron nitride nanosheets (BNNS) via thermolysis and subsequent hydrolysis using strong reactive agents, high temperatures and pressures were used to generate the oxygen radicals. Huang et al., used an autoclave treatment of

BNNTs in water-dimethyl sulfoxide to activate BN bonds through coordination for hydrolysis. Previous success with multiwalled carbon nanotubes functionalized with APTES led to improved compatibility with polymers in nanotube-based polymer matrix composites. In these cases, very little control over functionalization is offered and results are not replicated when applied to BNNTs .

The use of ultrasonication in aqueous media has been shown to exfoliate h-BN and attach hydroxyl groups to the edges, but this behavior is not seen in BNNTs due to the low reactivity of the radicals formed in water . Sonication has been shown to destabilize the B-N bond, attaching hydroxyl groups on the edge and surface of BNNTs . BNNTs sharpen, shorten and unzip producing BNNRs when BNNTs are treated by sonication in solutions of aqueous ammonia . In this reaction, ammonia coordinated to the B atom as a Lewis base, followed by hydrolysis of the BN bond . Sonication of multiwalled BNNTs induces alcoholysis, leading to sidewall peeling, producing boron nitride nanoribbons (BNNRs) . In these cases, low energy bath sonication was employed, for long durations of time (2-50 h) . It has been presented that alcohols coordinate to a BN bond, are activated, and another alcohol cleaves the BN bond through sonication assisted alcoholysis, releasing ammonia. Amine-functionalized BNNTs and amide-functionalized BNNTs have been obtained through harsh ammonia plasma treatment at high temperatures. Harsh acids have been used to solubilize BNNTs, but likewise, these techniques require harsh acids and produce undesirable byproducts. Such methods that have been shown to chemically modify the BNNT have also induced significant damage to the tube's structure, reducing the diameter of the tubes, shortening the tubes, leading to corrosion and sidewall peeling .

Fluorinated composites and polymer systems meet the needs for many high temperature applications due to their structural integrity and high resistance to solvents, acids and bases.

These composites and polymers can be made multifunctional by exploring addition of covalently functionalized h-BN nanoparticles and BNNTs. H-BN and BNNTs are insoluble in fluorinated solvents, and their addition into these fluorinated systems remains limited. Previously, we demonstrated successful addition of $-CF_2$ and $-CF_3$ groups in small quantities to two h-BN polymorphs, ($\sim 1 \mu\text{m}$, and $< 150 \text{ nm}$ diameter particles), begging the question as to whether the process would translate to BNNTs. In this study, we experimentally demonstrate h-BN platelets and oxidized and washed BNNTs can be covalently functionalized via a controlled sonication assisted alcoholysis at ambient pressures in non-aqueous solutions. To effectuate control over the process, heat, energy output (J) and time were measured to reduce damage to the BNNT structure.

Covalent Functionalization of BNNTs

Covalent functionalization is defined as the attachment of chemical moieties to the BNNT structure by forming covalent bonds. In a covalent bond, one pair of electrons is shared between the BNNT and the chemical moiety. In covalent sidewall functionalization, the goal is to improve dispersibility and reactivity of BNNTs. BNNTs are inherently non-reactive and hydrophobic. They are insoluble and incompatible with many existing chemical processing techniques, leading to aggregation and reduced electrical, mechanical, and thermal properties. Improving the reactivity of BNNTs is important for making BNNTs and h-BN nanoparticles compatible with polymer and composite materials systems.

In this paper, we report the use of a controlled, customizable surface functionalization technique that does not require harsh acids, damaging mechanical processes, or thermal processing methods that destroy the unique BNNT structure. This method provides essentially a

one-step, one-pot technique that reduces processing time and improves the solubility and stability of BNNTs in solvents.

Proposed Reaction Scheme

High energy probe sonication is used to induce alcoholysis reaction, producing reactive radical species in solution. This mechanism has been relied upon to exfoliate and hydroxylate h-BN platelets in water and unzip BNNTs. These radicals are short lived and hard to detect. Here, pulsed ultrasonic energy (exceeding $1 \cdot 10^5$ J) is used to destabilize the B-N bond and add small functional groups at the surface edges of the BN polymorph. In the case of BNNTs, there may be defects introduced during the synthesis and purification processes that are more reactive via ultrasonication. However, harnessing these sites for functionalization limits the potential for creating new defect sites, which can damage or limit the electronic properties of BNNT. Here, we propose a non-aqueous liquid phase approach. Ultrasonication produces hydroxyl radicals in solution that may react directly with existing defect sites to form covalent bonds. Due to the high energy output and the heat generated, coupled with the high intensity mechanic force of microbubble cavitation process, we predict these defect sites are temporarily destabilized, and reactive enough to form covalent bonds.

Figure 31. h-BN platelets are reacted with perfluorinated bifunctional alcohols in decafluoropentane.

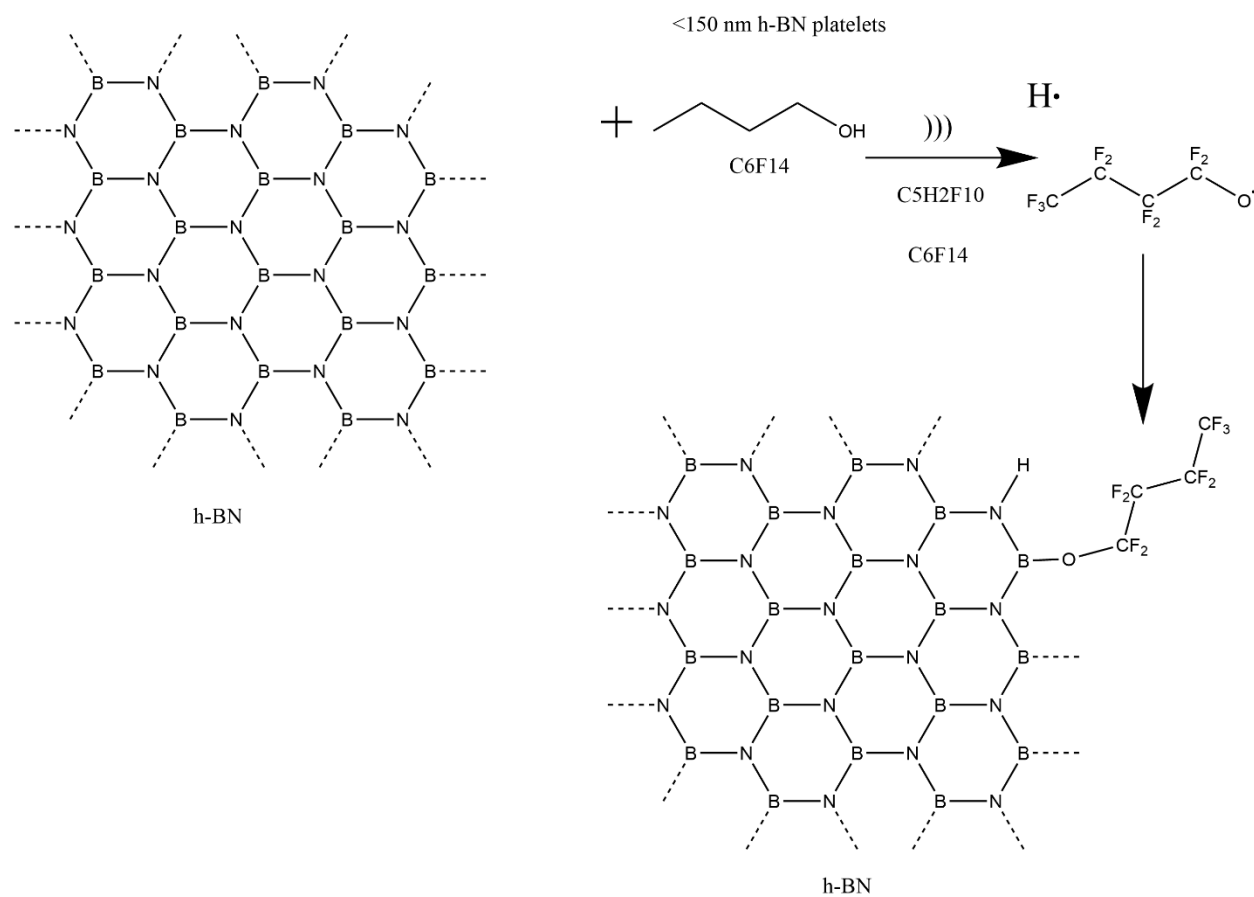
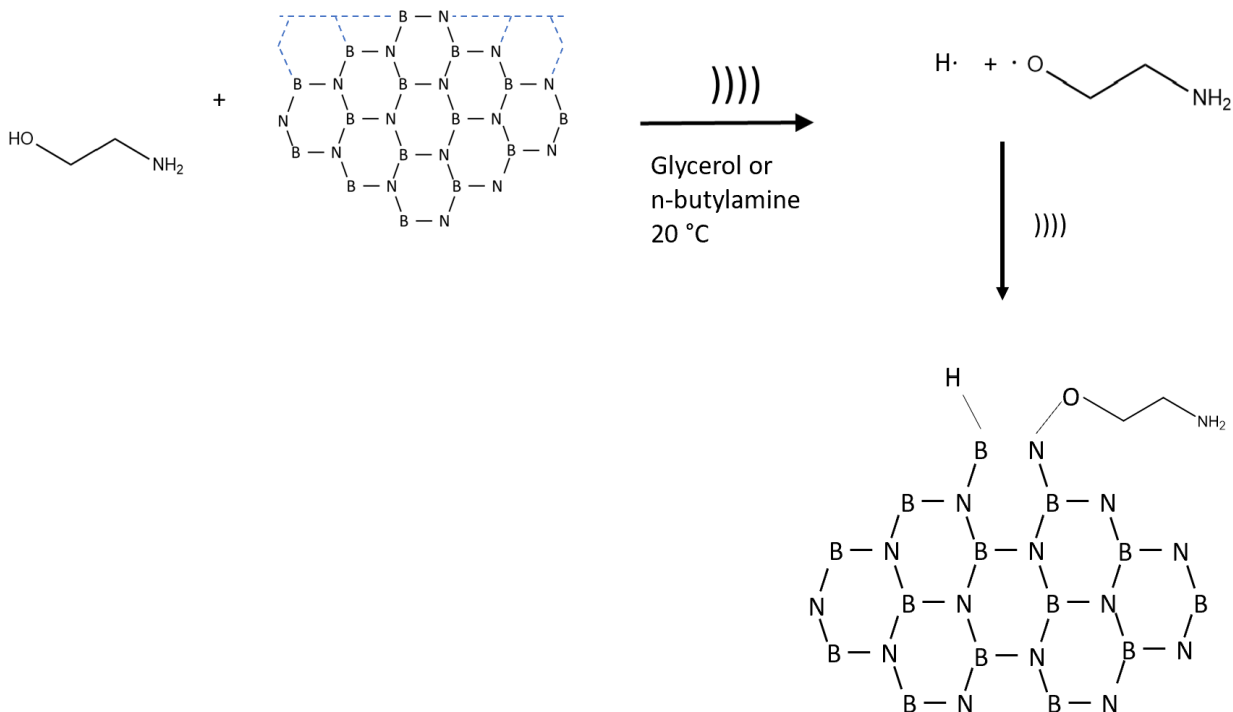


Figure 32. BNNTs or h-BN nano-sized platelets (<150 nm) are reacted with a bifunctional alcohol containing amine moieties in unreacted solvents. In these experiments, the solvents primarily used were either glycerol or n-butylamine, yielding amine functionalized h-BN or BNNTs. The non-aqueous solution is sonicated at high power (~70-80 W) and the temperature is controlled, such that a large amount of energy is created within the reaction vessel. This ultrasonication procedure produces short-lived hydroxyl radicals, which reacts

with B-N, producing NH₂-BNNTs and NH₂-h-BN nanoparticles.



Methods (BN)

Approach: Boron Nitride Purification

~1 μm h-BN platelets and <150 nm h-BN nanopowder was purchased from Sigma Aldrich and used without further purification. BNNTs were purchased from BNNT Materials, LLC. (Newport News, VA) were received in two batches. The first batch of unpurified BNNTs were received as a gray puffball and were purified before being used. The unpurified, gray tubes were oxidized at 800 °C for 1 h in a Thermo Scientific Thermolyne Muffle Furnace. The temperature inside the furnace was allowed to come back to room temperature stepwise, 10 °C increments before being removed. Upon removal from the furnace, the ball of oxidized BNNTs is bright white. The BNNTs are then transferred into a 1000 mL beaker and stirred for 24-48 h in

warm water (~80 °C). The BNNTs will begin to break up into smaller, swollen chunks. The water was then filtered out and the BNNTs are rinsed again for an additional 24 h in 5% ethanol.

Filtering Protocol

A 1000 mL borosilicate glass Erlenmeyer flask with one sidearm port was attached to a ground glass disc (diameter ~47 mm) and funnel, clamped with an aluminum spring clamp. The BNNTs were filtered over Teflon ~30 µm filter papers. The port was hooked up to vacuum filter and wash BNNTs. The BNNTs were washed three times in excess DI water, followed by two washes in ethanol. After washing, the BNNTs are no longer fluffy and separated, and are caked onto the filter. The filter is removed and placed directly into a standard Fisherbrand Isotemp heating oven to burn off the solvent for 1-2 h at 100 °C. The oven can come back to room temperature before the filter paper/BNNTs are removed. Upon removal from the oven, the BNNTs appear as a cracked, dense mat on the filter paper. 20 mL scintillation vials were rinsed with ethanol and allowed to air dry before use.

Temperature Control

A chiller loop was set to -15 °C for experiments where Vertrel XF and perfluorohexane were solvent due to their low boiling point (~70 °C). For solvents with higher boiling points such as glycerol and n-butylamine, the chiller loop was set to either -10 ° or -15 °C. A sufficiently large vessel was used to submerge at least the bottom half of the 20 mL reaction vessels and maintain temperature for the duration of the reaction. The cooling vessel was filled with acetone and the experiment can begin when the acetone reaches the desired temperature set by the chiller loop.

Temperature is evaluated and maintained during the reaction by the chiller loop, and an additional temperature probe is placed inside the vessel between sonication cycles. The

temperature within the reaction vessel itself is controlled to remain under 40 °C, the maximum temperature that allows the desired energy output by the ultrasonicator to remain stable.

Ultrasonication

A stand mounted probe ultrasonicator UP200St (26 kHz) from Hielscher Ultrasound Technology was used for all experiments. The instrument has the capacity to reach 200 W output, but for many of the experiments here, the optimal energy output was 80 W. The ultrasonicator probe tip was changed depending upon the area of the reaction vessel and volume of liquid being homogenized.

A Hielschler Ultrasound Technology UP200St probe sonicator (200 W, 26 kHz) was used for all experiments. The instrument has a capacity to reach a 200 W output, but for many of the experiments here, the optimal energy output was 80 W. The sonotrode was removable and could be changed depending upon the reaction vessel size, volume, and viscosity of the solvent. The ultrasonic homogenizer was fitted with a 7 mm titanium sonotrode, compatible with all solvent viscosities, excluding glycerol. For ultrasonication in glycerol, a glass probe tip was used due to its higher viscosity.

Sonotrode Selection

A series of sonotrodes were evaluated for the completion of this work. Titanium sonotrodes of different sizes were used depending upon the task at hand, volume and viscosity of liquid being sonicated. For homogenization only, for volumes of 2 mL up to 50 mL, a tapered 3 mm², 120 mm length probe tip was used. For homogenizing small volumes of liquids in microcentrifuge tubes, a titanium vial tweeter was employed to avoid splashing and loss of material. The vial tweeter was partially submerged into a deep (~25 cm depth) sheet of crushed ice to control temperature. For sonochemical reactions, either a 39 mm² or an 154 mm² titanium,

bell shaped probe tips were used with for volumes up to 100 mL. For homogenization in viscous solvents or strong bases, a glass and titanium 530 mm², 200 mm long probe tip was employed for volumes up to 100 mL. Ultrasonication was conducted within a soundproof box.

Additional Materials

For experiments requiring low energy sonication, a Branson Ultrasonics™ bath sonicator was used. The bath was degassed for 5 minutes before use. Mass was measured using a Mettler Toledo digital precision analytical balance as necessary. For solid nanopowders, wax weigh paper was used, and the balance was tared before and after each measurement was taken. Scoopulas and spatulas were cleaned with ethanol and wiped with a Kimwipe before and after each use.

Volumetric measurements were taken using 100 uL, 200 uL and 1000 uL pipettes and plastic pipette tips, supplied by Fisher Scientific. For polyimide aerogel synthesis, a 10 mL volumetric pipette was used with plastic pipette tips supplied by Fisher Scientific. Polyimide aerogel synthesis was conducted in 100 and 200 mL glass jars. Large hexagonal stirbars were used to stir the viscous solutions until gelation commenced. Gels were poured into silicone molds and left to age. Upon completion of the full aging process, the gels were removed from the silicone molds and submerged in solvent, in Tupperware vessels large enough to contain 4x the volume of pore solvent. The vessels are covered with matching Tupperware lids to keep the solutions air-tight.

Reagents

Reagents perfluorohexane (99%), 2H, 3H-perfluoropentane (99%) (Vertrel XF), Glycerol (98%), n-butylamine (99%), 1H, 1H, 2H, 2H- Perfluoro-1-octanol (97%), ethanolamine (99%), n-hexadecane (99%), and 3-dimethylamino 1-propanol (99%) were purchased from Sigma

Aldrich and used as received. Hexagonal BN (h-BN) in the form of boron nitride nanopowder (99%, <150 nm), and microscale platelets (98%, ~1 μm) were also supplied from Sigma Aldrich. Refined BNNTs (diameter 2-10 nm) were purchased from BNNT Materials, LLC (Newport News, LLC) and were used as-received without further purification.

Preparation of -CF functionalized h-BN and BNNTs

Vertrel XF (20 mL) was weighed into a 20 mL scintillation vial. BNNT (0.150 g) was then weighed and transferred into the vial. 1H, 1H, 2H, 2H- Perfluoro-1-octanol (1 mL) was weighed separately and transported into the same vial and capped. The details of the experimental methodology has been presented elsewhere and modified as follows. For each reaction scheme, a minimum of two samples were prepared. Three control samples were prepared for this study for this reaction scheme. Control samples prepared with reactant and were shaken gently instead of sonicated. Followed by extensive washing and drying to remove any unreacted material. One control sample was prepared without reactant and sonicated. Both samples were compared with a third sample, as-received BNNT (AR-BNNT) or <150 nm nanoplatelets. All samples were prepared such that the solvent volume (20 mL) and h-BN powder mass (150 mg) were held constant. The concentration of the reactant in solution was modified to determine whether the increase would lead to an increased reactivity and thereby increased functionalization of the nanomaterial. The concentration of the reactant was varied from ~.3 mL, and 1 mL, and 3 mL in excess. the volume of 1H, 1H, 2H, 2H-perfluoro-1-octanol was increased. The purpose of increasing the reactant concentration in some samples was to quantify whether an increase in the reaction concentration led to an increase the production of free radicals in the solution, potentially leading to a higher reactivity at the bonding sites at the edges and on the surface of the h-BN.

Table 5. Sonication energy output calculated in J for each reaction scheme.

Sample	Reactant	Vol Reactant (mL)	Vol Solvent (mL)	Mass BNNT (g)	Solvent	Power (W)	Total Energy Output (J)	Max Internal Temperature (°C)
NH ₂ -BNNT	ethanolamine	3	~17	0.15	glycerol	80	144000	40
NH ₂ -BNNT	ethanolamine	3	~17	0.15	N-butylamine	70	126000	40
CF-BNNT	Perfluoro-octanol	3	~17	0.15	Vertrel XF	70	126000	35

Preparation of -NH₂ Functionalized h-BNs and BNNTs

For the addition of -NH groups, reactants were selected due to availability, affordability, and ability to disperse BN nanostructures. For this work, bifunctional alcohols ethanolamine and 3-dimethyl amino 1-propanol were selected. A simple miscibility study was conducted to find suitable, nonreactive solvents, with reasonable freezing and boiling points. Due to the low temperatures required to control heat generated within the reaction vessel during ultrasonication, solvents that freeze above 0 °C were discouraged. Solvents that were immiscible or froze quickly include n-hexane (99%), n-hexadecane (99%), and pentane (98%). Compatible solvents selected for this work included n-butylamine (99%) and glycerol (99%). Solvent compatibility was also studied with h-BN due to the continued limited availability of purified BNNTs.

On the use of Glycerol: Green Solvent

There are concerns with using glycerol due to the presence of reactive hydroxyl groups, but glycerol has been shown to only be reactive in extremely acidic and basic conditions. The pH was measured before, during, and after the reactions to ensure neutrality was contained during the duration of the entire reaction. Due to the viscosity of glycerol, a glass (diameter, mm) probe tip was used, and a larger diameter mm reaction vessel was used to accommodate the larger

probe tip. The volume of solvent was likewise increased, the energy output was set at 80 W, pulsed at 3 s on 3 s off sonicated in 10 minute increments. The cycle was repeated 4 times.

h-BN reacted with excess ethanolamine, in glycerol

In early experiments, to avoid changing parameters such as surface area of the probe tip and scaling up the experimental volume, glycerol was mixed with excess quantities of ethanolamine to lower the viscosity. For h-BN and BNNT reactions, four samples were prepared. Glycerol (10 mL) was weighed into a ~20 mL scintillation vial. Nanoscale h-BN (<150 nm) (0.150 g) was then weighed and transferred directly into the vial. The vial is gently shaken, to confirm viscosity is lessened. Ethanolamine (10 mL) was weighed separately and transported into the same vial and capped. The reaction vessel is submerged into an acetone bath within the chiller loop for the duration of the experiment to limit the temperature reached inside the reaction vessel. A second sample was prepared without a solvent, meaning ethanolamine (20 mL) was directly reacted with h-BN nanoplatelets (<150 nm) (0.150 g). These two samples were compared with two control samples. 1) For the first control sample, glycerol (20 mL) was weighed into a 20 mL reaction vessel, and h-BN (150 mg) was added directly to the vial. Direct sonication was attempted, but it did not work due to the viscosity of the solution. The h-BN remained clumped, floating at the top of the solvent inside the vial. 2) The samples were compared with a sample of h-BN nanopowder.

Control samples were analyzed along with the amine-BNNTs via FT-IR and XPS. All samples were prepared such that the solvent volume (20 mL) and nanoscale h-BN mass (0.150 g) were held constant. The concentration of the reactant in solution was modified to determine whether the increase would lead to an increased reactivity and thereby increased functionalization of the nanomaterial, which remains unverified.

BNNT reacted with ethanolamine, in glycerol

Glycerol (40 mL) was weighed into a ~50 mL plastic reaction vessel. A portion of BNNT (0.150 g) was then weighed and transferred directly into the vial. The BNNT wetted immediately but did not break apart in solution with gentle agitation. Ethanolamine (1-3 mL) was weighed separately and transported into the same vial and capped. The reaction vessel is submerged into an acetone bath within the chiller loop for the duration of the experiment to limit the temperature reached inside the reaction vessel. For each reaction scheme, a minimum of two samples were prepared. 1) For the first control sample, glycerol (40 mL) was weighed into a 50 mL reaction vessel, and unmodified BNNT (150 mg) was added directly to the vial. The solution was ultrasonicated for 40 minutes total at 80 W. The sonicator was set to pulse 3 seconds on / 3 seconds off in 10 minute increments, totaling 4 cycles. Upon completion of the cycles, the BNNT was wetted, but remained in an aggregated ball. 2) For the second control sample, glycerol (40 mL) was weighed into a clean ~50 mL reaction vessel. Ethanolamine (1 mL) was added followed by 0.150 g BNNT. This vial was shaken vigorously by hand for several minutes. The BNNT was likewise wetted but remained densely aggregated in a single ball in the middle of the reaction vessel. 3) Both samples were characterized compared with a third sample of as received BNNT. These control samples were analyzed along with the amine-BNNTs via FT-IR and XPS. All samples were prepared such that the solvent volume (40 mL) and BNNT mass (0.150 g) were held constant. The concentration of the reactant in solution was modified to determine whether the increase would lead to an increased reactivity and thereby increased functionalization of the nanomaterial, which in this case, also remains unverified.

BNNT reacted with ethanolamine, in n-butylamine

Butylamine (17-20 mL) was weighed into a ~20 mL glass scintillation vial. A portion of BNNT (0.150 g) was then weighed and transferred directly into the vial. The BNNT wetted immediately but did not break apart in solution with gentle agitation. Ethanolamine (1-3 mL) was weighed separately and transported into the same vial and capped. The reaction vessel is submerged in acetone within the chiller loop ($-15\text{ }^{\circ}\text{C} \pm 3^{\circ}\text{C}$) for the duration of the experiment to limit the temperature reached inside the reaction vessel. For each reaction scheme, a minimum of two samples were prepared. 1) For the first control sample, n-butylamine (20 mL) was weighed into a 20 mL reaction vessel, and unmodified BNNT (150 mg) was added directly to the vial. The solution was ultrasonicated for 30 minutes total at 80 W. The sonicator was set to pulse 10 seconds on / 5 seconds off in 10 minute increments, totaling 3 cycles. Upon completion of the cycles, the BNNTs were breaking apart into strips resembling wet paper but remained mostly aggregated. 2) For the second control sample, n-butylamine (20 mL) was weighed into a clean ~20 mL reaction vessel. Ethanolamine (1 mL) was added followed by 0.150 g BNNT. This vial was shaken vigorously by hand for several minutes. The BNNT was likewise wetted but remained densely aggregated in large chunks suspended in the reaction vessel. 3) Both samples were characterized compared with a third sample of as received BNNT. These control samples were analyzed along with the amine-BNNTs via FT-IR and XPS. All samples were prepared such that the solvent volume (20 mL) and BNNT r mass (0.150 g) were held constant. The concentration of the reactant in solution was modified to determine whether the increase would lead to an increased reactivity and thereby increased addition of functional groups onto the nanomaterial surface, which remains unverified.

Temperature Control

It has been shown that careful control of temperature is required to control the volatility of the sonochemical reaction, enabling higher power to be used and longer duration experiments to be conducted. To gain control over the temperature and maintain a consistent energy and temperature profile across experiments, all samples were submerged in a jacketed flask, aiming to control temperature within the reaction vessel. The temperature of the loop was set to $-17\text{ }^{\circ}\text{C} \pm 3\text{ }^{\circ}\text{C}$. A thermocouple was placed into the acetone bath to constantly measure the temperature outside of the vessel during the reaction. Temperature inside the vessel was periodically measured as necessary. Due to the lower volatility of the non-fluorinated solvents, the probe sonication pulse time could be altered allowing longer periods of active sonication during each cycle. The probe sonicator power was set to 80 W, pulsed for 10 seconds on / 5 seconds off. The energy of the sonication was limited to the range between 33000 and 384000 J. After sonication, all samples were vacuum filtered, washed with the selected solvent (glycerol, n-butylamine) four times, and three times with MeOH. The washed solutions were dried in an oven at $200\text{ }^{\circ}\text{C}$ overnight hours to remove unreacted reagents.

The sonochemical process is governed by many factors, and the production of -OH radicals is favored at higher frequencies. Additionally, solvent properties such as vapor pressure, viscosity, surface tension and density were noted as cavitation is favored by solvents with higher vapor pressure and low density.

Characterization

Functionalized h-BNs and BNNTs were characterized by several analytical techniques. X-ray photoelectron spectroscopy (XPS) is used to determine the presence of functionalization groups. Absorption and Raman spectroscopy are used to verify covalent functionalization. Nuclear Magnetic Resonance spectroscopy (NMR) was used Imaging techniques such as

scanning electron microscopy (SEM) and transmission electron microscopy (TEM) are used to determine the lengths of the nanotubes and presence of aggregates. A Thermo Scientific ESCALAB Xi was used for photoelectron spectroscopy (XPS). An Agilent diamond ATR FT-IR was used for ATR FT-IR spectroscopy.

X ray Photoelectron Spectroscopy

XPS spectra were collected using a monochromatic Al source (200-500 μm), and a pass energy of 20.0 eV, with a spot size of 100-200 μm . XPS measurements were conducted on dry powdered samples in the case of h-BN nanomaterials. XPS measurements were conducted on $\sim 1 \times 1$ mm area of a washed/oven dried BNNT mat. To prevent charging at the surface, all sample surfaces were probed in the presence of a low energy electron flood gun. Atomic percent is calculated from XPS survey spectra conducted on each sample, and elements detected were studied at characteristic binding energies (BE) to quantify the presence of functional groups. The fluorine spectra was collected by targeting a binding energy of ~ 688 eV. The carbon spectra was collected by targeted a binding energy of ~ 285 eV, nitrogen spectra was collected by targeting ~ 400 eV, boron spectra was collected by targeting ~ 187 eV, and oxygen spectra was collected by targeting ~ 530 eV. Peak fitting was conducted using OriginPro 2021 fit with Gaussian functions on C1s, F1s or N1s high resolution spectra as necessary.

Atomic percentage (%) is calculated using the Avantage Xi software using different parameters. The first is based on the Full Width Half Maximum (FWHM) and the second is based on the Peak to Peak (PP), where the height is calculated as the difference between the maximum and minimum intensity within the specified elemental range. For this work, the atomic % referenced is based upon the FWHM calculation.

The atomic % is calculated to quantify the percentage of each element detected in the survey spectra. For the addition of fluorine groups, this is sufficient, but these techniques can be enhanced by evaluating the ratio of elements can be used to quantify the elemental composition differences between unfunctionalized samples and functionalized samples. This can be compared with a ratio of 1.18 for pristine BNNTs.

Fourier Transform Infrared Spectroscopy (FT-IR)

ATR FT-IR spectra were collected using a diamond ATR crystal from 400-4000 cm^{-1} . 20 scans were taken for each sample. In the case of detecting amine moieties, 100 scans were taken for each sample. FT-IR measurements were conducted on dry powdered samples with no further preparation. Samples were pressed directly onto the ATR crystal with a flat top to improve contact between the sample and the crystal surface. FT-IR was carried out on BNNT mats after washing, filtration and drying to remove unreacted reagents.

Preliminary evaluation of the AR-BNNT materials in our repository was conducted to establish the purity of the sample, as well as evaluate the type of impurities present. Figure 29 shows FT-IR spectra of BNNTs after thermal oxidation and washing. The absence of B_2O_3 peaks and -OH peaks ($\sim 3200\text{ cm}^{-1}$) confirms the oxidation and washing process successfully removed B, boron oxide contaminants and adequately removed solvent. BNNT has characteristic peaks at 1343 cm^{-1} and 789 cm^{-1} , corresponding with the radial breathing and transverse optical modes of BNNTs. An absorption band at 3424 cm^{-1} corresponds with the broad N-H bonds we want to see on the surface of functionalized BNNTs.

Figure 33. FT-IR was used to identify the presence of aliphatic C-N groups attached to the BNNT surface. Characteristic peaks are identified at between $\sim 1020\text{-}1250\text{ cm}^{-1}$, which can be attributed to the small molecule attachment. Also shown here are the transverse optical

and longitudinal modes ($\sim 1350\text{ cm}^{-1}$) and the out of plane buckling corresponding to the radial mode ($\sim 800\text{ cm}^{-1}$.)

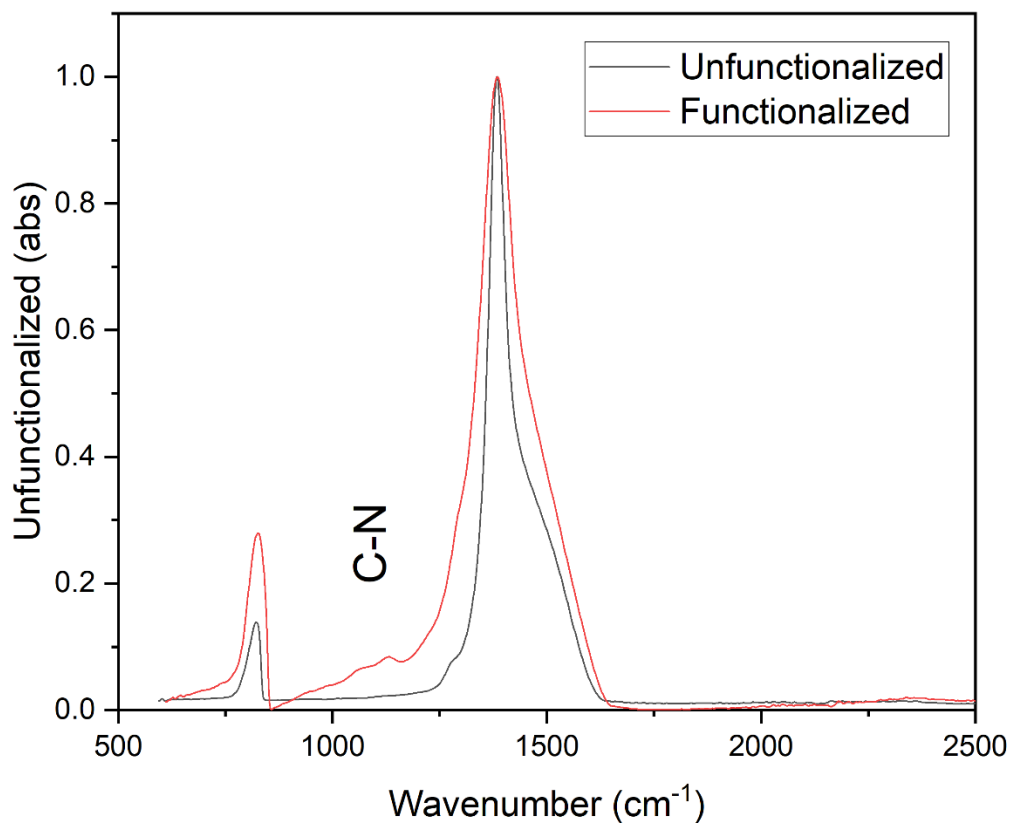
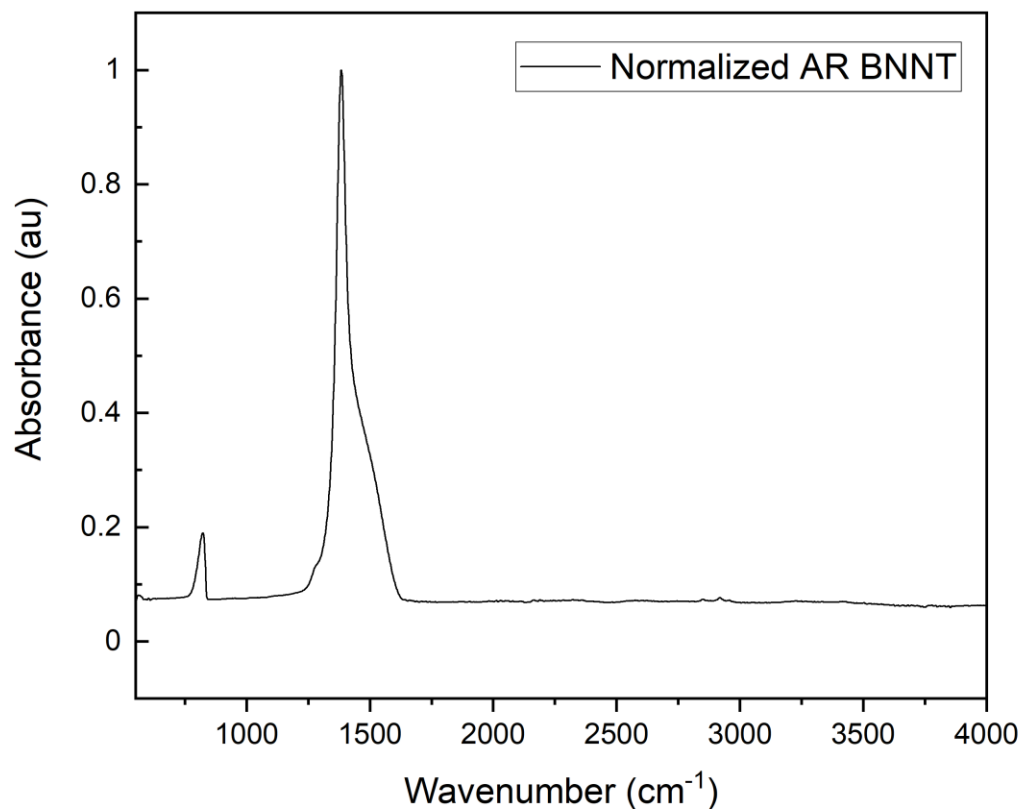


Figure 34. BNNT has characteristic peaks at 1343 cm⁻¹ and 789 cm⁻¹, corresponding with the radial breathing and transverse optical modes of BNNTs.



Dispersity Analysis

Colloids are suspensions of solid particles usually dispersed in a liquid media. This suspension is affected by interfacial forces such as van der Waals and electrostatic repulsive forces which exist between the particles.

To take preliminary evaluations of dispersion quality in different solvents, vials that have been standing for 48 hours can be evaluated side by side following ultrasonic treatment. It is readily obvious that successfully functionalized amine-hBN samples produce a more stable dispersion when compared with nonfunctionalized samples. In Figure 36, vial 1 (Right) shows n-hexane was used to produce NH₂- functionalized h-BN, producing a quasi-stable dispersion. Vial

2 (Left) shows h-BN dispersed in the solvent directly (n-hexane), the h-BN remains unfunctionalized, quickly crashing out of solution.

Figure 35. 150 mg h-BN platelets in solvent. (left) unfunctionalized (right) functionalized.

Amine Functionalized h-BN and BNNTs: UV/Visible Spectrophotometry (in NMP)



Functionalized BNNT (2 mg) was filtered and washed and suspended in N-methyl-2-pyrrolidone (NMP) (5 mL) ultrasonicated at low power (20 W) for 10 minutes, pulsed at 10 seconds on / 3 seconds off intervals. The sample was left to stand and observed. There were no visible chunks of swelled BNNTs in the solution immediately following ultrasonication. This sample was compared with a sample of unfunctionalized BNNTs (AR-BNNTs) undergoing the same treatment, and likewise observed. All samples were left to sit for 48 h, upon which the dispersion quality is evaluated. In the figure, it is evident that in the AR-BNNT suspension, there remains a mass of BNNT aggregates floating in the solution.

Figure 36. Suspensions of (left) amine-functionalized BNNTs in NMP, (right) unfunctionalized BNNTs after brief sonication.

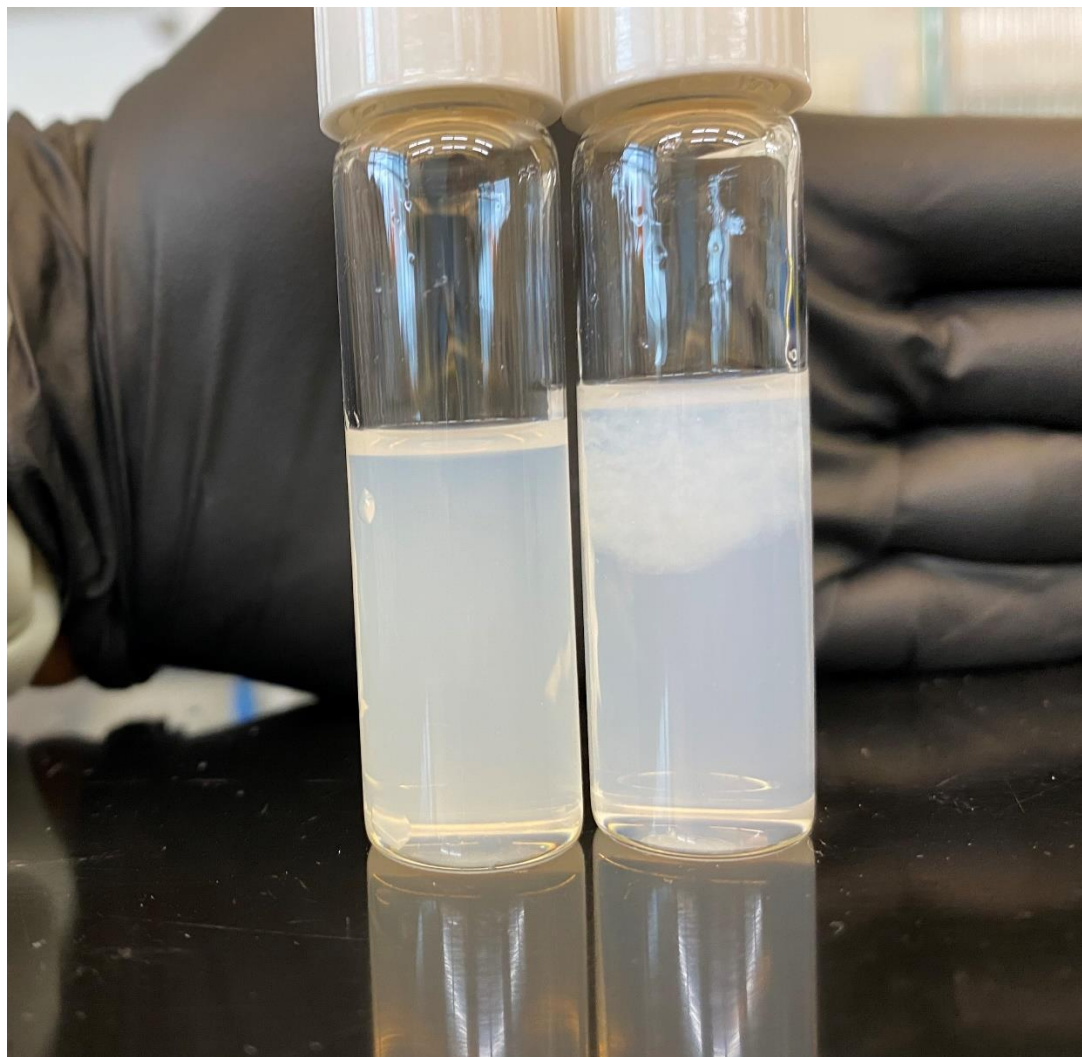


Table 6. Control sample (Top) was ultrasonication in glycerol, washed and dried. BNNTs were reacted with ethanolamine in glycerol to attach -NH₂ moieties to the edges and surface of BNNTs. The dried BNNTs were characterized via XPS, and elemental analysis was conducted to determine the composition of the materials. The B/N ratio was also calculated for reference. For a standard as-received BNNT sample, the ratio is 1.08, for NH₂-BNNTs, the ratio is 0.86.

Peak Table : NH ₂ -BNNT	
Name	Atomic %
B1s	45.83
N1s	42.22
C1s	8.33
O1s	3.62
Peak Table : ARBNNT	
Name	Atomic %
B1s	41.5
N1s	48.04
C1s	7.53
O1s	2.93

Table 7. Atomic % composition of AR-BNNT (Top) and CFx-BNNT (Bottom). Confirms attachment of fluoroalkyl groups to BNNT surface.

Peak Table : ARBNNT	
Name	Atomic %
B1s	41.5
N1s	48.04
O1s	2.93
C1s	7.53
F1s	0
Peak Table : CF-BNNT	
Name	Atomic %
B1s	50.25
N1s	42.37
O1s	2.37
C1s	3
F1s	2.02

Figure 37. High resolution C1s spectra of BNNT and NH-BNNT

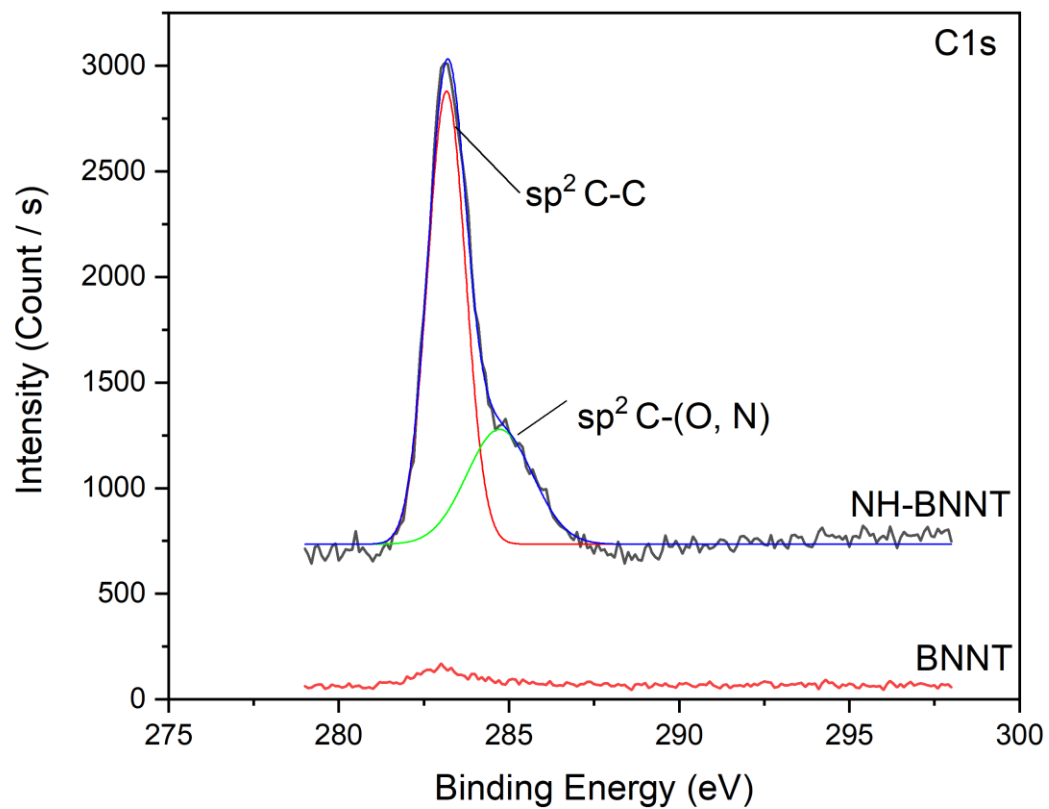


Figure 38. N1s high resolution spectra of NH-BNNT compared with BNNT.

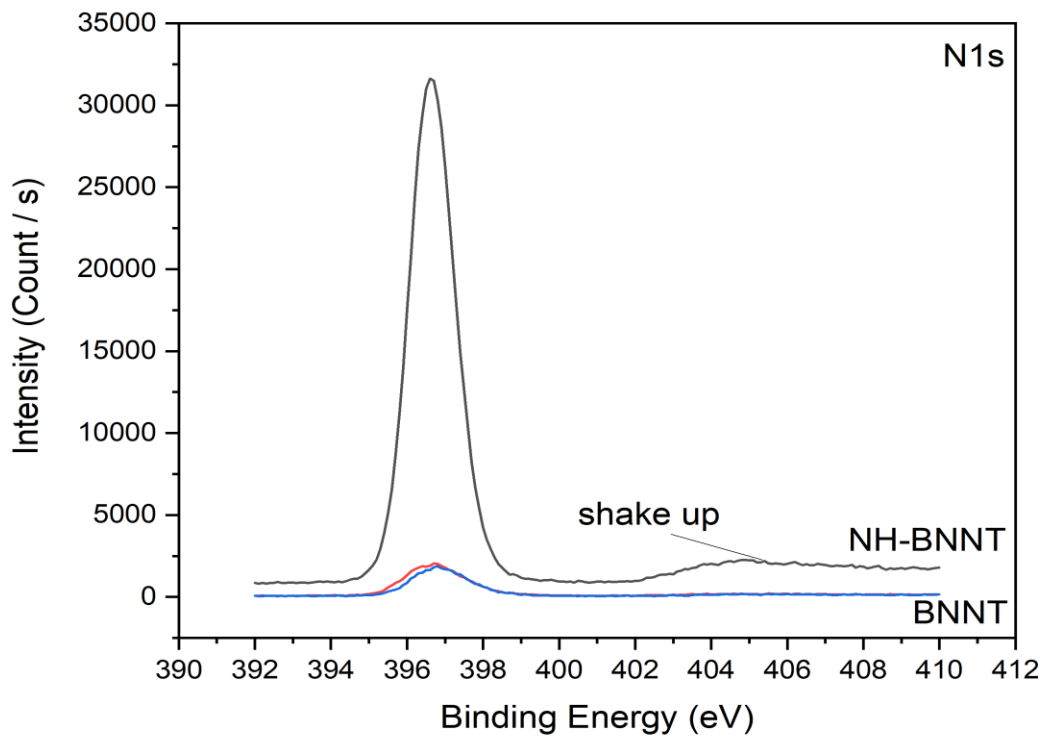


Figure 39. High resolution spectra valence region BNNT compared with NH-BNNT, highlighting the C2s bonding of surface BNNT (~18.1 eV).

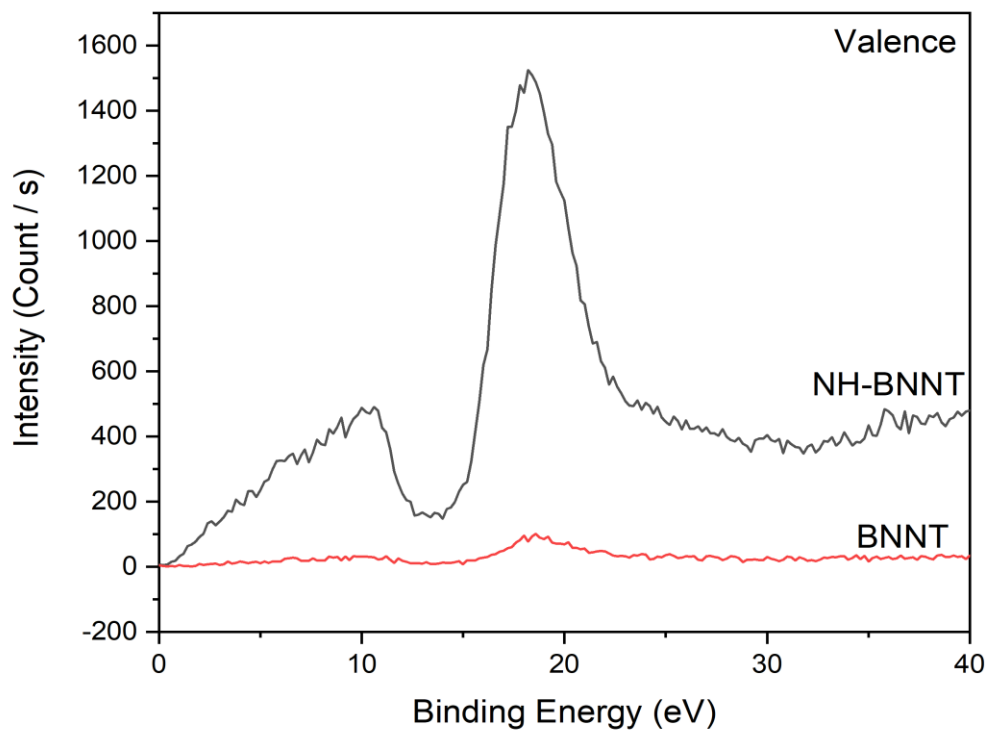
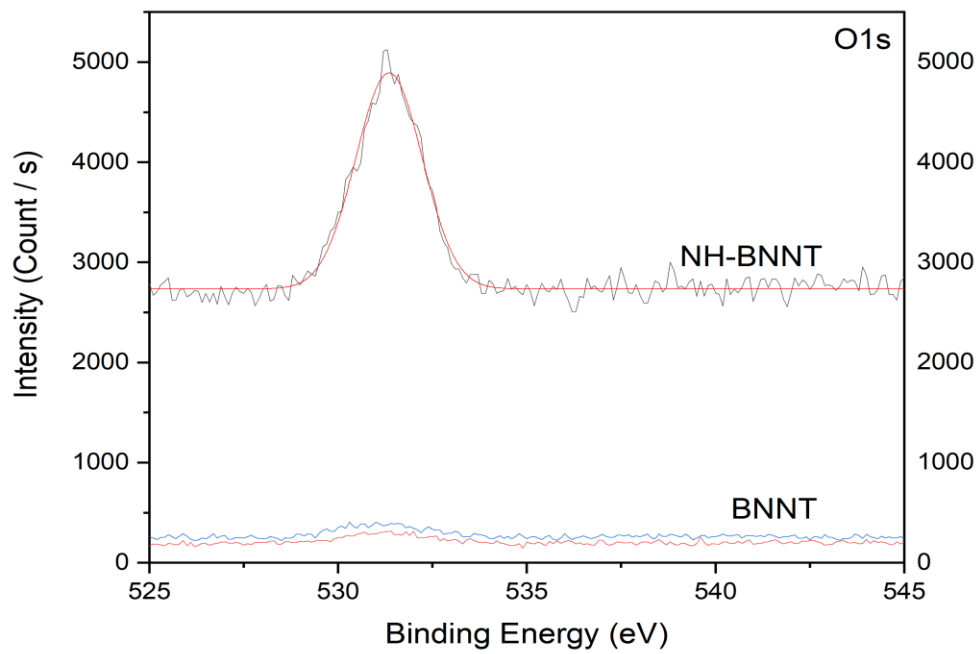


Figure 40. O1s high resolution spectra BNNT compared with NH-BNNT.



Discussion and Conclusions

Controllable BNNT functionalization methods are essential for improving the solubility and processability of BNNTs. Despite the significant challenges to altering the BNNT structure without inducing severe damage, significant strides continue to be made with these goals in mind. This dissertation presents an investigation into fundamental methods for purification and identifying h-BN impurities in BNNT commercial samples. With this dissertation, I also sought to answer whether sonochemical methods could be used to alter the surface of BNNTs via covalent functionalization, and in this dissertation, I investigated successful covalent functionalization using several functional groups. Additionally, we demonstrate the feasibility of expanding the use of sonication assisted alcoholysis from h-BN to BNNTs through the addition of small fluoroalkoxy and amine moieties across the BN bond in small concentrations. We present a mechanism for this reaction, and show increased stability of BNNTs in compatible solvents, such as NMP which can be important for improving the performance of future advanced composite and polymer applications.

BIBLIOGRAPHY

- A. Loiseau, F. Willaime, N. Demoncey, G. Hug, and H. Pascard. "Boron Nitride Nanotubes with Reduced Numbers of Layers Synthesized by Arc Discharge." *Physical Review Letters* 76, no. 25 (1996): 4737-40.
- Abraham L. Landis, Kreisler S.Y. Lau. *High Performance Polyimides and Related Thermoset Polymers: Past and Present Development, and Future Research Directions*. Handbook of Thermoset Plastics (Second Edition). 1998.
- Adeyuyi, Yusuf G. "Sonochemistry: Environmental Science and Engineering Applications." *Industrial & Engineering Chemistry Research* 40 (2001): 4681-715.
- Adnan, Mohammed, Daniel M. Marincel, Olga Kleinerman, Sang-Hyon Chu, Cheol Park, Samuel J. A. Hocker, Catharine Fay, *et al.* "Extraction of Boron Nitride Nanotubes and Fabrication of Macroscopic Articles Using Chlorosulfonic Acid." *Nano Letters* 18, no. 3 (2018/03/14 2018): 1615-19.
- Ahmad, Pervaiz, Mayeen Khandaker, and Yusoff Amin. "Synthesis of Boron Nitride Nanotubes by Argon Supported Thermal Chemical Vapor Deposition." *Physica E: Low-dimensional Systems and Nanostructures* 67 (11/07/2014 2014): 33-37.
- Ahmad, Pervaiz, Mayeen Uddin Khandaker, Ziaul Raza Khan, and Yusoff Mohd Amin. "Synthesis of Boron Nitride Nanotubes Via Chemical Vapour Deposition: A Comprehensive Review." *RSC Advances* 5, no. 44 (2015): 35116-37.
- Amanda L. Tiano, Cheol Park, Joseph W. Lee, Hoa H. Luong, Luke J. Gibbons, Sang-Hyon Chu, Samantha I. Applin, Peter Gnoffo, Sharon Lowther, Hyun Jung Kim, Paul M. Danehy, Jennifer A. Inman, Stephen B. Jones, Jin Ho Kang, Godfrey Sauti, Sheila A. Thibeault, Vesselin Yamakov, Kristopher E. Wise, Ji Sue, Catharine C. Fay. "Boron Nitride Nanotube: Synthesis and Applications." Paper presented at the SPIE Smart Structures and Materials + Nondestructive Evaluation and Health monitoring, San Diego, California, United States, 2014.
- Ansón-Casaos, A., J. M. González-Domínguez, and M. T. Martínez. "Separation of Single-Walled Carbon Nanotubes from Graphite by Centrifugation in a Surfactant or in Polymer Solutions." *Carbon* 48, no. 10 (8// 2010): 2917-24.
- Arnold, Michael S., Alexander A. Green, James F. Hulvat, Samuel I. Stupp, and Mark C. Hersam. "Sorting Carbon Nanotubes by Electronic Structure Using Density Differentiation." *Nat Nano* 1, no. 1 (10//print 2006): 60-65.
- Atasoy, Ahmet. "The Aluminothermic Reduction of Boric Acid." *International Journal of Refractory Metals and Hard Materials* 28, no. 5 (9// 2010): 616-22.
- Balint, M. G., and M. I. Petrescu. "An Attempt to Identify the Presence of Polytype Stacking Faults in Hbn Powders by Means of X-Ray Diffraction." *Diamond and Related Materials* 18, no. 9 (9// 2009): 1157-62.
- Ben Finney, Mark Jacobs. "Carbon Dioxide Temperature Pressure Phase Diagram." Wikimedia Creative Commons, 2018.
- "Bnnt-R, Boron Nitride Nanotube - Raw, Typical Properties, Product # 34236-A." In *BNNT-R, Boron Nitride Nanotube - Raw, Typical Properties, Product # 34236-A*: Tekna Advanced Materials Inc., www.tekna.com, 2017.
- "Bnnt P1 Beta, Technical Data/Specifications, Version 1.2." In *BNNT P1 Beta, Technical data/specifications, Version 1.2*: BNNT, Llc., www.bnnt.com, 2014.

- C. Y. Zhi, Y. Bando, T. Terao, C. C. Tang, H. Kuwahara, D. Golberg. "Chemically Activated Boron Nitride Nanotubes." *Chemistry - An Asian Journal* 4, no. 10 (2009): 1536-40.
- Cai, Qiran, Declan Scullion, Wei Gan, Alexey Falin, Shunying Zhang, Kenji Watanabe, Takashi Taniguchi, *et al.* "High Thermal Conductivity of High-Quality Monolayer Boron Nitride and Its Thermal Expansion." *Science Advances* 5, no. 6 (2019): eaav0129.
- Chee Huei, Lee, Wang Jiasheng, K. Kayatsha Vijaya, Y. Huang Jian, and Yap Yoke Khin. "Effective Growth of Boron Nitride Nanotubes by Thermal Chemical Vapor Deposition." *Nanotechnology* 19, no. 45 (2008): 455605.
- Chen, Hua, Ying Chen, Jun Yu, and James S. Williams. "Purification of Boron Nitride Nanotubes." *Chemical Physics Letters* 425, no. 4-6 (7/10/ 2006): 315-19.
- Chen, Ying, Jin Zou, Stewart J. Campbell, and Gerard Le Caer. "Boron Nitride Nanotubes: Pronounced Resistance to Oxidation." *Applied Physics Letters* 84, no. 13 (2004): 2430-32.
- Cho, Hyunjin, Steven Walker, Mark Plunkett, Dean Ruth, Robyn Iannitto, Yadienka Martinez Rubi, Keun Su Kim, *et al.* "Scalable Gas-Phase Purification of Boron Nitride Nanotubes by Selective Chlorine Etching." *Chemistry of Materials* 32, no. 9 (2020/05/12 2020): 3911-21.
- Chopra, Nasreen G., R. J. Luyken, K. Cherrey, Vincent H. Crespi, Marvin L. Cohen, Steven G. Louie, and A. Zettl. "Boron Nitride Nanotubes." *Science* 269, no. 5226 (1995-08-18 00:00:00 1995): 966-67.
- Ciofani, Gianni, Giada Graziana Genchi, Ioannis Liakos, Athanassia Athanassiou, Dinuccio Dinucci, Federica Chiellini, and Virgilio Mattoli. "A Simple Approach to Covalent Functionalization of Boron Nitride Nanotubes." *Journal of Colloid and Interface Science* 374, no. 1 (5/15/ 2012): 308-14.
- Cohen, Marvin L., and Alex Zettl. "The Physics of Boron Nitride Nanotubes." *Physics Today* 63 (January 01, 2010 2010): 34.
- Cui, Zhenhua, Andrew J. Oyer, A. Jaeton Glover, Hannes C. Schniepp, and Douglas H. Adamson. "Large Scale Thermal Exfoliation and Functionalization of Boron Nitride." *Small* 10, no. 12 (2014): 2352-55.
- Cuiping Yu, Jun Zhang, Wei Tian, Xiaodong Fan and Yagang Yao. "Polymer Composites Based on Hexagonal Boron Nitride and Their Application in Thermally Conductive Composites." *Royal Society of Chemistry Advances* 8 (2018).
- Deng, Xiaoyong, Dongmei Xiong, Haifang Wang, Dandan Chen, Zheng Jiao, Haijiao Zhang, and Minghong Wu. "Bulk Enrichment and Separation of Multi-Walled Carbon Nanotubes by Density Gradient Centrifugation." *Carbon* 47, no. 6 (5// 2009): 1608-10.
- Dengxiong Shen, Jingang Liu, Haixia Yang, Shiyong Yany. "Highly Thermally Resistant and Flexible Polyimide Aerogels Containing Rigid-Rod Biphenyl, Benzimidazole, and Triphenylpyridine Moieties: Synthesis and Characterization." *Chemistry Letters* 42, no. 12 (2013): 1545-47.
- Deshmukh, Aarti R., Ji Wan Jeong, Su Jung Lee, Go Un Park, and Beom Soo Kim. "Ultrasound-Assisted Facile Green Synthesis of Hexagonal Boron Nitride Nanosheets and Their Applications." *ACS Sustainable Chemistry & Engineering* 7, no. 20 (2019/10/21 2019): 17114-25.
- Fathalizadeh, Aidin, Thang Pham, William Mickelson, and Alex Zettl. "Scaled Synthesis of Boron Nitride Nanotubes, Nanoribbons, and Nanococoons Using Direct Feedstock

- Injection into an Extended-Pressure, Inductively-Coupled Thermal Plasma." *Nano Letters* 14, no. 8 (2014/08/13 2014): 4881-86.
- Feng, Ye, Yasumitsu Miyata, Kiyoto Matsuishi, and Hiromichi Kataura. "High-Efficiency Separation of Single-Wall Carbon Nanotubes by Self-Generated Density Gradient Ultracentrifugation." *The Journal of Physical Chemistry C* 115, no. 5 (2011/02/10 2011): 1752-56.
- Fisher, Thermo. "Xps Knowledge Base."
- Freimanis, B. R. Bikson and YA. F. "Cause of the Discolouration of Aromatic Polyimides." *Polymer* (1970).
- Ghazizadeh, Mahdi, Joseph E Estevez, and Ajit Kelkar. *Boron Nitride Nanotubes for Space Radiation Shielding*. 2015. doi:10.19070/2167-8685-150007e.
- Golberg, Dmitri, Yoshio Bando, Yang Huang, Takeshi Terao, Masanori Mitome, Chengchun Tang, and Chunyi Zhi. "Boron Nitride Nanotubes and Nanosheets." *ACS Nano* 4, no. 6 (2010/06/22 2010): 2979-93.
- Greenblatt, A. M. Buckley and M. "The Sol-Gel Preparation of Silica Gels." *Journal of Chemical Education* 71, no. 7 (1994): 599.
- Haiquan Guo, Mary Ann B. Meador, Jessica Lynn Cashman, David Tresp, Bushara Dosa, Daniel Scheiman, and Linda S McCorkle. "Flexible Polyimide Aerogels with Dodecane Links in the Backbone Structure." *Applied Materials and Interfaces* (2020).
- Haiquan Guo, Mary Ann B. Meador, Linda McCorkle, Derek J. Quade, Jiao Guo, Bart Hamilton, and Miko Cakmak. "Tailoring Properties of Cross-Linked Polyimide Aerogels for Better Moisture Resistance, Flexibility, and Strength." *Applied Materials and Interfaces* 4 (2012): 5422-29.
- Hales, Stephen J, Joel A Alexa, Brian J Jensen, and Donald L Thomsen. "Radio Frequency Plasma Synthesis of Boron Nitride Nanotubes (Bnnts) for Structural Applications: Part I." *Radio Frequency Plasma Synthesis of Boron Nitride Nanotubes (BNNTs) for Structural Applications: Part I* NASA/TP-2016-219001 (2016).
- Haley B. Harrison, Jeffrey R. Alston. "Sonochemical Functionalization of Boron Nitride Nanomaterials." *MRS Advances*, 2020.
- Haley Harrison, Jason T. Lamb, Kyle S. Nowlin, Andrew J. Guenther, and Ajit D. Kelkar and Jeffrey R. Alston Kamran B. Ghiassi. "Quantification of Hexagonal Boron Nitride Impurities in Boron Nitride Nanotubes Via Ftir Spectroscopy†." *Nanoscale Advances* (2019).
- Harrison, Haley B., and Jeffrey R. Alston. "Sonochemical Functionalization of Boron Nitride Nanomaterials." *MRS Advances* 5, no. 14-15 (2020): 709-16.
- Harrison, Haley, Jason T. Lamb, Kyle S. Nowlin, Andrew J. Guenther, Kamran B. Ghiassi, Ajit D. Kelkar, and Jeffrey R. Alston. "Quantification of Hexagonal Boron Nitride Impurities in Boron Nitride Nanotubes Via Ftir Spectroscopy." *Nanoscale Advances*, no. 1 (2019): 1693-701.
- Huang, Qing, Yoshio Bando, Chunyi Zhi, Dmitri Golberg, Keiji Kurashima, Fangfang Xu, and Lian Gao. "Chemical Peeling and Branching of Boron Nitride Nanotubes in Dimethyl Sulfoxide." *Angewandte Chemie International Edition* 45, no. 13 (2006): 2044-47.
- Ikuno, T., T. Sainsbury, D. Okawa, J. M. J. Fréchet, and A. Zettl. "Amine-Functionalized Boron Nitride Nanotubes." *Solid State Communications* 142, no. 11 (6// 2007): 643-46.

- Jason P. Randall, Mary Ann B. Meador, and Sadhan C. Jana. "Tailoring Mechanical Properties of Aerogels for Aerospace Applications." *ACS Applied Materials & Interfaces* 3 (2011): 613-26.
- Jerôme, Yanlong Gu and Francois. "Glycerol as a Sustainable Solvent for Green Chemistry." *Green Chemistry* 12, no. 7 (2010): 1127-38.
- Jiang, Fang, Siqu Cui, Na Song, Liyi Shi, and Peng Ding. "Hydrogen Bond-Regulated Boron Nitride Network Structures for Improved Thermal Conductive Property of Polyamide-Imide Composites." *ACS Applied Materials & Interfaces* 10, no. 19 (2018/05/16 2018): 16812-21.
- Jilin Wang, Yunle Gu, Laiping Zhang, Guowei Zhao, and Zhanhui Zhang. "Synthesis of Boron Nitride Nanotubes by Self-Propagation High-Temperature Synthesis and Annealing Method." *Hindawi Journal of Nanomaterials* 2010 (2010).
- Juan, Li, Li Jianbao, Yin Yanchun, Chen Yongjun, and Bi Xiaofan. "Water-Assisted Chemical Vapor Deposition Synthesis of Boron Nitride Nanotubes and Their Photoluminescence Property." *Nanotechnology* 24, no. 36 (2013): 365605.
- Jung, Choong-Hwan, Man-Jong Lee, and Chan-Joong Kim. "Preparation of Carbon-Free B₄c Powder from B₂O₃ Oxide by Carbothermal Reduction Process." *Materials Letters* 58, no. 5 (2// 2004): 609-14.
- Junkai Ren, Luigi Stagi, Carlo Maria Carbonaro, Luca Malfatti, Maria Francesca Casula, Pier Carlo Ricci, Antonio Esau Del Rio Castillo, Francesco Bonaccorso, Laura Calvillo, Gaetano Granozzi and Plinio Innocenzi. "Defect-Assisted Photoluminescence in Hexagonal Boron Nitride Nanosheets." *2D Materials* 7, no. 4 (2020).
- Kai Wu, Chuxin Lei, Weixing Yang, Songgang Chai, Feng Chen, Qiang Fu. "Surface Modification of Boron Nitride by Reduced Graphene Oxide for Preparation of Dielectric Material with Enhanced Dielectric Constant and Well-Suppressed Dielectric Loss." *Composites Science and Technology* 134, no. 6 (2016): 191-200.
- Kantesh Balani, Vivek Verma, Arvind Agarwal, Roger Narayan. "Physical, Thermal, and Mechanical Properties of Polymers." Chap. A1 In *Biosurfaces: A Materials Science and Engineering Perspective*, edited by Inc. John Wiley and Sons: Kantesh Balani, Vivek Verna, Arvind Agarwal, Roger Narayan, 2015.
- Kawagishi, Ken, Hiromu Saito, Hidemitsu Furukawa, and Kazuyuki Horie. "Superior Nanoporous Polyimides Via Supercritical CO₂ Drying of Jungle-Gym-Type Polyimide Gels." *Macromolecular Rapid Communications* 28, no. 1 (2007/01/05 2007): 96-100.
- Keun Su, Kim, Kim Myung Jong, Park Cheol, C. Fay Catharine, Chu Sang-Hyon, T. Kingston Christopher, and Simard Benoit. "Scalable Manufacturing of Boron Nitride Nanotubes and Their Assemblies: A Review." *Semiconductor Science and Technology* 32, no. 1 (2017): 013003.
- Kim, Dukeun, Sayuka Nakajima, Toshiki Sawada, Mahiro Iwasaki, Susumu Kawauchi, Chunyi Zhi, Yoshio Bando, Dmitri Golberg, and Takeshi Serizawa. "Sonication-Assisted Alcoholysis of Boron Nitride Nanotubes for Their Sidewalls Chemical Peeling." *Chemical Communications* 51, no. 33 (2015): 7104-07.
- Kim, Jaewoo, Sol Lee, Young Rang Uhm, Jiheon Jun, Chang Kyu Rhee, and Gil Moo Kim. "Synthesis and Growth of Boron Nitride Nanotubes by a Ball Milling–Annealing Process." *Acta Materialia* 59, no. 7 (2011/04/01/ 2011): 2807-13.

- Kim, Jun Hee, Hyunjin Cho, Thang Viet Pham, Jae Hun Hwang, Seokhoon Ahn, Se Gyu Jang, Hunsu Lee, *et al.* "Dual Growth Mode of Boron Nitride Nanotubes in High Temperature Pressure Laser Ablation." *Scientific Reports* 9, no. 1 (2019/10/30 2019): 15674.
- Kim, Jun Hee, Thang Viet Pham, Jae Hun Hwang, Cheol Sang Kim, and Myung Jong Kim. "Boron Nitride Nanotubes: Synthesis and Applications." *Nano Convergence* 5, no. 1 (2018/06/28 2018): 17.
- Kim, Keun Su, Christopher T. Kingston, Amy Hrdina, Michael B. Jakubinek, Jingwen Guan, Mark Plunkett, and Benoit Simard. "Hydrogen-Catalyzed, Pilot-Scale Production of Small-Diameter Boron Nitride Nanotubes and Their Macroscopic Assemblies." *ACS Nano* 8, no. 6 (2014/06/24 2014): 6211-20.
- Kim, Tan Young, Eun Ho Song, Byung Hyun Kang, Se Jung Kim, Yun-Hi Lee, and Byeong-Kwon Ju. "Hydrolyzed Hexagonal Boron Nitride/Polymer Nanocomposites for Transparent Gas Barrier Film." *Nanotechnology* 28, no. 12 (2017/02/21 2017): 12LT01.
- Kistler, Samuel S. "Coherent Expanded Aerogels and Jellies." *Nature* 127, no. 3211 (1931/05/01 1931): 741-41.
- Kumari, Sangita, Om P. Sharma, Rashi Gusain, Harshal P. Mungse, Aruna Kukrety, Niranjana Kumar, Hiroyuki Sugimura, and Om P. Khatri. "Alkyl-Chain-Grafted Hexagonal Boron Nitride Nanoplatelets as Oil-Dispersible Additives for Friction and Wear Reduction." *ACS Applied Materials & Interfaces* 7, no. 6 (2015/02/18 2015): 3708-16.
- Laszlo, Endrey Andrew. "Aromatic Polyimide Particles from Polycyclic Diamines." edited by United States Patent and Trademark Office. United States: El Du Pont de Nemours and Co, 1963.
- Lee, C. H., S. Bhandari, B. Tiwari, N. Yapici, D. Zhang, and Y. K. Yap. "Boron Nitride Nanotubes: Recent Advances in Their Synthesis, Functionalization, and Applications." [In eng]. *Molecules* 21, no. 7 (Jul 15 2016).
- Lee, Chee, Shiva Bhandari, Bishnu Tiwari, Nazmiye Yapici, Dongyan Zhang, and Yoke Yap. "Boron Nitride Nanotubes: Recent Advances in Their Synthesis, Functionalization, and Applications." *Molecules* 21, no. 7 (2016): 922.
- Lee, Chee Huei, Shiva Bhandari, Bishnu Tiwari, Nazmiye Yapici, Dongyan Zhang, and Yoke Khin Yap. "Boron Nitride Nanotubes: Recent Advances in Their Synthesis, Functionalization, and Applications." *Molecules* 21 (2016).
- Lee, Chee Huei, Ming Xie, Vijaya Kayastha, Jiasheng Wang, and Yoke Khin Yap. "Patterned Growth of Boron Nitride Nanotubes by Catalytic Chemical Vapor Deposition." *Chemistry of Materials* 22, no. 5 (2010/03/09 2010): 1782-87.
- Li, Ling, Xiaowei Liu, Luhua Li, and Ying Chen. "High Yield Bnnts Synthesis by Promotion Effect of Milling-Assisted Precursor." *Microelectron. Eng.* 110 (2013): 256-59.
- Li, Yanjiao, Jing'en Zhou, Kai Zhao, Simon Tung, and Eric Schneider. "Synthesis of Boron Nitride Nanotubes from Boron Oxide by Ball Milling and Annealing Process." *Materials Letters - MATER LETT* 63, no. 20 (08/01 2009): 1733-36.
- Liao, Yunlong, Zhongfang Chen, John W. Connell, Catharine C. Fay, Cheol Park, Jae-Woo Kim, and Yi Lin. "Chemical Sharpening, Shortening, and Unzipping of Boron Nitride Nanotubes." *Advanced Functional Materials* 24, no. 28 (2014): 4497-506.
- Libor Matejka, Karel Dusek, Josef Plestil, Jaroslav Kriz, Frantisek Lednicky. "Formation and Structure of the Epoxy-Silica Hybrids." *Polymer* 40 (1998): 178-81.

- Lourie, Oleg R., Carolyn R. Jones, Bart M. Bartlett, Patrick C. Gibbons, Rodney S. Ruoff, and William E. Buhro. "Cvd Growth of Boron Nitride Nanotubes." *Chemistry of Materials* 12, no. 7 (2000/07/01 2000): 1808-10.
- M. Mutz, Eric Eastwood, and M. D. Dadmun. "Quantifying the Solubility of Boron Nitride Nanotubes and Sheets with Static Light Scattering and Refractometry." *Journal of Physical Chemistry C* 117, no. 25 (June 2013 2013): 13230- 38.
- Ma, Jinrui, Nian Luo, Zilong Xie, Feng Chen, and Qiang Fu. "Preparation of Modified Hexagonal Boron Nitride by Ball-Milling and Enhanced Thermal Conductivity of Epoxy Resin." *Materials Research Express* 6, no. 10 (2019/09/20 2019): 1050d8.
- Mahmoud S. Amin, Bennett Atwater, Robert D. Pike, Kurt E. Williamson, David E. Kranbuehl, and Hannes C. Schniepp. "High-Purity Boron Nitride Nanotubes Via High-Yield Hydrocarbon Solvent Processing." *Chemistry of Materials* 31 (2020): 8351–57.
- Marincel, Daniel M., Mohammed Adnan, Junchi Ma, E. Amram Bengio, Mitchell A. Trafford, Olga Kleinerman, Dmitry V. Kosynkin, *et al.* "Scalable Purification of Boron Nitride Nanotubes Via Wet Thermal Etching." *Chemistry of Materials* 31, no. 5 (2019/03/12 2019): 1520-27.
- Mary Ann B. Meador, * Christian R. Aleman, † Katrina Hanson, † Nakaira Ramirez, † Stephanie L. Vivod,, and ‡ and Linda McCorkle Nathan Wilmoth. "Polyimide Aerogels with Amide Cross-Links: A Low Cost Alternative for Mechanically Strong Polymer Aerogels." *Applied Materials and Interfaces* 7, no. 2 (2015): 1240-49.
- Mary Ann B. Meador, Christian R. Aleman, Katrina Hanson, Kakaira Ramirex, Stephanie L. Vivod, Nathan Wilmoth, Linda McCorkle. "Polyimide Aerogels with Amide Cross-Links: A Low Cost Alternative for Mechanically Strong Polymer Aerogels." *American Chemical Society: Applied Materials and Interfaces* 7 (2015): 1240-49.
- Mary Ann B. Meador, Ericka J. Malow, Rebecca Silva, Sarah Wright, Derek Quade, Stephanie L. Vivod, Haiquan Guo, Jiao Guo and Miko Cakmak. "Mechanically Strong, Flexible Polyimide Aerogels Cross-Linked with Aromatic Triamine." *Applied Materials and Interfaces* 4 (2012): 536-44.
- Mary Ann B. Meador, Sarah Wright, Anna Sandberg, Baochau N. Nguyen,, Carl H. Mueller Frederick W. Van Keuls, Rafael Rodríguez-Solís,, and and Felix A. Miranda. "Low Dielectric Polyimide Aerogels as Substrates for Lightweight Patch Antennas." *Applied Materials and Interfaces* 4, no. 11 (2012): 6346-53.
- Maryam Anafcheh, Elaheh Ahmadi, Mansour Zahedi. "Addition of Borazine to Boron Nitride Nanotubes: [2+2] Cycloaddition or Bond Cleavage." *Chemical Monthly* 150, no. 6 (2019): 1019-24.
- Meador, Mary Ann B., and Stephanie L. Vivod. "Polyimide Synthesis." In *Encyclopedia of Polymeric Nanomaterials*, edited by Shiro Kobayashi and Klaus Müllen, 1-11. Berlin, Heidelberg: Springer Berlin Heidelberg, 2014.
- Michael, W. Smith, C. Jordan Kevin, Park Cheol, Kim Jae-Woo, T. Lillehei Peter, Crooks Roy, and S. Harrison Joycelyn. "Very Long Single- and Few-Walled Boron Nitride Nanotubes Via the Pressurized Vapor/Condenser Method." *Nanotechnology* 20, no. 50 (2009): 505604.
- Mittal, Vikas. *High Performance Polymers and Engineering Plastics*. Edited by Vikas Mittal. Salem, MA: John Wiley and Sons, 2011.

- Mohammed Adnan, Daniel M. Marincel, Olga Kleinerman, Sang-Hyon Chu, Cheol Park, Samuel J.A. Hocker, Catharine Fay, Sivaram Arepalli, Yeshayahu Talmon, and Matteo Pasquali. "Extraction of Boron Nitride Nanotubes and Fabrication of Macroscopic Articles Using Chlorosulfonic Acid." *Nano Letters* (2018).
- N.H. Ince, G. Tezcanli, R.K. Belen, P.I.G. Apikyan. "Ultrasound as a Catalyzer of Aqueous Reaction Systems: The State of the Art and Environmental Applications." *Applied Catalysis B: Environmental* 29, no. 3 (2001): 167-76.
- Nambiar, Shruti, and John T. W. Yeow. "Polymer-Composite Materials for Radiation Protection." *ACS Applied Materials & Interfaces* 4, no. 11 (2012/11/28 2012): 5717-26.
- Olga Kleinerman, Mohammed Adnan, Daniel M Marincel, Anson W K Ma, E Amram Bengio, Cheol Park, Sang-Hyon Chu, Matteo Pasquali, Yeshayahu Talmon. "Dissolution and Characterization of Boron Nitride Nanotubes in Superacid." *Langmuir* 33, no. 15 (2017).
- P. Riesz, D. Berdahl, and C. L. Christman. "Free Radical Generation by Ultrasound in Aqueous and Nonaqueous Solutions." *Environmental Health Perspectives* 84 (1985): 233-52.
- Pakdel, A., C. Zhi, Y. Bando, T. Nakayama, and D. Golberg. "A Comprehensive Analysis of the Cvd Growth of Boron Nitride Nanotubes." [In eng]. *Nanotechnology* 23, no. 21 (Jun 1 2012): 215601.
- Palanisamy, Periasamy, Murthy Chavali, Enamala Manoj Kumar, and Krishna Chitanya Etika. "Chapter 10 - Hybrid Nanocomposites and Their Potential Applications in the Field of Nanosensors/Gas and Biosensors." In *Nanofabrication for Smart Nanosensor Applications*, edited by Kaushik Pal and Fernando Gomes, 253-80: Elsevier, 2020.
- Pankaj Chowdhury, T. Viraraghavan. "Sonochemical Degradation of Chlorinated Organic Compounds, Phenolic Compounds and Organic Dyes – a Review." *Science of the Total Environment* 407 (2008): 2474-92.
- Pokropivny, Vladimir V. "Non-Carbon Nanotubes (Review). Part 2. Types and Structure." *Powder Metallurgy and Metal Ceramics* 40, no. 11 (2001/11/01 2001): 582-94.
- "Polyimides: Chemistry and Structure-Property Relationships-Literature Review."
- "Purification and Assembly of DNA-Stabilized Boron Nitride Nanotubes into Aligned Films." (2019).
- Qunhong Weng, Xuebin Wang, Xi Wang, Yoshio Bando and Dmitri Golberg. "Functionalized Hexagonal Boron Nitride Nanomaterials: Emerging Properties and Applications." *Chemical Society Reviews* 45 (2016): 3989-4012.
- Ratta, Varun. "Polyimides: Chemistry and Structure-Property Relationships." 1999.
- Ren, Junkai, Luigi Stagi, and Plinio Innocenzi. "Hydroxylated Boron Nitride Materials: From Structures to Functional Applications." *Journal of Materials Science* 56, no. 6 (2021/02/01 2021): 4053-79.
- Rigacci, Alain C. Pierre and Arnaud. *Sio2 Aerogels*. Aerogels Handbook, Advances in Sol-Gel Derived Materials and Technologies. Edited by M.A. Aegerer et al. Springer Science + Business Media, LLC2001. doi:DOI 10.1007/978-1-4419-7589-8_2,.
- Roy, Arup Kumer, Byoungnam Park, Kang Seok Lee, Sung Young Park, and Insik In. "Boron Nitride Nanosheets Decorated with Silver Nanoparticles through Mussel-Inspired Chemistry of Dopamine." *Nanotechnology* 25, no. 44 (2014/10/17 2014): 445603.
- Rubio, Angel, Jennifer L. Corkill, and Marvin L. Cohen. "Theory of Graphitic Boron Nitride Nanotubes." *Physical Review B* 49, no. 7 (02/15/ 1994): 5081-84.

- Saban Kalay, Zehra Yilmaz, Ozlem Sen, Melis Emanet, Emine Kazanc and Mustafa Çulha. "Synthesis of Boron Nitride Nanotubes and Their Applications." *Beilstein Journal of Nanotechnology* 6 (2015): 84-102.
- Sainsbury, Toby, Arlene O'Neill, Melissa K. Passarelli, Maud Seraffon, Dipak Gohil, Sam Gnaniah, Steve J. Spencer, Alasdair Rae, and Jonathan N. Coleman. "Dibromocarbene Functionalization of Boron Nitride Nanosheets: Toward Band Gap Manipulation and Nanocomposite Applications." *Chemistry of Materials* 26, no. 24 (2014/12/23 2014): 7039-50.
- Sainsbury, Toby, Amro Satti, Peter May, Arlene O'Neill, Valeria Nicolosi, Yurii K. Gun'ko, and Jonathan N. Coleman. "Covalently Functionalized Hexagonal Boron Nitride Nanosheets by Nitrene Addition." *Chemistry – A European Journal* 18, no. 35 (2012): 10808-12.
- Sainsbury, Toby, Amro Satti, Peter May, Zhiming Wang, Ignatius McGovern, Yurii K. Gun'ko, and Jonathan Coleman. "Oxygen Radical Functionalization of Boron Nitride Nanosheets." *Journal of the American Chemical Society* 134, no. 45 (2012/11/14 2012): 18758-71.
- Saner Okan, Burcu, Züleyha Özlem Kocabaş, Asli Nalbant Ergün, Mustafa Baysal, Ilse Letofsky-Papst, and Yuda Yürüm. "Effect of Reaction Temperature and Catalyst Type on the Formation of Boron Nitride Nanotubes by Chemical Vapor Deposition and Measurement of Their Hydrogen Storage Capacity." *Industrial & Engineering Chemistry Research* 51, no. 35 (2012/09/05 2012): 11341-47.
- Sang-Woo Jeon, Shin-Hyun Kang, Jung Chul Choi and Tae-Hwan Kim. "Dispersion of Boron Nitride Nanotubes by Pluronic Triblock Copolymer in Aqueous Solution." *Polymer* 11, no. 4 (2019).
- Seo, Tae Hoon, Gun Hee Lee, Ah Hyun Park, Hyunjin Cho, Jun-Hee Kim, S. Chandramohan, Seong-Ran Jeon, *et al.* "Boron Nitride Nanotubes as a Heat Sinking and Stress-Relaxation Layer for High Performance Light-Emitting Diodes." *Nanoscale* 9, no. 42 (2017): 16223-31.
- Shin, Homin, Jingwen Guan, Marek Z. Zgierski, Keun Su Kim, Christopher T. Kingston, and Benoit Simard. "Covalent Functionalization of Boron Nitride Nanotubes Via Reduction Chemistry." *ACS Nano* 9, no. 12 (2015/12/22 2015): 12573-82.
- Shuqiong Lin, Behnam Ashrafi, Kurtis Laqua, Keun Su Kim and Benoit Simard. "Covalent Derivatization of Boron Nitride Nanotubes with Peroxides and Their Application in Polycarbonate Composites." *New Journal of Chemistry* 41, no. 15 (2017).
- "Silica Aerogel: Synthesis and Applications." (2010).
- Simón-Herrero, Carolina, Xiao-Yuan Chen, Maria Luz Ortiz, Amaya Romero, José L. Valverde, and Luz Sánchez-Silva. "Linear and Crosslinked Polyimide Aerogels: Synthesis and Characterization." *Journal of Materials Research and Technology* 8, no. 3 (2019/05/01/ 2019): 2638-48.
- Singh, Dilip K., P. K. Iyer, and P. K. Giri. "Diameter Dependence of Interwall Separation and Strain in Multiwalled Carbon Nanotubes Probed by X-Ray Diffraction and Raman Scattering Studies." *Diamond and Related Materials* 19, no. 10 (10// 2010): 1281-88.
- Singhal, S. K., A. K. Srivastava, R. P. Pant, S. K. Halder, B. P. Singh, and Anil K. Gupta. "Synthesis of Boron Nitride Nanotubes Employing Mechanochemical Process and Its Characterization." *Journal of Materials Science* 43, no. 15 (2008/08/01 2008): 5243-50.
- "The Sol-Gel Process." (1990).

- Song, Yangxi, Bin Li, Siwei Yang, Guqiao Ding, Changrui Zhang, and Xiaoming Xie. "Ultralight Boron Nitride Aerogels Via Template-Assisted Chemical Vapor Deposition." *Scientific Reports* 5 (05/15/online 2015): 10337.
- Sroog, C. E. "Polyimides." *Journal of Polymer Science: Macromolecular Reviews* 11, no. 1 (1976): 161-206.
- Stephanie L Vivod, Mary Ann B. Meador, Coleen Pugh, Melissa Wilkosz, Kerah Calomino, and Linda S McCorkle. "Toward Improved Optical Transparency of Polyimide Aerogels." *Applied Materials and Interfaces* 12, no. 7 (2019): 8622-33.
- Subramaniam Iswar, Geert M.B.F. Snellings, Shanyu Zhao, Rolf Erni,, Jing Wang Yeon Kyoung Bahk, Marco Lattuada, Matthias M. Koebel,, and Wim J. Malfait. "Reinforced and Superinsulating Silica Aerogel through in Situ Crosslinking with Silane Terminated Prepolymers." *Acta Materialia* 147 (2018): 322-28.
- Suenaga, K., F. Willaime, A. Loiseau, and C. Colliex. "Organisation of Carbon and Boron Nitride Layers in Mixed Nanoparticles and Nanotubes Synthesised by Arc Discharge." *Applied Physics A* 68, no. 3 (1999/03/01 1999): 301-08.
- "Surfactant-Assisted Individualization and Dispersion of Boron Nitride Nanotubes." *Nanoscale Advances* (2019).
- Takekoshi, Tohru. *Polyimides: Fundamentals and Applications*. Plastics Engineering. Edited by Kash L. Mittal Malay K. Ghosh. Vol. 36, New York 1996.
- Talk, Mary Ann B. Meador ACS. "Improvements to the Synthesis of Polyimide Aerogels." edited by National Aeronautics and Space Administration, 2011.
- Tang, Chengchun, Yoshio Bando, and Tadao Sato. "Catalytic Growth of Boron Nitride Nanotubes." *Chemical Physics Letters* 362, no. 3-4 (8/19/ 2002): 185-89.
- Tang, Chengchun, Yoshio Bando, Tadao Sato, and Keiji Kurashima. "A Novel Precursor for Synthesis of Pure Boron Nitride Nanotubes." *Chemical Communications*, no. 12 (2002): 1290-91.
- Tang, Yi-Ren, Da-Wei Lin, Yang Gao, Jun Xu, and Bao-Hua Guo. "Prominent Nucleating Effect of Finely Dispersed Hydroxyl-Functional Hexagonal Boron Nitride on Biodegradable Poly(Butylene Succinate)." *Industrial & Engineering Chemistry Research* 53, no. 12 (2014/03/26 2014): 4689-96.
- Tanur, Adrienne E., Jiasheng Wang, Arava L. M. Reddy, Daniel N. Lamont, Yoke Khin Yap, and Gilbert C. Walker. "Diameter-Dependent Bending Modulus of Individual Multiwall Boron Nitride Nanotubes." *The Journal of Physical Chemistry B* 117, no. 16 (2013/04/25 2013): 4618-25.
- Tay, Roland Yingjie, Hongling Li, Siu Hon Tsang, Lin Jing, Dunlin Tan, Mingwei Wei, and Edwin Hang Tong Teo. "Facile Synthesis of Millimeter-Scale Vertically Aligned Boron Nitride Nanotube Forests by Template-Assisted Chemical Vapor Deposition." *Chemistry of Materials* 27, no. 20 (2015/10/27 2015): 7156-63.
- Thang, Pham, Anna P. Goldstein, James P. Lewicki, Sergei O. Kucheyev, Cheng Wang, Thomas P. Russell, Marcus A. Worsley, *et al.* "Nanoscale Structure and Superhydrophobicity of Sp(2)-Bonded Boron Nitride Aerogels." *Nanoscale* 7, no. 23 (2015 2015): 10449-58.
- Thomas, J., N. E. Weston, and T. E. O'Connor. "Turbostratic1 Boron Nitride, Thermal Transformation to Ordered-Layer-Lattice Boron Nitride." *Journal of the American Chemical Society* 84, no. 24 (1962/12/01 1962): 4619-22.

- Tiano, A. L., L. Gibbons, M. Tsui, S. I. Applin, R. Silva, C. Park, and C. C. Fay. "Thermodynamic Approach to Boron Nitride Nanotube Solubility and Dispersion." *Nanoscale* 8, no. 7 (2016): 4348-59.
- Velayudham, Singaravelu, Chee Huei Lee, Ming Xie, Dominique Blair, Nicholas Bauman, Yoke Khin Yap, Sarah A. Green, and Haiying Liu. "Noncovalent Functionalization of Boron Nitride Nanotubes with Poly(P-Phenylene-Ethynylene)S and Polythiophene." *ACS Applied Materials & Interfaces* 2, no. 1 (2010/01/27 2010): 104-10.
- Vieira, S. M., and D. L. Carroll. "Purification of Boron Nitride Multiwalled Nanotubes." [In eng]. *J Nanosci Nanotechnol* 7, no. 9 (Sep 2007): 3318-22.
- Vivod, S. L., Meador, M. A. B., Pugh, C., Wilkosz, M., Calomino, K., & McCorkle, L. S. "Toward Improved Optical Transparency of Polyimide Aerogels." *Applied Materials and Interfaces* 12 (2020): 8622-33.
- Vivod, Stephanie. "Influence of Trifluoromethyl Substituents on Structural and Thermal Stability of Polyimide Aerogel Matrix." (2019).
- Wang, X. Z., Q. Wu, Z. Hu, and Y. Chen. "Template-Directed Synthesis of Boron Nitride Nanotube Arrays by Microwave Plasma Chemical Reaction." *Electrochimica Acta* 52, no. 8 (2007): 2841-44.
- Wang, Zhujun, Qian Li, Jinfeng Liu, Huayi Li, and Shuirong Zheng. "Covalent Surface Functionalization of Boron Nitride Nanotubes Fabricated with Diazonium Salt." *Journal of Nanomaterials* 2018 (2018/04/18 2018): 6717046.
- Wei Fan, Xiang Zhang, Yi Zhang, Youfang Zhang, Tianxi Liu*. "Lightweight, Strong, and Super-Thermal Insulating Polyimide Composite Aerogels under High Temperature." *Composites Science and Technology* 173 (2019): 47-52.
- Wirtz, Ludger, Angel Rubio, Raul Arenal de la Concha, and Annick Loiseau. "Ab Initio Calculations of the Lattice Dynamics of Boron Nitride Nanotubes." *Physical Review B* 68, no. 4 (07/30/ 2003): 045425.
- Wu, K., Lei, C., Yang, W., Chai, S., Chen, F., Fu, Q. "Surface Modification of Boron Nitride by Reduced Graphene Oxide for Preparation of Dielectric Material with Enhanced Dielectric Constant and Well-Suppressed Dielectric Loss." *Composites Science and Technology* 134, no. 6 (2016).
- Xiao, Feng, Sina Naficy, Gilberto Casillas, Majharul H. Khan, Tomas Katkus, Lei Jiang, Huakun Liu, Huijun Li, and Zhenguo Huang. "Edge-Hydroxylated Boron Nitride Nanosheets as an Effective Additive to Improve the Thermal Response of Hydrogels." *Advanced Materials* 27, no. 44 (2015): 7196-203.
- Xiaoliang Zeng, Lei Ye, Rong Sun, Jianbin Xu, and Ching-Ping Wongcd. "Observation of Viscoelasticity in Boron Nitride Nanosheet Aerogel." *Physical Chemistry Chemical Physics* 17 (May 2015 2015): 16709-14.
- Xiujuan, J. Dai, Chen Ying, Chen Zhiqiang, R. Lamb Peter, H. Li Lu, Plessis Johan du, G. McCulloch Dougal, and Wang Xungai. "Controlled Surface Modification of Boron Nitride Nanotubes." *Nanotechnology* 22, no. 24 (2011): 245301.
- "An Xps and Low-Temperature Nitrogen Adsorption Study of the Structure of Carbon-Fluorocarbon Nanocomposites." (2018).
- Y. Chen, J. Fitz Gerald, J.S. Williams, S. Bulcock "Synthesis of Boron Nitride Nanotubes at Low Temperatures Using reactive Ball Milling." *Chemical Physical Letters* 299, no. 3-4 (1999): 260-64.

- Yahachi Saito, Masatomo Maida, Takehisa Matsumoto. "Structure of Boron Nitride Nanotubes with Single Layer and Multilayer Produced by Arc Discharge." *Japanese Journal of Applied Physics* 38, no. 1R (1999).
- Yamaguchi, Maho, Dai-Ming Tang, Chunyi Zhi, Yoshio Bando, Dmitry Shtansky, and Dmitri Golberg. "Synthesis, Structural Analysis and in Situ Transmission Electron Microscopy Mechanical Tests on Individual Aluminum Matrix/Boron Nitride Nanotube Nanohybrids." *Acta Materialia* 60, no. 17 (2012/10/01/ 2012): 6213-22.
- Yang, Huang, Lin Jing, Tang Chengchun, Bando Yoshio, Zhi Chunyi, Zhai Tianyou, Dierre Benjamin, Sekiguchi Takashi, and Golberg Dmitri. "Bulk Synthesis, Growth Mechanism and Properties of Highly Pure Ultrafine Boron Nitride Nanotubes with Diameters of Sub-10 nm." *Nanotechnology* 22, no. 14 (2011): 145602.
- Yeh, Yao-Wen, Yevgeny Raitses, Bruce E. Koel, and Nan Yao. "Stable Synthesis of Few-Layered Boron Nitride Nanotubes by Anodic Arc Discharge." *Scientific Reports* 7, no. 1 (2017/06/08 2017): 3075.
- Ying Chen, Lewis T. Chadderton, John Fitz Gerald, James S. Williams. "A Solid-State Process for Formation of Boron Nitride Nanotubes." *Applied Physics Letters* 74, no. 20 (1999): 2960-62.
- Yu, J., Y. Chen, and B. M. Cheng. "Dispersion of Boron Nitride Nanotubes in Aqueous Solution with the Help of Ionic Surfactants." *Solid State Communications* 149, no. 19 (2009/05/01/ 2009): 763-66.
- Yu, Jun, Ying Chen, Richard Wuhrer, Zongwen Liu, and Simon P. Ringer. "In Situ Formation of Bn Nanotubes During Nitriding Reactions." *Chemistry of Materials* 17, no. 20 (2005/10/01 2005): 5172-76.
- Zheng, Zhuoyuan, McCord Cox , and Bin Li "Surface Modification of Hexagonal Boron Nitride Nanomaterials: A Review.". *Journal of Materials Science* 53, no. 1 (2018): 66-99.
- Zhi, C. Y., Y. Bando, C. C. Tang, Q. Huang, and D. Golberg. "Boron Nitride Nanotubes: Functionalization and Composites." *Journal of Materials Chemistry* 18, no. 33 (2008): 3900-08.
- Zhi, Chunyi, Yoshio Bando, Chengchun Tan, and Dmitri Golberg. "Effective Precursor for High Yield Synthesis of Pure Bn Nanotubes." *Solid State Communications* 135, no. 1-2 (7 2005): 67-70.
- Zhi, Chunyi, Yoshio Bando, Chengchun Tang, Susumu Honda, Kazuhiko Sato, Hiroaki Kuwahara, and Dmitri Golberg. "Covalent Functionalization: Towards Soluble Multiwalled Boron Nitride Nanotubes." *Angewandte Chemie International Edition* 44, no. 48 (2005): 7932-35.
- . "Purification of Boron Nitride Nanotubes through Polymer Wrapping." *The Journal of Physical Chemistry B* 110, no. 4 (2006/02/01 2006): 1525-28.
- Zhuoyuan Zheng, McCord Cox, and Bin Li. "Surface Modification of Hexagonal Boron Nitride Nanomaterials: A Review." *Journal of Materials Science*, no. 53 (August, 2017 2018): 66-99.
- Zois Syrgiannis, Michele Melchionna and Maurizio Prato. "Covalent Carbon Nanotube Functionalization." *Encyclopedia of Polymeric Nanoaterials* (2014).